Structural and Biochemical Characterization of the Human Serine Protease HtrA1

Inaugural-Dissertation

zur

Erlangung des Doktorgrades

Dr. rer. nat.

der Fakultät für

Biologie und Geografie

an der

Universität Duisburg-Essen

vorgelegt von

Linda Trübestein

aus Berlin

April 2010

Gutachter:

Prof. Michael Ehrmann, Prof. Peter Bayer

Prüfungsdatum:

18.06.2010

Parts of this work are included in the following publications:

Tennstaedt, A., Truebestein, L., Hauske, P., Schmidt, N., Irle, I., Kaiser, M., Brandt, R., Sickmann, A., Egensperger, R., Baldi, A., Dehmelt, L. und Ehrmann M., „HtrA1 is a tau protease.“ (in revision in PNAS)

Truebestein, L., Tennstaedt, A., Krojer, T., Hauske, P., Kaiser, M., Clausen, T., and Ehrmann, M., „Substrate binding remodels active site of HtrA1 and regulates protease activity.” (submitted to Nat Struc & Mol Biol)

Acknowledgements

First of all I would like to thank Michael Ehrmann for his constant support and supervision during my PhD. Thanks for giving me the chance to work on this very interesting project and for all the trust you had in me.

I am thankful to all the members in the Ehrmann Lab for creating a very nice working atmosphere, for all the discussions and the nice time we had.

I want to thank Tim Clausen for giving me the great chance to work in his lab and for always giving me the feeling that I am very welcome. Thanks for all the motivation and the supervision during my PhD.

Furthermore I would like to thank all the members of the Clausen Lab in Vienna. You were such fantastic colleges! I can hardly imaging to find something like this again. I want to thank Linn, Doris, Justyna, Flavia, Juliane, Sonja, Becky, Bastian, Jakob, Tobias, Robert, Anita and Alex for the warm welcome and for sharing lab space, equipment and knowledge so generously with me. I will never forget all the hours of chatting and laughing. It was a wonderful time.

Especially I want to thank Tobias for all his support and his patience. You became never tired of discussing all my questions again and again and to keep me on the right track.

I am very thankful to Justyna, Linn and Tobias for discussions and correcting my thesis.

I want to thank Evi and Nina for always listening to my problems inside and outside the lab and for all their optimism and support during the ups and downs in my life. It makes life so much easier to have such good friends like you.

I want to thank Roger for stepping into my life. You showed me what is important and how to keep the right balance. Nothing better than you could have happened to me.

Finally I would like to thank my sister Nora, my parents and my step-parents with all my heart. Thanks for always believing in me and giving me the strength to go on. I can not imagine a happy life without you.

Table of Contents

List of Figures

List of Tables

Abbrevations

amp	ampicillin
APS	ammonium persulfate
BSA	bovine serum albumin
CIAP	calf intestine alkaline phosphatase
CV	column volumes
DFP	diisopropyl fluorophosphate
DMSO	dimethyl sulfoxide
DLS	dynamic light scattering
dNTP	deoxynucleotides
DTT	dithiothreitol
Fig.	figure
hrs	hours
Hepes	N-[2-Hydroxyethyl]piperazine-N'-[2-ethanesulphonic acid]
IGFBP	Insulin-like growth factor binding proteins
IPTG	isopropyl-β-D-thiogalactopyranoside
kDa	kilo dalton
NiNTA	nickel-Nitrilotriacetic acid
MM	minimal medium
min	minutes
LB	Luria Bertani
OD	optical density
on	over night
PAGE	polyacrylamide gel electrophoresis
PEG	polyethylene glycol
PCR	polymerase chain reaction
PDZ	protein-protein interaction domain
rpm	revolutions per minute
RT	room temperature
SDS	sodium dodecyl sulphate
SEC	size exclusion chromatography
SeMet	selenomethionine
Tab.	table
TBS	Tris buffered saline
TCA	trichloroacetic acid
TEMED	N,N,N',N'-Tetramethylethylenediamine
TRIS	tris[hydroxymethyl]aminomethane
wt	wild-type
v/v	volume per volume
w/v	weight per volume

1 Introduction

1.1 Protein quality control

Cell function and viability are depending on correct protein folding. Although all information necessary for a protein to obtain a native conformation is encoded in its amino acid sequence (Anfinsen 1973), *in vivo* protein folding requires the assistance of chaperones, folding catalysts and proteases to monitor and regulate this process. Accordingly, cells have developed a sophisticated system of chaperones and proteases to control the folding state of proteins (Wickner *et al.* 1999). Failure in the quality control machinery can lead to damaged proteins that can be hazardous for cells as they tend to form large aggregates.

Mistakes in transcription and translation that result in mutations of only one amino acid can lead to destabilization and thus prevent normal folding. In addition, environmental stress conditions such as macromolecular crowding, inappropriate ionic strength, oxidative, temperature or pH stress can cause the formation of misfolded proteins or slowly reacting intermediates (Wickner *et al.* 1999). Stress conditions can also promote the partial unfolding of fully folded native proteins. Exposed hydrophobic regions on non-native proteins bind to similar regions on nearby proteins by highly specific self association (Rajan *et al.* 2001). The aggregating species can continue to bind exposed hydrophobic regions of neighbouring proteins and form various stable structures, including soluble aggregates and insoluble deposits (Demuro *et al.* 2005). Insoluble protein aggregates contribute to the pathology of a variety of serious human diseases, including amyloidoses that are characterized by insoluble, fibrillar protein aggregates with a ß-sheet-rich structure. In this situation both proteases and chaperones serve to maintain quality control of cellular proteins. Any of the two protein families has to recognize regions that are commonly found in misfolded or unfolded proteins but not in native proteins (Wickner *et al.* 1999) and it could be demonstrated, that both systems recognize hydrophobic regions exposed in unfolded proteins (Wickner *et al.* 1999). The number of diseases linked to aberrant protein conformations include Huntington's disease, Alzheimer's disease, Parkinson's disease, and more (Dobson 2004; Macario and Conway de Macario 2005). They underline the importance of an effective protein quality control for cell viability and survival.

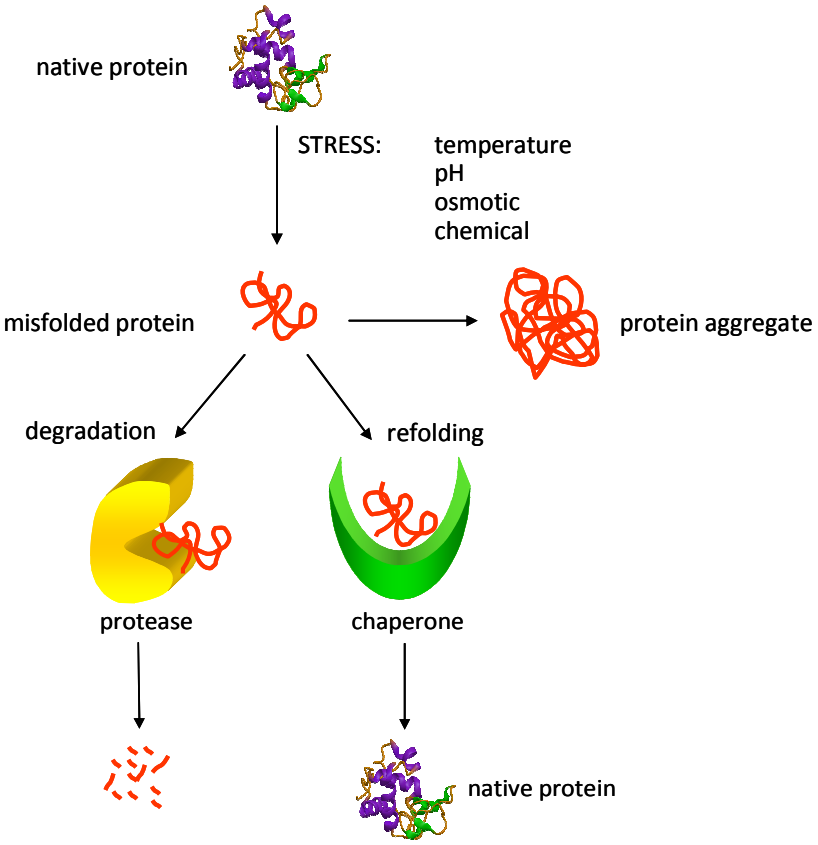

Fig. 1.1 Principles of protein quality control
Non-native proteins can either be refolded by molecular chaperones or degraded by proteases. Both principles serve the same goal, namely the avoidance of protein aggregates, which are lethal for the cell. Achieving the correct balance between folding and degradation of misfolded proteins is critical for cell viability.

1.2 Proteolysis and proteolytic enzymes

Proteases are an important class of enzymes that hydrolyse peptide bonds. They can either work as exo- or endopeptidases. Exopeptidases cleave one, two or three residues from the N- or C-terminus of a polypeptide chain. Therefore they are called aminopeptidases or carboxypeptidases, respectively. Endopeptidases cleave somewhere in the middle of a polypeptide chain, depending on their substrate specificity. According to the nomenclature of Rawlings and Barrett, endoproteases can be divided into five groups depending on their active site residues and their functional groups. Four of these groups, namely serine proteases, cysteine proteases, aspartate proteases and metalloproteases (Barrett, 1994) have been well studied and are well understood (Rawlings *et al.* 1994, 1995, 1995). Proteases perform a variety of fundamental biological activities. They are used for such different functions as food digestion, cleavage of signal peptides, the precise processing of

proteins in the blood clotting cascade (Fersht 1999) or the degradation of abnormal proteins (Wickner *et al.* 1999). Proteases are furthermore associated with a variety of diseases and therefore they are potential targets for new drugs (Fersht 1999).

The biological implications of proteolytic reactions are immense. Proteases provide an important link between genetics and biochemistry as they often act as key players in regulatory events, for example in important signaling cascades such as apoptosis (Shi 2002, Degterev *et al.* 2003) and the regulation of the unfolded protein response (Patil *et al.* 2001).

Proteases also show a high degree of specificity towards binding and processing their substrates. Thereby substrate specificity is often defined by the structural properties of the active site or by adaptor proteins that can feed substrates to the protease (Gottesman 2003). Bacterial DegS is an example where binding of C-termini of outer membrane proteins to the PDZ domain triggers the activation of the protease (Walsh *et al.* 2003). As mentioned before, proteases bind to hydrophobic patches which are normally buried in the native conformation (Wickner *et al.* 1999). Therefore it is obvious that potential cleavage sites have to become accessible as a result of unfolding or the loss of interaction partners. A further concept to control the accessibility of catalytic sites is the compartmentalization of active sites within a large protease particle. In cage forming proteases, as examplified by the proteasome or the DegP protease from *E. coli*, the active sites are located in an inner cavity that can be accessed only by unfolded proteins (Larsen *et al.* 1997, Clausen *et al.* 2002, Krojer *et al.* 2008). This principle is an elegant way to prevent degradation of folded proteins. Proteases are often involved in degradation events which are depending on the action of more than one protease which represents an additional level of regulation. Inhibition and activation of proteases describes another principle of regulation. Many of the classical proteases such as trypsin are synthesized as inactive zymogens that are converted into the active form by proteolysis of a propeptide (Khan *et al.* 1998, Lazure 2002, Wiederanders 2003). Zymogen activation was long considered to be irreversible however, recent reports indicate reversible zymogen activation where either other proteins (Friedrich *et al.* 2003) or external factors such as concentrated salts (Huang *et al.* 2001), temperature (Spiess *et al.* 1999) and binding of substrates (Ehrmann *et al.* 2004, Hasselblatt *et al.* 2007, Krojer *et al.* 2008) can switch protease activity on or off. Yet another level of regulation of proteases is the existence of various natural inhibitors. According to the principle of exosite binding (Krishnaswamy 2005, Guillin *et al.* 1995), the common feature of these inhibitors is that they are tightly bound to the protease by occupying the substrate-specificity pockets (Bode *et al.* 2000, Ye *et al.* 2001).

1.3 Serine proteases

Serine proteases have been extensively studied and are a group of well-characterized enzymes. They have been studied by both by kinetic methods in solution and by x-ray structural studies to high resolution. Most of them contain the typical catalytic triad composed of histidine, aspartate and serine. So far, also serine proteases with novel catalytic triads, (e.g. Ser-His-His) and dyads (e.g. Ser-Lys) have been additionally discovered (Blow 1997, Hedstrom 2002, Pólgar 2005). The following paragraph gives a short description of the catalytic mechanism and the main determinants of substrate specificity of serine proteases considering chymotrypsin as example. It should be noted, that this overview is mainly adopted from the book Carl Brandon and John Tooze (Introduction to protein structure, 1999) and from Alan Fersht (Structure and mechanism in protein science, 1999) and Arthur Lesk (Introduction to protein structure, 2001).

1.3.1 The catalytic mechanism

The mechanism for the hydrolysis of the peptide bond is an addition-elimination reaction involving two tetrahedral intermediates. The catalytic triad spans the active site cleft with Ser195 on one side and Asp102 and His57 on the other side (using the chymotrypsin numbering). The reaction proceeds in two steps: during the first step the peptide bond is cleaved. The sidechain of the substrate at the residue N-terminal to the scissile bond binds to the specificity pocket and the catalytic triad Asp102-His57-Ser210 positions and polarizes the sidechain of Ser195 for nucleophilic attack on the C-atom of the peptide bond. The C_1 of the substrate is covalently bound to the hydroxyl group of the active site serine in the protease forming an acyl-enzyme intermediate. The intermediate with the carbon atom in a tetrahedral state is stabilized by the ‘oxyanion hole’. Both Gly193 and Ser195 can donate backbone hydrogens for hydrogen bonding to the negatively charged oxygen of the substrate (formerly the carbonyl oxygen of the peptide group of the peptide bond) (Fig. 1.3). A proton is transferred from Ser195 to His57 releasing the C-terminal moiety of the substrate. One peptide product is now attached to the protease and the other peptide product diffuses away. In the second step the acyl-intermediate is deacylated to restore the catalytic triad and to release the second peptide product. This step also proceeds through a tetrahedral transition state with H_2O in the role of the NH_2-group of the peptide. A nucleophilic attack by the hydroxyl group of a water molecule that is hydrogen bonded to His57 releases the carboxylic acid product restoring the protease in its initial state (Hedstrom, 2002).

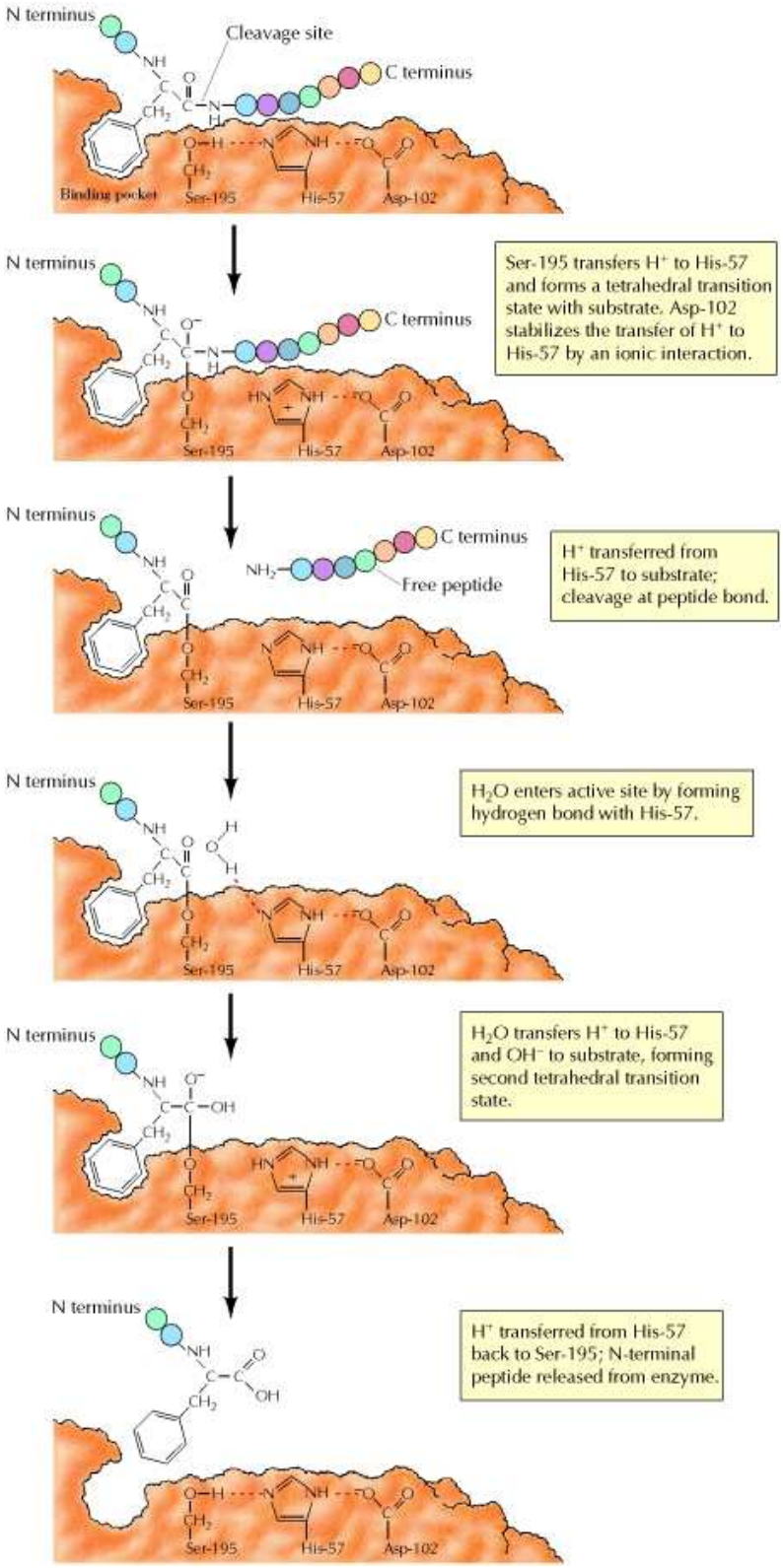

Fig. 1.2 The mechanism of chymotrypsin

The catalytic cycle is schematically shown. Acylation includes extraction of a proton from Ser195 by His57, attack of the scissile peptide bond by Ser195 and formation of the tetrahedral intermediate. Donation of a proton to the peptide nitrogen from His57 and cleavage of the peptide bond releases the first product. Deacylation includes the attack of the acyl-enzyme intermediate by H_2O that donates a proton to His57. The remaining OH attacks the acyl carbon forming a second tetrahedral transition state. His57 donates a proton to the Ser195 oxygen. The ester bond is cleaved and the second product is released. The figure is adapted from Geoffrey M. Coopers "The Cell", 2nd edition 2000.

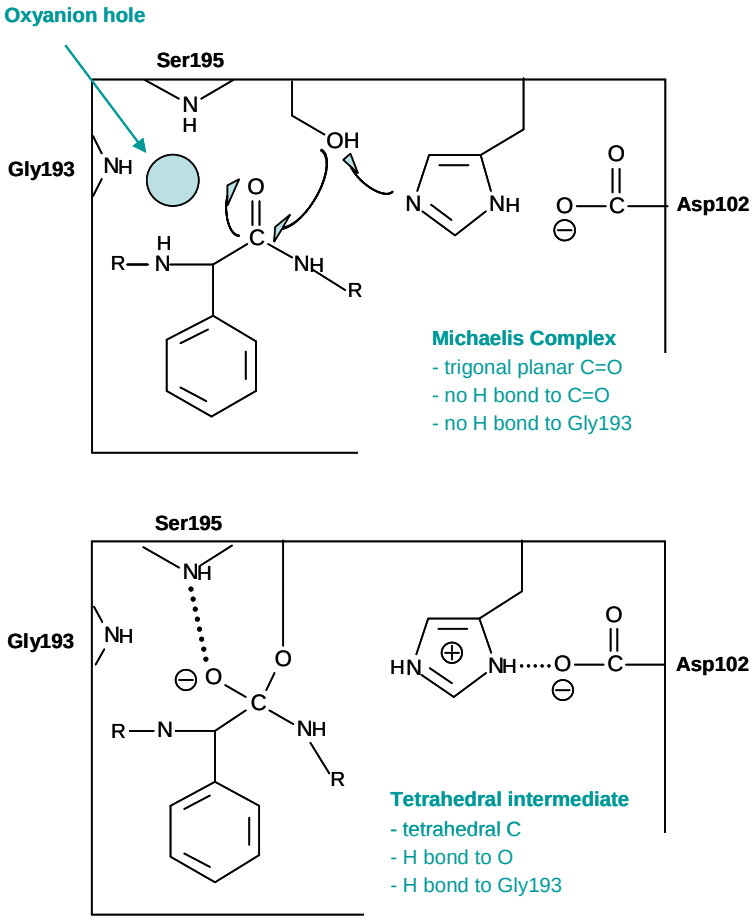

Fig. 1.3 Contribution of the oxyanion hole to the enzymatic mechanism of chymotrypsin
During the formation of the tetrahedral intermediate, the carbonyl oxygen of the substrate obtains a partial negative charge and moves to the oxyanion hole. Two hydrogen bonds are formed in the oxyanion hole that stabilise the tetrahedral transition state. The picture was adapted from Dr. Jakubowski's Biochemistry online.

1.3.2 S1 specificity pocket

The binding site for a polypeptide substrate consists of a series of subsites across the surface of the enzyme. However, very often only the primary binding pocket, also called the S1 specificity pocket is well defined. The specificity of the pocket depends on its depth as well as on the electrostatic properties of the residues forming the surface of the pocket. Digestive proteases such as try sin, chemotropism or lactase have very similar three dimensional structures but show different substrate specificity. They cleave their substrates after positively charged, bulky aromatic or small uncharged side chains respectively (Blow 1997; Edstrom *et al.* 2002). Studies on protease specificity usually focused on the P1/S1 interaction (based on the nomenclature of Schuster and Berger (1967). P1 (peptide 1) represents the first residue of the N-terminal side of the scissile bond. The subsites on the protease, for example S1 (subside 1) interact with the substrate. Three residues determine the different preferences. In chymotrypsin, residues 189-192, 214-216 and 224-228 form the S1 pocket

and the specificity is determined by residues Ser189, Gly216 and Gly226 (Perona and Craik 1995; Czapinska and Otlewski 1999). These three residues create a deep hydrophobic pocket that binds to hydrophobic residues of the substrate. In contrast, in trypsin Asp189, Gly216 and Gly226 create a negatively charged specificity pocket that interacts with Arg or Lys side chains at the P1 site of the substrate (Huber *et al.* 1974, Hedstrom *et al.* 2002). Elastase prefers small uncharged residues as Val216 and Thr226 line the specificity pocket (Shotton and Watson, 1969, Hedstrom *et al.* 2002). Besides the S1 specificity pocket the substrate interacts with additional binding pockets. Mainly the main chain of residues 214-216 interact with the backbone of residues P1 to P3 of the substrate forming an antiparallel beta sheet (Hedstrom *et al.* 2002). Additional structural features that generate substrate specificity and modulate enzyme activity are ions such as Na^+ and Ca^{2+}, surface insertion loops and exosites that are linked to the polypeptide binding sites and active site (DiCera and Krem 2003).

1.4 PDZ domains

PDZ domains are protein-protein interaction modules and are present in all kingdoms of life from bacteria to vertebrates. The name PDZ domain (also known as GLGF repeat) derives from the first three identified PDZ domain containing proteins: the postsynaptic protein PSD-95, the Drosophila disc large tumor suppressor, Dlg and the tight junction protein ZO-1 (reviewed in Hung *et al.* 2002). PDZ domains are found within diverse multi-domain proteins and recognize mainly the carboxy termini of their target proteins (Beebe *et al.* 2000). They often play important roles in organizing and linking multi-protein networks involved in signalling pathways and subcellular transports (Milev *et al.* 2007). Beside binding substrates through their C-termini also internal PDZ binding motifs exist which mimic a C-terminus (Harris *et al.* 2001). PDZ domains are composed of 90 to 120 amino acids and share a common three-dimensional structure (Fig. 1.4). The fold comprises six "ß-strands ("ßA – "ßF), forming two antiparallel sheets stacked onto each other with two α helices (αA and αB) packed against the edges of the ß sandwich to build the hydrophobic core (Milev *et al.* 2007). The peptide binding site is on the opposite side to the closely to each other located N- and C-termini (Harris *et al.* 2001). Although there are only small variations in the structure of different PDZ domains they show different specificity towards substrates. A nomenclature to describe the last few C-terminal amino acids bound by a PDZ domain has been developed. The C-terminal residue of the substrate is referred to as the P0 residue, negatively counting towards the N-terminus for subsequent residues. Based on

the interaction with the -2 position three classes of PDZ domains have been described. Residues at -1 and -3 are supposed to mediate the fine tuning of the binding (Milev *et al.* 2007, Songyang *et al.* 1997). Peptide binding to a PDZ domain is defined by two important features. First, peptides bind in an extended groove on the surface between ßB and αB forming an additional, antiparallel ß-strand (Fig. 1.4). Second, the C-terminal residue of the ligand points into a deep hydrophobic pocket, built by conserved residues (Doyle *et al.* 1996). The highly conserved GLGF loop motif which binds the COOH-terminus of the peptide and a positively charged residue (arginine or lysine) are important features for binding C-terminal peptides in a canonical fashion (Harris *et al.* 2001).

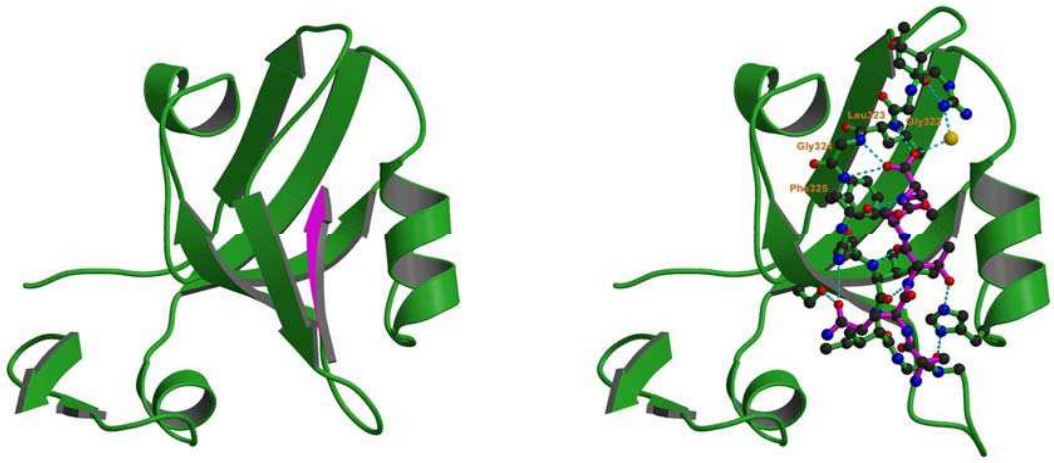

Fig. 1.4 Canonical peptide binding mode
A) Ribbon diagram of the third PDZ domain from the synaptic protein PSD-95 in complex with a peptide ligand (Doyle *et al.*, 1996). Peptides bind in the groove between ßB and αB forming an additional antiparallel ß-sheet (shown in magenta). B) Chemical interactions involved in peptide binding. The PDZ domain is coloured in green and the ligand in purple. Hydrogen bonds are indicated by dotted lines coloured in cyan. The Protein Data Bank entry code is 1BE9.

In addition several PDZ domains were identified which bind internal recognition motifs (Hillier *et al.* 1999, Harris *et al.* 2001). Here the binding does not depend on recognition of a typical carboxyl-terminal motif but the domains interact in a linear head-to-tail fashion (Hillier *et al.* 1999). One example is the PDZ domain of neuronal nitric oxide synthase (nNOS) which can heterodimerize with the PDZ domain of postsynaptic density protein 95 (PSD95) by mimicking a peptide ligand which binds into the peptide binding groove of PSD95, except that a sharp ß-turn replaces the normally required carboxyl terminus (Hillier *et al.* 1999). This can explain how PDZ domains participate to assemble protein networks. Identifying the substrate specificity of a particular PDZ domain can shed light on its distinct binding behaviour and help to find physiological substrates to understand its distinct function.

1.5 The HtrA-family of serine proteases

The HtrA (high temperature requirement) family represents a class of oligomeric serine proteases. The defining feature of the over 180 family members is the combination of a catalytic domain with one or more C-terminal PDZ domains (Clausen *et al.* 2002) (Fig. 1.5). Some members of this family possess additional N-terminal domains, such as transmembrane or insulin-like growth factor-binding domains (IGFBP) (Kim and Kim 2005). Functionally, HtrAs monitor protein homeostasis in the cell. Prokaryotic HtrAs underlie processes involved in tolerance against various folding stresses and pathogenicity (Jones *et al.* 2001, Cortes *et al.* 2002, Mo *et al.* 2006). The four human homologues are suggested to be involved in the onset of diseases related to deficient protein quality control including arthritis, cancer, ageing, Alzheimer´s or Parkinson´s disease (Clausen *et al.* 2002, Grau *et al.* 2005 and 2006, Nie *et al.* 2005, Plun-Favreau *et al.* 2007). The cellular localization of HtrAs is connected to extracytoplasmic compartments such as the periplasm in Gram-negative bacteria or membranes in Gram-positive organisms. In eukaryotes HtrA proteases were found in the extracellular matrix, mitochondria and chloroplasts (Huesgen *et al.* 2006, Zurawa-Janicka *et al.* 2007, Vande Walle *et al.* 2008).

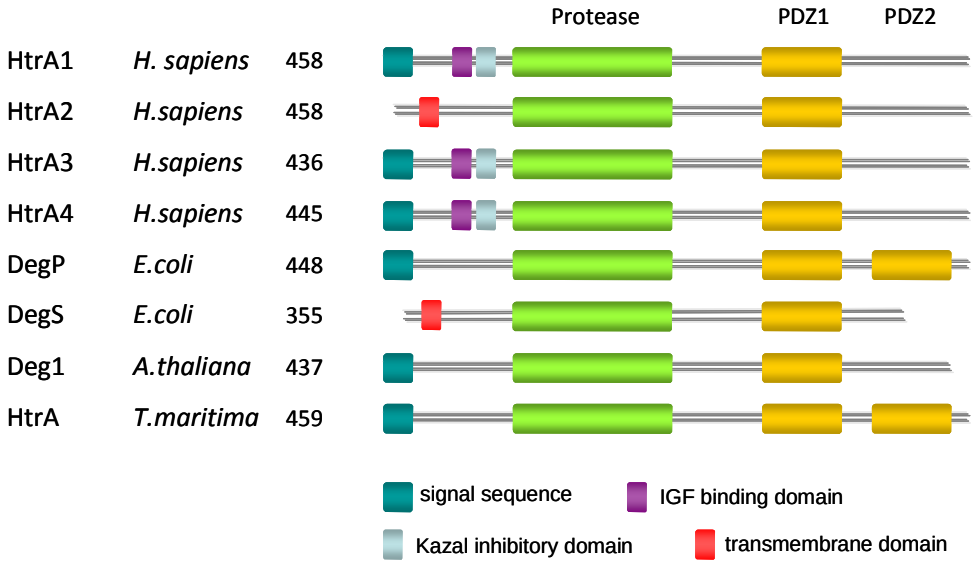

Fig. 1.5 Domain architecture of the HtrA family of serine proteases
Schematic representation of the domain organization of selected HtrAs. The protease domain is colored in green, PDZ1 and PDZ2 in orange. The N-terminal segments contain a signal sequences (olive), a transmembrane domain (red), an insulin-like growth factor (IGF) binding domain (violet) or a Kazal-like inhibitory domain (light blue). The amino acid lengths are indicated. Figure adapted from Clausen *et al.* 2002.

Another interesting feature of the HtrA proteins is that protease activity can be reversibly switched on and off by the novel mechanism of reversible zymogen activation (Ehrmann *et al.* 2004).

1.5.1 Family of bacterial HtrAs

Three HtrA proteins, DegP, DegQ and DegS, have been identified in *E. coli.* DegP and DegS have become well understood in the last years whereas DegQ is less well understood. DegP (also named HtrA or protease Do) was discovered more than 25 years ago, when Goldberg and co-workers systematically analysed the proteases in *E. coli* (Swamy *et al.* 1983). DegP is synthesized as a precursor protein with an N-terminal signal peptide that targets the protease to the periplasm (Pallen and Wren 1997). DegP was identified as a heat-shock protein and transcription of its gene is regulated by both σ_E and Cpx pathways in response to stress due to unfolded proteins in the cell envelope (Erickson and Gross 1989, Danese *et al.* 1995). Biochemical data shows that the protease recognizes denatured or unfolded proteins and that it exhibits strong preference for cleavage after small hydrophobic residues like valine or isoleucine (Kolmar *et al.* 1996). Based on these studies it was proposed that DegP degrades misfolded proteins in the periplasm reducing damage. DegP was furthermore shown to display chaperone activity additionally to its digestive properties (Spiess *et al.* 1999). The switch between these two functions is mediated by temperature: the chaperone activity is present at low temperatures (28°C) whereas the protease activity is most apparent at elevated temperatures (42°C) (Spiess *et al.* 1999). The large variety of substrates indicates that DegP is a key factor controlling protein fate in the cell envelope. Besides this physiological impact, DegP represents the first well-studied protein quality control factor that acts in an ATP-independent manner. Like DegP, DegQ is located in the periplasm of *E. coli* and shows similar substrate specificity as DegP (Kolmar *et al.* 1996). It is suggested to functionally substitute for DegP if it is over expressed in *E. coli* (Waller *et al.* 1996). That is supported by the fact that DegQ can complement the temperature sensitivity of *degP* null mutants (Waller *et al.* 1996).

DegS is homologous to DegP and DegQ but differs in substrate specificity, oligomeric state and function. DegS has an N-terminal transmembrane segment and is localized in the inner membrane of *E. coli*. It has a trimeric structure with the active sites surface exposed (Ades *et al.* 1999, Alba *et al.* 2002). In the latent state, the active site of DegS is present in an inactive conformation, in which substrate binding as well as catalysis is prevented (Wilken *et al.* 2004). After binding of stress peptides to its PDZ domains DegS is activated and cleaves the antisigma factor RseA at one specific position (Hasselblatt *et al.* 2007). Cleavage of RseA leads to the onset of a proteolytic cascade which causes the expression of several factors dealing with protein folding stress in the periplasm (Hasselblatt *et al.* 2007).

1.5.2 Family of human HtrAs

The mammalian HtrA family of serine proteases is, like the other family members defined by a characteristic trypsin-like serine protease domain and one or two C-terminal PDZ domains. Four mammalian HtrA proteins have been identified to date, HtrA1–4. In analogy to their bacterial homologues, it seems likely that the human HtrA proteases also function in protein quality control (Maurizi 2002, Gray *et al.* 2000). Protein quality control involves protein diagnosis, stress response, protein repair and degradation. The bacterial members of the HtrA family are involved in most of these tasks in the bacterial periplasm. A specific system for extracelluar stress response in mammals has yet to be identified and therefore the potential involvement of human HtrA proteases in protein quality control (Grau *et al.* 2005) represents an interesting target.

The four human family members can be divided into two groups mainly based on their domain architecture. HtrA2 possesses a transmembrane anchor and a large section of the N-terminus is removed during maturation. In contrast, the N-termini of HtrA1, 3 and 4 contain predicted signal sequences as well as domains that are known as insulin-like growth factor binding protein (IGFBP) and protease inhibitor domains (Fig. 1.5). Initial evidence suggests that stress response pathways might be involved in their regulation. HtrA1, 2 and 3 are better understood meanwhile and are discussed below. In contrast HtrA4 is not characterized so far.

1.5.3 HtrA1

HtrA1 (also called PRSS11) is a ubiquitously expressed serine protease which contains a signal sequence for secretion to the ECM, an insulin-like growth factor binding protein domain (IGFBP), and a Kazal-type serine protease inhibitor domain in addition to the serine protease domain and one C-terminal PDZ domain (Clausen *et al.* 2002).

The HtrA1 gene (PRSS11) was initially identified as being expressed in human fibroblasts but not after transformation with SV40 (simian virus) (Zumbrunn *et al.* 1996). Studies indicate that PRSS11 mRNA is either absent or significantly downregulated in several types of cancer e.g. in ovarian cancer (Shridhar *et al.* 2002, Chien *et al.* 2004), leukaemia, Burkitt's lymphoma (Nie *et al.* 2003), melanomas (Baldi *et al.* 2002) and mesotheliomas (Baldi *et al.* 2008). In addition, overexpression of HtrA1 inhibited proliferation *in vitro* and tumor growth *in vivo* (Baldi *et al.* 2002). These results suggest HtrA1 having a tumor suppressor function. A tumor suppressor phenotype of a protease would be novel as so far this function was mainly attributed to protease inhibitors.

HtrA1 was also shown to influence tumor response to chemotherapy by modulating chemotherapy-induced cytotoxicity. Downregulation of HtrA1 attenuated cisplatin- and paclitaxel-induced cytotoxicity, while forced expression of HtrA1 enhanced cisplatin- and paclitaxel-induced cytotoxicity (Chien *et al.* 2006). Therefore HtrA1 is suggested to be a potential prognostic factor to measure the success of chemotherapies (Chien *et al.* 2006).

HtrA1 expression is not induced by heat shock (in contrast to HtrA2) but could be regulated by a more general stress pathway. This notion is supported by upregulation of HtrA1 during osteo- (Hu *et al.* 1998, Chamberland *et al.* 2009) and rheumatoid arthritis (Grau *et al.* 2005), ageing (Ly *et al.* 2000) and Duchenne muscular dystrophy (Bakay *et al.* 2002). As a secreted protease, HtrA1 is likely to be involved in the degradation of extracellular matrix proteins, which could be important for both arthritis and tumor progression and invasion. Several recent reports describe e.g. the role of HrA1 in arthritis as HtrA1 contributes to degrading cartilage (Grau *et al.* 2006, Chamberland *et al.* 2009). Fibronectin from synovial liquids could be identified as a HtrA1 substrate and the treatment with HtrA1 leads to the expression of MMP1 and MMP3 implicating a role of HtrA1 in degradation of the ECM and that HtrA1 acts as a critical protease involved in proteoglycan turnover and cartilage degradation during degenerative joint disease (Grau *et al.* 2006). Recently it was shown by Chamberland *et al.* (2009) that aggrecan, a proteoglycan and major structural component of cartilage, is degraded by HtrA1 and that the proteoglycan content is dramatically reduced by HtrA1 overexpression. Furthermore a genetic variation at the HTRA1 gene promoter locus is associated with spinal disc degeneration, suggesting once more an involvement of the htrA1 gene in osteoarthritis (Urano *et al.* 2010).

HtrA1 is moreover degrading APP and APP-fragments like Aß and co-localizes with Aß plaques in the human brain (Grau *et al.* 2005) implicating a role of HtrA1 in Alzheimer´s disease.

The existence of a single nucleotide polymorphism (SNPs) in the promoter region of the htrA1 gene (rs11200638) is a major genetic risk factor for wet age-related macular degeneration (AMD) (Dewan *et al.* 2006, Yang *et al.* 2006). The wet form of AMD is characterized by the formation of new blood vessels beneath the retina and therefore the irreversible loss of vision. The allele with the SNP is associated with an increased mRNA- and protein expression of HtrA1 (Yang *et al.* 2006). Recently, recombinant HtrA1 was shown to cleave RPE (retinal pigmented epithelium) secreted proteins like clusterin and fibromodulin which are involved in the regulation of the complement pathway and like alpha 2 macroglobulin and ADAM9 which are involved in amyloid deposition (An *et al.* 2010).

There is also evidence that HtrA1 is involved in the TGFß signalling pathway. The expression of HtrA1 during mouse embryonic development is restricted to tissues which are depending on the pathway during differentiation. Furthermore it was shown that HtrA1 binds to several TGFß-family proteins

like Bmp4, Gdf5 or activin, inhibiting the signalling mediated by these factors (Oka *et al.* 2004). Patients with CARASIL (Cerebral Autosomal Recessive Arteriopathy with Subcortical Infarcts and Leukoencephalopathy) show mutations in the htrA1 gene which leads to the synthesis of a protein that is less active and (therefore) less potent to inhibit the TGFß signalling pathway (Hara *et al.* 2009). These facts support the role of HtrA1 in the TGFß signalling pathway.

During pregnancy the expression of HtrA1 is regulated dynamically displaying low expression levels in the first trimester and strong increased expression in the third trimester (De Luca *et al.* 2004). This expression pattern of HtrA1 in human placentas strongly implicates a role for HtrA1 in placental development and function. Moreover, on the basis of its subcellular distribution it was postulated that HtrA1 acts on different targets, such as intracellular growth factors or extracellular matrix proteins, to favor the correct formation and function of the placenta (De Luca *et al.* 2004).

HtrA1 was also shown to cleave IGFBP-5, a factor which binds to IGFI and II thereby regulating the amount of these growth factors (Hue *et al.* 2005). Factors that alter IGFBP affinity have the capacity to regulate IGF actions. So far, it is not understood how cleavage of IGFBP-5 by HtrA1 alters the activity of IGFBP-5.

Recently it was reported that human HtrA1 is a microtubule-associated protein and modulates microtubule stability and cell motility (Chien *et al.* 2009). It was shown that HtrA1 binds to microtubules via its PDZ domain, that is co-sediments with α- and ß-tubulin and that both proteins are a substrate for HtrA1 implicating a role in MT organization associated with cell migration (Chien *et al.* 2009).

1.5.4 HtrA2

In contrast to its paralogs HtrA1, 3 and 4, HtrA2/Omi contains a mitochondrial localization signal and is present in the mitochondrial intermembrane space (IMS). It is expressed as a 49-kDa proenzyme that is targeted to the mitochondrial IMS (Hedge *et al.* 2002, Martins *et al.* 2002) although a fraction of the endogenous HtrA2/Omi protein pool has been detected in the nucleus of resting cells (Martins *et al.* 2002, Gray *et al.* 2000, Kuninaka *et al.* 2007). HtrA2 is anchored via its transmembrane domain to the mitochondrial inner membrane, where it undergoes proteolytic maturation. The fully processed protein lacks the first 133 amino acids and exposes an N-terminal inhibitor of apoptosis protein (IAP)-binding motif (IBM). The motif is related to those found in the Drosophila IAP inhibitors Reaper, Hid and Grim and the mammalian IAP antagonist Smac/DIABLO (Hedge *et al.* 2002, Martins *et al.* 2002). If autodegradation or cleavage by another protease is required for maturation is still under discussion.

Protein levels of HtrA2 were shown to be upregulated several times after heat shock and after induction of the unfolded protein response induced by tunicamycin treatment (Gray *et al.* 2000).
Several reports describe a regulatory function of the processed form of HtrA2 in apoptosis, a process that is necessary to remove excess, damaged or infected cells (Hegde *et al.* 2002, Martins *et al.* 2002, Suzuki *et al.* 2001, Van Loo *et al.* 2002, Verhagen *et al.* 2002). Nuclear DNA damage, death receptor activation and numerous other apoptotic insults trigger the translocation of the mature protease into the cytosol, where it contributes to apoptosis through both caspase-dependent and -independent mechanisms. The substrates of HtrA2 are proteins involved in apoptosis as well as inhibitors of apoptosis (IAPs) (Suzuki *et al.* 2004, Hedge *et al.* 2002, Martins *et al.* 2002).
Evidence is present that HtrA2 is additionally involved in neurodegenerative disorders like Parkinson´s or Alzheimer´s disease. Two single nucleotide polymorphisms in the HtrA2/Omi gene cause missense mutations (A141S and G399S) and affect the enzymatic activity of the protease. They have been associated with the development of Parkinson's disease in humans (Strauss *et al.* 2005). It was furthermore shown that the proteolytic activity of HtrA2 is regulated by PINK, a kinase associated with Parkinson s disease (Plu-Favreau *et al.* 2007). Additionally, HtrA2 was identified in a yeast-two-hybrid screen to bind to presenilin-2 and cleaving APP, implicating a role for HtrA2 in Alzheimer´s disease (Gupta *et al.* 2004, Park *et al.* 2006). Recent studies indicate that HtrA2 interacts with different proteins to maintain homeostasis of mitochondria (Dagda *et al.* 2009).
The crystal structure of the maturated form of HtrA2 was solved in 2002 by Li *et al.* and is discussed in chapter 1.62.

1.5.5 HtrA3

HtrA3 shows 59% identity and 84% similarity to HtrA1 and shows the same domain architecture (Fig. 1.5). In addition, the expression profile of HtrA3 in embryonic mouse tissues is similar to the expression profile of HtrA1 (Oka *et al.* 2004) and as HtrA1, HtrA3 also binds to several TGFß-like proteins inhibiting the signalling of Bmp4 and Bmp2 (Oka *et al.* 2004). HtrA3 is as well capable of cleaving ß-casein and some ECM-proteoglycans (Tocharus *et al.* 2004). Together these facts suggest that HtrA3 and HtrA1 fullfil overlapping tasks and have similar functions.
The expression of HtrA3 is upregulated during development of mouse or human placenta (Nie *et al.* 2006), but the physiological role is not yet understood. Recent studies about the expression levels of HtrA3 in ovaries of rats implicate that the protease is important for the development of this organ as well as its differentiation (Bowden *et al.* 2009).

HtrA3 mRNA levels are downregulated during progression of endometrial cancer (Bowden *et al.* 2006). Thus, a decreased expression level of HtrA3 might be important for the development of cancer. Recent results suggest that similar to HtrA2, HtrA3 is located to the mitochondria and is released by treatment with drugs against lung cancer (Beleford *et al.* 2010). Thus, it is suggested to be a mitochondrial cell death factor whose serine protease function may be crucial to modulate etoposide- and cisplatin-induced cytotoxicity in lung cancer cell lines (Beleford *et al.* 2010).

1.6 Serine protease structures of the HtrA family

So far, five crystal structures are known for members of the HtrA family. These include the structure of human HtrA2/Omi (Li *et al.* 2002), the bacterial members DegP (Krojer *et al.* 2002, Krojer *et al.* 2008) and DegS (Wilken *et al.* 2004, Hasselblatt *et al.* 2007) and of HtrA from *M. tuberculosis* (Mohamedmohaideen *et al.* 2008). The structure of the protease domain of HtrA from *T. maritima* (Kim *et al.* 2003) and of the PDZ domain of human HtrA3 (Runyon *et al.* 2007) have been furthermore solved.

All known structures have in common that the functional unit appears to be a trimer, which is stabilised by residues of the protease domains. The protease domain adopts a chymotrypsin like fold with two antiparallel ß-barrels, each containing six ß-strands. The catalytic triad is composed of histidine, aspartate and serine. The PDZ domains are mobile elements; they act as molecular gatekeepers of the proteolytic chamber (DegP) or regulators of proteolytic activity (DegS, and HtrA2/Omi).

1.6.1 Crystal structures of bacterial DegP

Two crystal structures are available of DegP. The first crystal structure shows the protein in the inactive conformation. DegP is arranged as a hexamer composed of two stacked trimers forming an inner cavity (Fig. 1.6) (Krojer *et al.* 2002). The active sites of the protease are located in the inner cavity and are accessible only from the side (Fig. 1.6). The chamber is lined with hydrophobic patches that might constitute the substrate binding sites for non native polypeptides. The PDZ domains are highly flexible and form the side walls that restrict access to the active sites. In the same crystal two different conformations of DegP were found regarding the PDZ domains. In the so called ´open state´

they protrude outwards creating a lateral passage with a freely accessible inner cavity while in the ´closed state´ they close the entrances to the inner cavity (Fig. 1.6).

The fact that regarding the PDZ domains two conformations were found could imply the following roles for the PDZ domains. First they are responsible for substrate binding and second for the translocation of the substrate into the inner chamber (Clausen *et al.* 2002, Krojer *et al.* 2002). Although the PDZ domains do not mediate the essential hexameric interactions in the ´open state´, the PDZ2 domains have been demonstrated to be indispensable for the hexamer formation in solution (Sassoon *et al.* 1999, Iwanczyk *et al.* 2007).

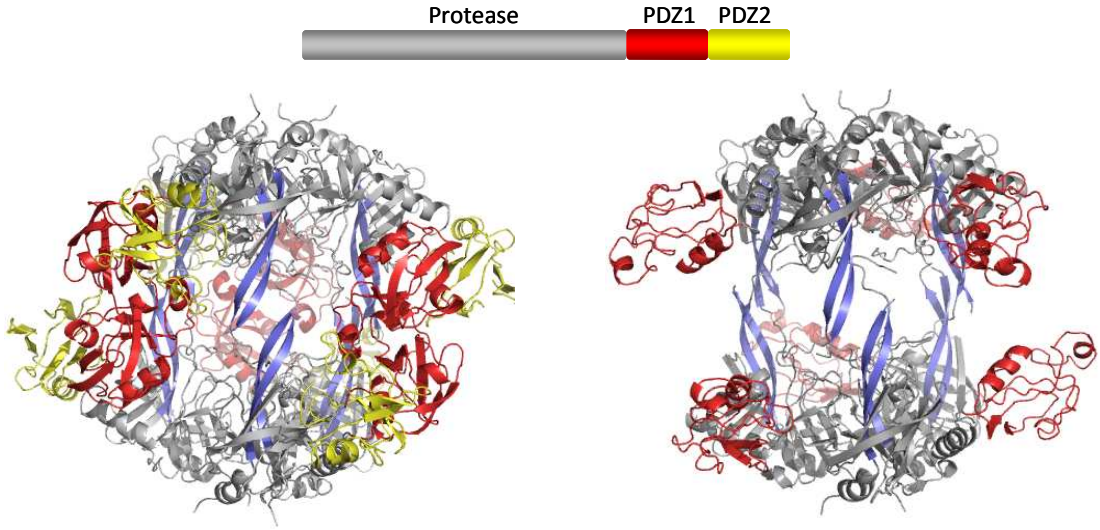

Fig. 1.6 Open and closed state of the DegP hexamer
Side view of DegP hexamer in two states: 'open state' (left) and 'closed state' (right). Trimeric rings of the protease domain (grey) are connected by 'loop LA pillars' by forming an inter-subunit β-sheet (blue). PDZ domains are depicted in red (PDZ1) and yellow (PDZ2). The PDZ2 domains of the 'open state´ were too flexible to be included in the model. The images of the structures were produced using PyMOL (DeLano 2002).

Dimerization of the two trimeric rings is mediated by the interactions between loops LA from opposite trimers protruding into the active sites of the opposite trimer (Fig. 1.7). Loop LA* interacts with the active site loops L1 and L2 thereby distorting the active site meaning that proper adjustment of the catalytic triad and formation of the oxyanion hole is prevented (Krojer *et al.* 2002). In summary the hexameric structure of DegP shows a proteolytically inactive conformation and could thus represent a resting state of the protease/chaperone.

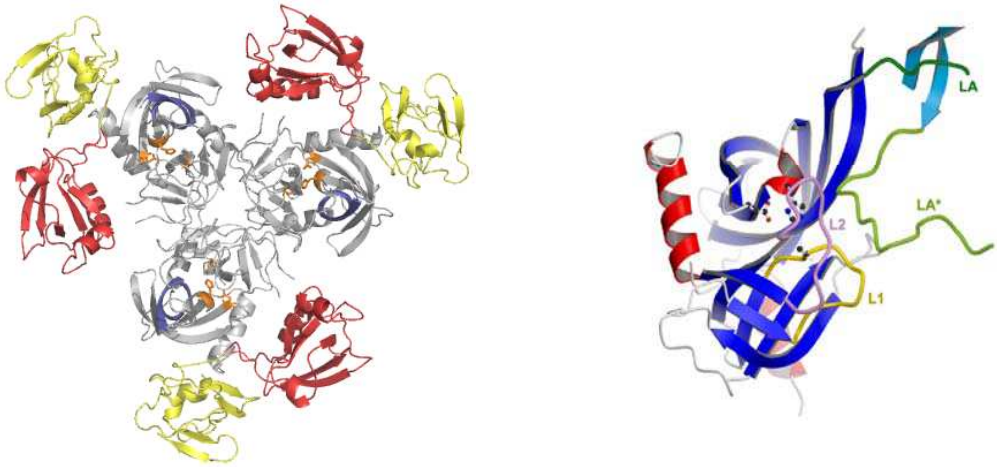

Fig. 1.7 DegP hexamer in the inactive conformation
Loop LA (LA*) protrudes into the active site of the opposite monomer and distorts the conformation of the active site loops L1 and L2. Active site residues are depicted in ball and stick representation. An inactive Ser210Ala mutant was used for crystallization. PDB entry code for DegP: 1ky9 (Krojer, Garrido-Franco *et al.* 2002). The images of the structures were produced using PyMOL (DeLano 2002).

Upon substrate binding DegP transforms from a hexamer into 12-meric and 24-meric multimers which show the catalytically active conformation (Krojer *et al.* 2008). In the crystal structure of the DegP 24mer (Krojer *et al.* 2008) eight trimers are located at the vertices of an octahedron. Figure 1.8 shows the overall structure of the DegP 24mer. In contrast to the structure of the DegP hexamer both PDZ domains are well defined and part of the model. The 24mer has a molecular mass of 1.13 MDa with an impressive cavity volume roughly 8-fold that of the bacterial chaperone GroEL (Krojer *et al.* 2008).

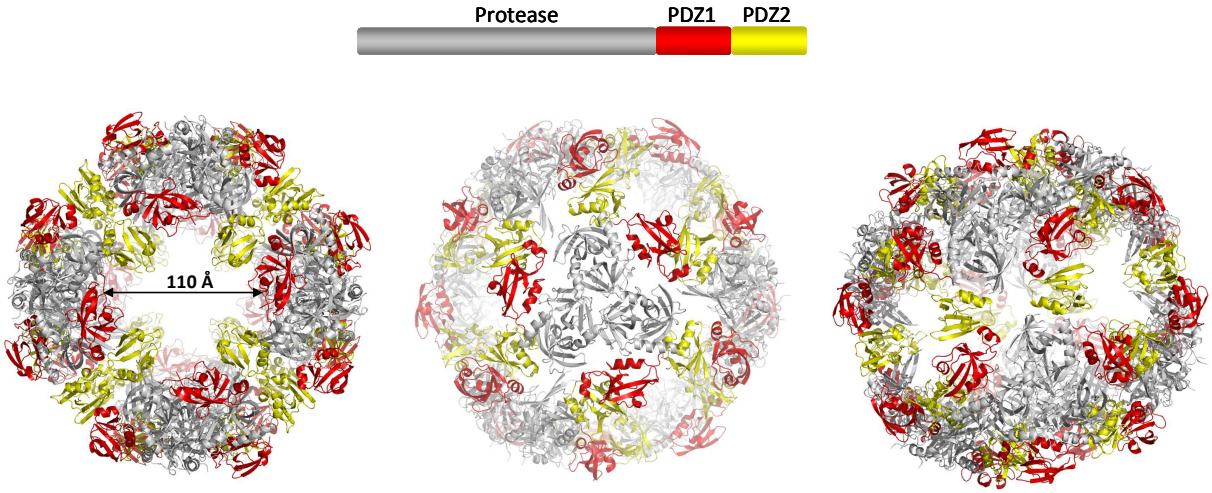

Fig. 1.8 Overall structure of the DegP 24mer
The DegP 24mer is shown in three different orientations along the molecular four-fold, three-fold and two-fold axes. The inner cavity has a diameter of 110 Å. PDZ domain1 is coloured in red, PDZ domain 2 in yellow. PDB entry code for DegP: 3cs0. The images of the structures were produced using PyMOL (DeLano 2002) and adapted from Krojer *et al.* 2008.

These data indicate that by transforming from the hexamer into the 24mer the enzyme transforms from the inactive into the active conformation. Loop LA, which in the inactive conformation interacts with the active site of the neighbouring monomer and therefore distorts the active site by interacting

with loops L1 and L2, is now extracted and loop L1 and L2 are oriented to set up a functional proteolytic side (Fig.1.9) Therefore it has been suggested that the conversion from hexameric into higher oligomeric species is crucial for regulating the protease activity (Krojer *et al.* 2008).

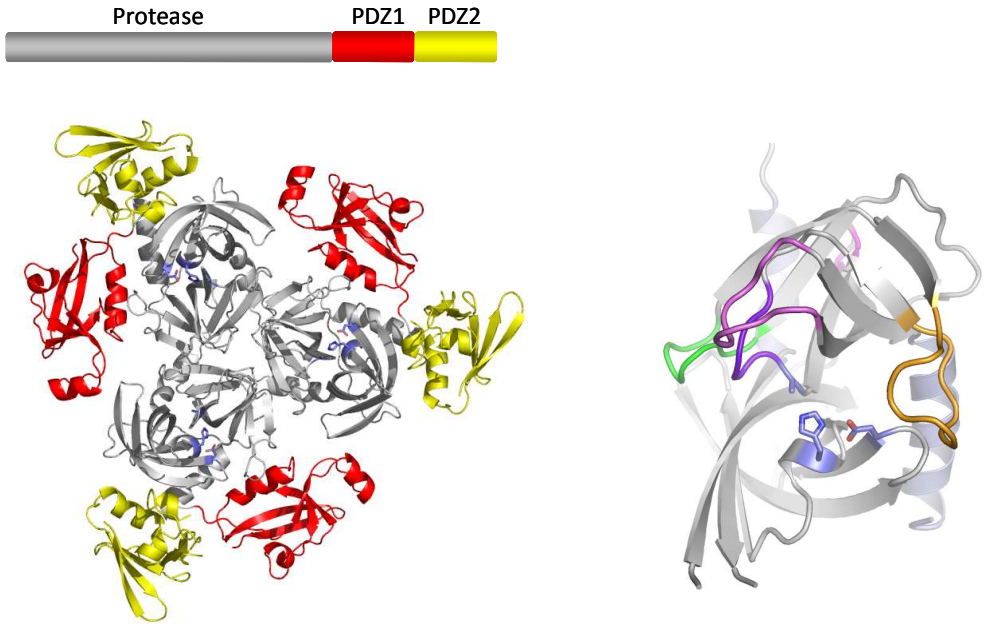

Fig. 1.9 Conversion from the inactive into the active conformation in DegP24mer
Active site residues are depicted in ball and stick representation. An inactive Ser210Ala mutant was used for crystallization. PDB entry code for DegP: 3cs0 (Krojer *et al.* 2008). Catalytically important loops are coloured in blue loop L1, in magenta loop L2, in orange loop L3 and in greed loop LD. The images of the structures were produced using PyMOL (DeLano 2002).

In the structure of the 24mer (and the EM structure of the 12mer) additional density was found in the inner cavity. Further analysis of DegP oligomers identified this density as folded outer-membrane proteins like OmpA, OmpC and OmpF. Thus it can be concluded that the inner cavity serves antagonistic functions. The encapsulation of folded outer-membrane proteins protects these proteins from degradation in the periplasm and might be necessary to safely transfer them to their destination in the outer membrane of *E. coli* (Krojer *et al.* 2008). In contrast, misfolded proteins are degraded in the inner cavity. It was proposed that the mechanism of oligomerization upon substrate binding could also be true for the regulation of other HtrA family proteases.

1.6.2 Crystal structure of human HtrA2

The only known crystal structure of a human family member is the one of HtrA2/Omi (Li *et al.* 2002). The structure was solved for the inactive (serine to alanine mutation) mature protein lacking the 133 N-terminal residues. As the basic building block of all family members is the trimer, also HtrA2 forms a pyramide shaped homotrimer. Contacts between the monomers are mediated exclusively by the protease domain (Li *et al.* 2002) (Fig. 1.10).

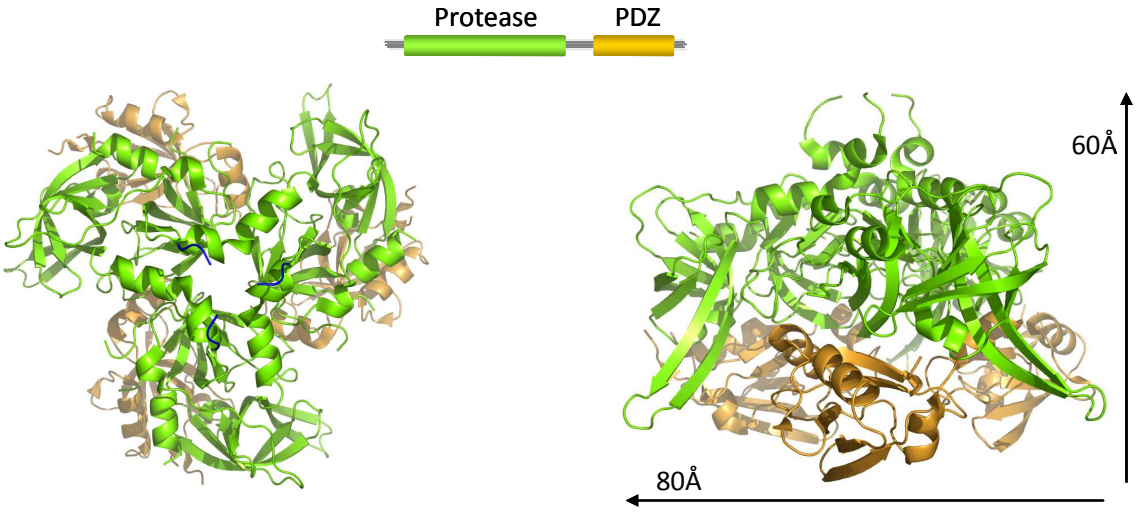

Fig. 1.10 Crystal structure of human HtrA2/Omi
The HtrA2/Omi forms a homotrimer, which is viewed along (left) or perpendicular to (right) the three-fold symmetry axis. Trimerization is mediated exclusively by the serine protease domain. On top of the trimer at the N-terminus the IAP (inhibitor of apoptosis-binding tetrapeptide) motif is shown. The PDZ domains are located opposite at the base. Figure was produced using PyMOL and adapted from Li *et al.* 2002.

Unlike the other structures of bacterial DegP hexamer or DegS, the PDZ domains of HtrA2 do not protrude outwards, but are located on top of the protease domain thereby restricting access to the active site. It has been proposed that the PDZ domains regulate protease activity and modulate HtrA2-mediated cell death activity (Li *et al.* 2002). Figure 1.11 shows a proposed working model for HtrA2.

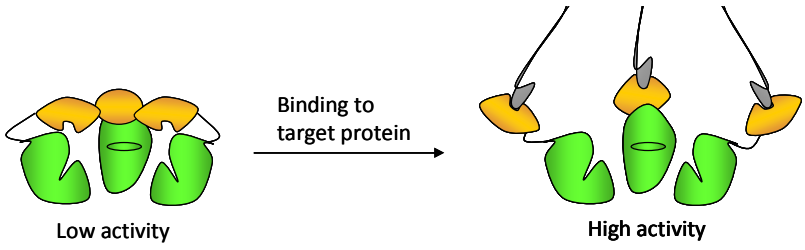

Fig. 1.11 Activation of HtrA2
Activation of HtrA2 is proposed to proceed by binding of a trimeric ligand to the PDZ domains. In the basal state the PDZ domains restrict access to the active site resulting in a low activity of HtrA2/Omi. Upon binding of the ligand the PDZ domains protrude outwards, opening up the active site an allowing entrance for substrates. HtrA2/Omi probably targets trimeric ligands such as the DISC because it functions as a homotrimer. Picture adapted from Li *et al.* 2002.

2 Aims

The HtrA (high temperature requirement) family represents a new class of oligomeric serine proteases in which a catalytic domain is combined with one or more C-terminal PDZ (protein-protein interaction) domains. These proteins are widely conserved and found in most organisms from bacteria to mammals. The biological implications of only some bacterial HtrAs are known while the human HtrAs are not well characterised and their precise functions are not understood in detail.

In this thesis, studies should be performed to obtain an understanding of the structural properties of HtrA1 and the regulation of its proteolytic activity.

To access the structural properties of HtrA1 different deletion contructs of the proteolytic active and inactive form of HtrA1 were applied for crystallization. Crystallization and subsequent structure solution consist of several consecutive steps, beginning with the establishment of an efficient and reproducible protein purification procedure. After purification, the protein can be characterized by N-terminal sequencing, mass spectrometry, size-exclusion chromatography and dynamic light scattering in order to detect any unwanted post-translational modifications, to elucidate the molecular weight of the oligomer in solution and the homogeneity of the sample. The crystallization of the protein can be performed by employing the widely used sparse-matrix screening methods. After production of diffraction quality crystals, the crystal structure of HtrA1 can be solved by molecular replacement (MR). With the crystal structure of HtrA1, it should be possible to elucidate the organization of the oligomer, the structural determinants of the active site and the role of the PDZ domains.

In the second part of the study, the development of an activity assay and the measurement of enzymatic activity of different deletion constructs is the main focus. Furthermore it shall be tried to find inhibitors, peptides and substrates to characterize their interaction with HtrA1 and to co-crystallize them with HtrA1 in order to specify the regulations of enzymatic activity.

3 Materials and Methods

3.1 Materials

3.1.1 Chemicals and their suppliers

antibiotics	Sigma
crystallization kits	Hampton Research
Ni-NTA-agarose	Qiagen
Superdex-200	PHARMACIA
further chemicals	Merck, Fluka, Serva, Sigma

3.1.2 Bacterial strains

Tab. 3.1 Bacterial strains

Strain	Genotype	Origin
DH5α	F-, supE44, ΔlacU169, [Φ80lacZΔM15], hsdR17, recA1, endA1, gyrA96, thi-1, (res-, mod+), deoR (Hanahan 1983)	
CLC 198	MC4100 *degP*::Tn*10*	
One Shot® Chemically Competent *E. coli* Mach1	F^- ϕ80(*lac*Z)ΔM15 Δ*lac*X74 *hsd*R($r_K^- m_K^+$) Δ*rec*A1398 *end*A1 *ton*A nupG	**Invitrogen**
BL21 (DE3) (RIL)	F^- *ompT hsdS*$_B$(r_B^- m_B^-) *gal dcm* (DE3)	**Novagen**

BL21-CodonPlus (DE3)-RIL	*E. coli* F^- *ompT hsdS*$_B$(r_B^- m_B^-) *dcm*$^+$ Tet^r *gal* λ (DE3) *endA* The [*argU ileY leuW* Cam^R)	**Stratagene**
BL21 (DE3) Rosetta	F^- *ompT hsdS*$_B$(r_B^- m_B^-) *gal dcm* (DE3) pRARE[1] (Cam^R)	**Novagen**
BL21 (DE3) Origami B	F^- *ompT hsdS*$_B$(r_B^- m_B^-) *gal dcm lacY1 ahpC gor522::* Tn*10 trxB* (Kan^R, Tet^R)	**Novagen**
B834	F^- *ompT hsdS*$_B$(r_B^- m_B^-) *gal dcm met*	**Novagen**

1 pRARE contains the tRNA genes *argU, argW, ileX, glyT, leuW, proL, metT, thrT,tyrU, and thrU.* The rare codons AGG, AGA, AUA, CUA, CCC, and GGA are supplemented.

3.1.3 Plasmids and vectors

Tab. 3.2 Plasmids

Name	Genotype	Reference / source	Resistence
pCS20	pQE60 derivative with *lac IQ*, *degP* (C-terminal His_6-tag)	(Spiess *et al.* , 1999)	amp
pET 21d	pBR322 derivative	Novagen	amp
pET 26b	pBR322 derivative	Novagen	kan
pCS21	pQE60 derivative with *lac IQ*, $degP_{S210A}$ (C-terminal His_6-tag)	(Spiess *et al.*1999)	amp
pET32a	pBR322 derivative	Novagen	amp

3.1.4 Oligonucleotides for Cloning

All oligonucleotides were synthesized by Life Technologies.

Tab. 3.3 Nucleotides for Cloning

Name	Nucelotidsequence 5´- 3´
Cloning in pET 21d	
Fw: LT_HtrA1_Helix1_NcoI	**CATGCCATGGGGCAGGAAGATCCCAACAGTTTGCGCCATAA**
LT_HtrA1_Helix2_NcoI	**CATGCCATGGCAAAATATAACTTTATCGCGGACGTGGTGGA**
LT_HtrA1_SC_NcoI	**CATGCCATGGCACTGCAGCGCGGAGCCTGCGGCCAA**
Cloning in pET 21d and pET 26b	
LT_HtrA1_dSS_4_NcoI	**CATG CCATGGCG CAG CTG TCC CGG GCC GGC CGC**
LT_deltamacHtrA1_XhoI	**CCG CTCGAGAGA TCT TGG GTC AAT TTC TTC GGG**
LT_HtrA1_Kazal_1_XhoI	**CCG CTCGAGTTG GCC GCA GGC TCC GCG CTG CAG GAC**
LT_HtrA1_Kazal_2_XhoI	**CCG CTCGAGCTG CCC TTG GCC GCA GGC TCC GCG**
LT_HtrA1_dSS_SG_NcoI	**CATGCCATGGCACAGCTGTCCCGGGCCGGCCGCTCG**
LT_HtrA1_Kazalonly_NcoI	**CATG CCATGGTGCGG CGG CGC GCG CAG GCC GGC**
LT_HtrA1_IGFBPonly_XhoI	**CCG CTCGAGCGTGGCCGAGGCTGGCACCCCGAA GGG**
Cloning in pET 21d with Strep-tag	
LT_deltamacHtrA1_Strep (NotI)	**ATAAGAAT GCGGCCGC TTA TTTTTCGAACTGCGGGTGGCT CCAAGCGCT (Strep) TGG GTC AAT TTC TTC GGG AAT CAC**
LT_HtrA1_Kazal_2_Strep (NotI)	**ATAAGAATGCGGCCGC TTA TTTTTCGAACTGCGGGTGGCTC CAAGCGCT (Strep) CTG CCC TTG GCC GCA GGC TCC GCG**
Cloning in pET32a as Trx-fusion	
LT_HtrA1_ KpnI_Prec	**CGG GGT ACC CTGGAAGTTCTGTTCCAGGGGCCC (Precs.) GATTCTGAGATG GCGCAGCTGTCCCGGGCCGGCCGC**
LT_deltamacHtrA1_BamHI	**GGAGGA GGATCC AGATCTTGGGTCAATTTCTTCGGG**
LT_deltamacHtrA1_BamHI_stop	**GGACGC GGATCC TTAAGATCTTGGGTCAATTTCTTCGGG**

LT_deltamacHtrA1_BamHI_corr	**GGACGC GGATCC TGGGTCAATTTCTTCGGGAATCAC**
LT_HtrA1_Kazal2_BamHI	**GGA CGC GGATCC CTG CCC TTG GCC GCA GGC TCC GCG**
LT_HtrA1_Kazal2_BamHI_stop	**GGA CGC GGATCC TTA CTG CCC TTG GCCGCAGGC TCCGCG**
LT_deltamacHtrA1_XhoI_stop	**CCG CTCGAG TTA AGA TCT TGG GTC AAT TTC TTC GGG**
LT_HtrA1_Kazal_2_XhoI_stop	**CCG CTCGAG TTA CTG CCC TTG GCC GCA GGC TCC GCG**
Cloning in PDDII83 (Gal – TEV - myc vector) for yeast expression	
LT_Fw_Yeast_BamHI	**GGA CGC GGATCC ATG GCG CAGCTGTCCCGGGCCGGC CGC**
LT_ FL_Yeast_NotI	**ATAAGAAT GCGGCCGC TGGGTCAATTTCTTC GGGAATCAC**
LT_ Kazal2_Yeast_NotI	**ATAAGAATGCGGCCGC CTG CCC TTG GCC GCAGGCTCC GCG**
LT_ FL_Yeast_His_NotI	**ATAAGAAT GCGGCCGC TTA GTGGTGGTGGTGGTGGTG (His-Tag) TGGGTCAATTTCTTC GGGAATCAC**
LT_ Kazal2_Yeast_His_NotI	**ATAAGAAT GCGGCCGC TTA GTGGTGGTGGTGGTGGTG (His-Tag) CCC TTG GCC GCA GGC TCC GCG**
Cloning in pET 21d with SUMO-taq	
LT_HtrA1_dSS_4_NcoI	**CATG CCATGG CG CAG CTG TCC CGG GCC GGC CGC**
LT_deltamacHtrA1_BamHI_stop	**GGA CGC GGATCC TTA AGA TCT TGG GTC AATTTCTTC GGG**
LT_HtrA1_Kazal2_BamHI_stop	**GGA CGC GGATCC TTA CTG CCC TTG GCCGCAGGCTCC GCG**

3.1.5 Media

LB (Luria Bertani) medium:
10 g Bacto-tryptone
5 g Yeast extract
10 g NaCl
made up to 1 l with H_2O and autoclaved

LB (Luria Bertani) Agar:
1 l LB medium
15 g Agar

NM-medium:

740 ml H_2O
100 ml 10x salts
100 ml 10x amino acids
60 ml 1 mg/ml seleno-DL-methionine
autoclave H_2O, then add the other sterile filtered components

10x salts:

1 M $(NH_4)_2SO_4$	75 ml
5 M NaCl	17 ml
1 M $MgSO_4$	10 ml
1 M Glucose	200 ml
1 mg/ml $CaSO_4$ x $2H_2O$	10 ml
Trace elements	10 ml
10 mg/ml Thiamine	10 ml
10 mg/ml Biotine	10 ml
$FeNH_4(SO_4)_2$ x $6H_2O$	1 ml (add before use)
H_2O	65 ml

Trace elements:

10 mg/ml $MnCl_2$	5 µl
10 mg/ml $CuSO_4$ x $5H_2O$	5 µl
10 mg/ml Na_2MoO_4	5 µl
10 mg/ml $ZnSO_4$	5 µl
made up to 50 ml with H_2O	

10x amino acids:

H_2O	274 ml
1M K_2HPO_4	476 ml
1M KH_2PO_4	220 ml
Alanine	0.5 g
Arginine	0.5 g
Aspartate	0.5 g
Aspartic acid	0.5 g
Cysteine	0.5 g
Glutamic acid	0.5 g

	Glutamate	0.5 g
	Glycine	0.5 g
	Histidine	0.5 g
	Isoleucine	0.5 g
	Leucine	0.5 g
	Lysine	0.5 g
	Proline	0.5 g
	Serine	0.5 g
	Threonine	0.5 g
	Valine	0.5 g
Amino acids II:	H_2O	28.5 ml
	Phenylalanine	0.5 g
	Tryptophan	0.5 g
	Tyrosine	0.5 g
	32% (v/v) HCl	1.5 ml

3.1.6 Antibiotics

Ampicillin: 50 mg/ml in H_2O stock solution, stored at -20°C

Kanamycin: 50 mg/ml in H_2O stock solution, stored at -20°C

Tetracyclin: 50 mg/ml in H_2O stock solution, stored at -20°C

3.1.7 Proteins and enzymes

Tab. 3.4 Proteins and Enzymes for Cloning

Protein/Enzyme	Origin
BSA (Bovine serum albumin)	Sigma-Aldrich, München
DNAseI	Sigma-Aldrich, München
CIP	NEB
T4 Ligase	Roche
Herculase	Roche

Phusion High Fidelity Polymerase	Finnzymes, NEB, Ipswich, MA, USA
Restriction enzymes	NEB, Ipswich, MA, USA

3.1.8 Protein and nucleic acid standards

Tab. 3.5 Protein- and Nucleic Acid Standards for SDS-PAGE and Agarosegels

Standard	Company
FPLC Gelfiltration LMW&HMW Standard	Bio-Rad, München
BSA (Rinderserumalbumin)	Sigma-Aldrich, München
Prestained SDS-PAGE Standard	Bio-Rad, München
Unstained SDS-PAGE Standard	Bio-Rad, München
Quick-Load 2-Log DNA Ladder	NEB, Ipswich MA, USA

3.2 Methods

3.2.1 Microbiological methods

3.2.1.1 *Sterilisation*

Media and solutions were sterilised by autoclaving. In the course of this, they were heated to 120°C with a pressure of 1 bar for 20 min. Heat sensitive solutions were sterile filtered with a 0.22 µm filter (Millipore).

3.2.1.2 *Growth conditions*

Liquid cultures were grown in Erlenmeyer flasks of appropriate size. In order to improve the oxygen supply, the flasks contained chicanes. The flasks were shaken at 180 rpm and incubated at a temperature of approx. 37°C. Recombinant ΔN-HtrA1 and HtrA1-prot (wild type and S328A mutant) were expressed in *E. coli* BL21 (DE3) cells. Full length HtrA1 and NT-HtrA1 were expressed in *E. coli* Origami B cells (Novagen). All proteins contained a C-terminal His_6-tag, the full length and NT-HtrA1 protein additionally an N-terminal TrxA-tag and a His_6-tag. The cells were grown in LB-medium with 50 µg/ml ampicillin at 37°C until they reached an OD_{600} of 0.8 to 1.0 followed by induction with 500 µM IPTG. Cells with full length protein or the N-terminal domain were grown for 3 hrs at 37°C, cells

with other constructs for 16 hrs at 28°C. *E. coli* B834 cells were used for the expression of ΔN-HtrA1(SeMet) and treated the same way.

3.2.1.3 *Determination of the cell density in liquid cultures*

The cell density of liquid cultures was determined by measurement of the optical density in a photometer at a wavelength of 600 nm. LB media was used as a blank.

3.2.1.4 *Polymerase chain reaction (PCR)*

To PCR amplify DNA fragments (Mullis *et al.* 1992) an initial denaturation step at 95°C for 5 min, followed by 35 cycles of 10 sec denaturation, 20 sec annealing at 55°C to 60°C and 44 sec extension at 72°C was performed. Finally the reaction was heated to 72°C for 10 min and then cooled to 4°C. A typical pipetting scheme is given below (Tab. 3.6).

Tab. 3.6 Pipetting scheme for PCR reaction

Volume [µl]	Component
5	10x Herculase buffer
5	dNTPs (jeweils 10 mM)
0.5	*Primer forward* (10 µM)
0.5	*Primer reverse* (10 µM)
0.5	Herculase
5	DMSO
0.5	*Template*
ad 50 µl	H_2O

DMSO was used in every PCR reaction as the GC-rich region of the *htrA1* gene had the potential to form secondary structures which could be relaxed by DMSO. The results of the PCR reaction were checked by agarose gel electrophoresis (3.2.1.6).

3.2.1.5 *Colony PCR*

To select for positive clons after transformation a colony PCR was performed. Per plate 3 to 5 colonies were picked with a sterile pipette tip and directly pipette into a prepared PCR mixture.

Tab. 3.7 Colony PCR pipetting scheme

Volume [µl]	Component
2.5	10x Thermo Pol-Puffer
0.3	dNTP (10 mM each)
0.5	*Primer forward* (10 µM)
0.5	*Primer reverse* (10 µM)
2.5	DMSO
0.5	*Taq*-Polymerase
ad 25 µl	H_2O

PCR-program:

1.	94°C	2 min	
2.	94°C	15 s	40 cycles
3.	55°C	15 s	
4.	72°C	45 s	
5.	72°C	5 min	

For analysis of PCR products 5 µl are loaded to an agarose gel (3.2.1.6) to identify positive clons for plasmid mini preps (3.2.1.12).

3.2.1.6 *Agarose gel electrophoresis*

Agarose gel electrophoresis was employed to separate double-stranded DNA molecules according to their molecular mass after restriction enzyme digestion and to quickly determine the yield and purity of a DNA isolation or PCR reaction. The agarose concentration of the gel depends on the various sizes of the separating DNA fragments to be visualized; generally a 1% (w/v) solution was used. The agarose was dissolved in 1x TAE by heating in a microwave oven. Ethidium bromide was added to enable fluorescent visualization of the DNA fragments under UV light and the cooled (approx. 50°C) gel was poured into a gel casting form containing the gel comb. After cooling down, 1x TAE electrophoresis buffer was added to the buffer reservoirs until the gel was covered. The samples (1–20 µl) were mixed with 1/10 of their volume with DNA loading buffer and subjected to electrophoresis for one hour at 70 V. Additionally, a DNA size-marker (Lambda Eco/Hind III) was co-electrophoresed with the DNA samples to identify fragments between 500–22,000 bp. After electrophoresis, the DNA-intercalated ethidium bromide was detected under UV light at 302 nm.

50x TAE-Puffer:	50 mM EDTA 2 M Tris-Acetat, pH 8.0
6x DNA-Probenpuffer:	30% (v/v) glycine 0.25% (w/v) bromophenol blue 0.025% (w/v) xylencyanole

3.2.1.7 *DNA isolation from agarose gels*

DNA gel extraction and PCR purification protocols were performed as described in "QIAquick Spin Handbook" using a microcentrifuge (July 2002), applying the QIAquick Gel Extraction Kit and QIAquick PCR Purification Kit. The purified DNA was eluted in 30–50 µl 1xTE buffer.

3.2.1.8 *Determination of DNA concentration*

The absorbance of the DNA samples at 260 nm was measured with a micro-volume UV-Vis spectrophotometer (Nanodrop 2000) and the concentration was calculated according to the Lambert Beer Law. The ratio of absorptions at 260 nm versus 280 nm is used to assess the purity of the sample with respect to protein contamination, since protein (in particular, the aromatic amino acids) tends to absorb at 280nm. Absorption at 230 nm can be caused by contamination by phenolate ion, thiocyanates, and other organic compounds. For a pure nucleic acid sample, the 260:230 ratio should be around 2.

3.2.1.9 *Restriction enzyme digestion, dephosphorylation, ligation*

Restriction digests were performed using the supplied buffers at recommended temperatures (Fermentas). Typically, 1-2 units of enzyme were used per 1 µg of DNA. To prepare the vectors for cloning, they were digested as described above. To avoid self-ligation and increase ligation efficiency, 15 U calf intestinal phosphatase (CIP) was added for 1 h at 37°C to remove 5' phosphates of cut vector. After successful restriction digestion of the insert and the vector, both were purified by gel extraction (Gel Extraction Kit, Qiagen). To perform ligation insert and vector were mixed in a 3:1 ratio, respectively. The reaction mix was incubated with 1 U T4 DNA ligase in the appropriate 10x buffer at 20°C for 2 hrs or left overnight at 4°C. DH5α cells were transformed and plated out for selection on LB plates.

3.2.1.10 *Production of chemically competent E. coli cells*

Chemically competent B834 and Origami B cells were prepared using the following protocol. LB media containing the appropriate antibiotics was inoculated with a single colony and grown over night at 37°C. 50 ml LB media was inoculated the next day to an OD_{600} of 0.1 and grown till an OD_{600} of 0.5. Cells were incubated 15 min on ice and centrifuged for 15 min at 4°C in a 50 ml falcon tube. The pellet was carefully resuspended in 1/3 cold RF I solution, incubated on ice for 15 min. and again centrifuged for 15 min at 4°C. Subsequently the pellet was resuspended in 1/12 RF II, incubated 15 min on ice, aliquoted and frozen in liquid nitrogen. The cells were stored at -80°C.

RF I: 100 mM RbCl, 50 mM $MnCl_2$, 10 mM $CaCl_2$, 30 mM potassium acetate, 15% glycerin, pH adjusted to 5.8 with acetic acid

RF II: 10 mM MOPS, 10 mM RbCl, 75 mM $CaCl_2$, 15% glycerin
pH adjusted to 6.8 with NaOH

3.2.1.11 *Transformation of chemically competent E. coli cells*

The plasmids were cloned into DH5α cells during the cloning and selection procedures, whereas supercompetent BL21 (DE3) and Origami B cells were transformed for overexpression. Aliquots of cells (100 µl DH5α; 50 µl BL21 Star (DE3), 25 µl Origami B cells) were transformed with 1 µl of plasmid DNA and incubated on ice for 20 min before exposure to 42°C for 90 sec. After incubation for 1 min on ice 1 ml LB medium was added to the cells were incubated at 37°C for 1 h on a shaker (1200 rpm). Afterwards, they were either transferred into liquid LB media or plated on LB selective media containing the appropriate antibiotic and grown overnight at 37°C.

3.2.1.12 *Plasmid isolation*

Two different plasmid purification kits were employed. For low scale plasmid preparation, used for identifying colonies containing the correct plasmid, the Plasmid Mini kit (Qiagen) was used. After sequencing larger amounts of plasmid DNA of positive clons was needed for transformation, therefore plasmid purification was done using Plasmid Midi kit (Qiagen). For minipreps 5 ml, for midipreps 100 ml of LB media, containing 50 µg/ml ampicillin for selection was inoculated with a single bacterial colony of ampicillin resistant *E. coli* and incubated overnight at 37°C. Grown cells

were harvested by centrifugation (4000 rpm in Heraeus Multifuge 4 KR, 15 min for minipreps; 25 min for midipreps) and afterwards purified following the manufacturer‘s instructions according to the alkaline lysis method. Purified DNA was eluted in 50 µl TE buffer for minipreps and 200 µl TE buffer for midipreps. For storage the plasmid DNA was frozen at -20°C. For the determination of the yield of purified midiprep DNA the sample was 1:50 diluted and the concentration was measured by UV spectrophotometry at 260 nm (Ultrospec 3300 pro, Amersham Biosciences). The quality of the DNA was determined by calculating the ratio of the optical density at 260 nm and 280 nm.

3.2.1.13 *Cloning of full length HtrA1 and NT-HtrA1*

Full length protein and the N-terminus of HtrA1 (NT-HtrA1, residues 22 – 159) lacking the signal sequence (residues 1-21) were cloned in fusion with a thioredoxin A-tag (TrxA-tag) to support proper folding of HtrA1 which contains 18 cysteines in the N-terminal domain. TrxA contains in its active center a disulfide bond … The protein was cloned into a pET32a vector (Novagen) which provides the possibility to express the protein of interest in fusion with TrxA. The vector contains cleavage sites to cleave the tag with factor Xa and TEV. Instead HtrA1 was cloned with a PreScission cleavage site which was inserted by PCR with the forward primer. PreScission protease is described to be more efficient and more importantly does not require DTT for activity as e.g. TEV. In addition PreScission is a cysteine protease and therefore any impurity would not interfere in activity assays. HtrA1 was PCR amplified from pSG 7 and pSG 13 (SA mutant) and restriction sites for *Kpn*I and *Xho*I were introduced by PCR as well as the PreScission cleavage site. The Tag is fused N-terminal and contains itself a C-terminal His_6 tag. HtrA1 was cloned either in frame or out of frame with a C-terminal His_6-tag provided by the vector.

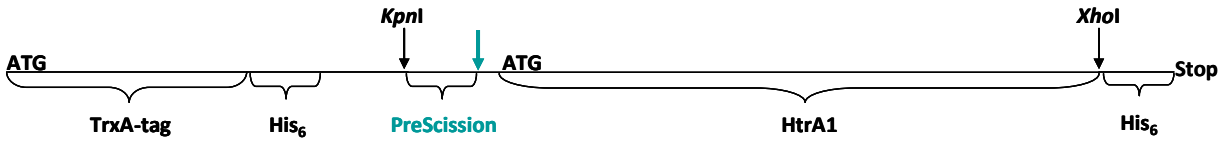

Fig. 3.1 Cloning strategy for full length HtrA1 in pET32a
PET32a provides a TrxA-tag in frame with an C-terminal His-tag. Via PCR the gene of interest is amplified introducing a C-terminal *Kpn*I and a PreScission cleavage site and a N-terminal *Xho*I cleavage site. The PCR product is subsequently cloned into pET32a in frame with the TrxA-tag and a second N-terminal His-tag.

3.2.2 Biochemical methods

3.2.2.1 *SDS polyacrylamide gel electrophoresis (SDS-PAGE)*

SDS-PAGE was used for the electrophoretic separation of proteins according to the method of Laemmli (Laemmli, 1970). The stacking and the separating gel were prepared as described below (table 3.8). Gels were poured in an apparatus for 8 minigels. The protein samples were mixed with 5 µl of 2x sample buffer, boiled for 5 min and loaded onto the gel. The electrophoresis was performed at 110 to 200 V for about 60 min. Afterwards the gel could either be blotted (3.2.2.4) or stained with Coomassie brilliant blue (3.2.2.2).

Tab. 3.8 Composition of polyacrylamid gels

component	separating gel (12.5%)	stacking gel (5%)
buffer A	37.5 ml	-
buffer B	-	2.5 ml
acrylamide stock	40 ml	8.3 ml
H_2O	21 ml	38.4 ml
10% (w/v) SDS	1 ml	0.5 ml
TEMED	80 µl	40 µl
10% (w/v) APS	800 µl	400 µl

Buffer A: 1 M Tris/HCl pH 8.8

Buffer B: 2.5 M Tris/HCl pH 6.8

Acrylamide stock: 30% (w/v) Acrylamide 0.8% (w/v) Bisacrylamide

Sample buffer: 1.25 ml 2 M Tris/HCl, pH 6.8,
3.2 ml Glycerol (87%)
180 µl 2-Mercaptoethanol
+ a few grains of bromophenolblue

	0.8 g SDS
	filled with H_2O to 10 ml
Running buffer:	25 mM Tris/HCl
	200 mM Glycine
	0.1% (w/v) SDS
	pH 8.3
2x SDS-Sample-buffer:	0.2 M Tris-HCl, pH 6,8
	8% (w/v) SDS
	40% (v/v) Glycerol
	0.04% (w/v) Bromophenol blue
	30 mM DTT

3.2.2.2 *Coomassie blue staining*

The polyacrylamide gels were stained by soaking in a staining solution and boiling for 20 sec in a microwave oven. Afterwards, the gels were gently shaken for 10min at RT. For destaining, the gels were transferred to a destaining solution and again boiled for several seconds and subsequently shaken for approximately one hour at RT. The destaining procedure was repeated until the gel was completely free of background stain.

Staining solution:	2.5 g Coomassie brilliant blue R-250
	250 ml Ethanol
	80 ml acetic acid
	filled with H_2O to 1 l
Destaining solution:	250 ml ethanol
	80 ml acetic acid
	filled with H_2O to 1 l

3.2.2.3 *Determination of protein concentration*

Two distinct methods have been used in order to measure the protein concentration of a given sample. Note that concentrations measured by the Bradford method are given in mg/ml, whereas the concentrations determined by absorbance at 280nm are given in molar concentrations.

a) Bradford protein assay

For the determination of the protein concentration according to the method of Bradford (Stoscheck, 1990) 795 µl H_2O were mixed with 5 µl of protein solution and 200 µl of Bradford-solution (BioRad, Germany) in a plastic-cuvette. The Absorption of this mixture was measured in a photometer at a wavelength of 595nm against a blank solution containing 800 µl H_2O and 200µl of Bradford-solution. The corresponding protein concentration was calculated from a calibration curve using BSA as a standard.

b) Absorbance at 280 nm

The Absorbance of a protein sample at 280 nm has been measured with a Nanodrop 2000 (Thermo Scientific). The concentration was calculated according to the Beer-Lambert relation: $A = \varepsilon \times c \times d$, where A is the absorption at 280 nm, ε is the molar absorbance coefficient, c the molar concentration of the protein solution and d is the cell length of the cuvette. The molar absorbance coefficient of HtrA1 has been calculated as described by Gill and von Hippel (Gill and Vonhippel, 1989). The molar absorbance coefficient of full length HtrA1 is 11430 $M^{-1}\,cm^{-1}$ assuming all cysteines residues appear as half and 10430 $M^{-1}\,cm^{-1}$ assuming that no cysteine residues appear as half cysteines. The coefficient for ΔN-HtrA1 is 8940 $M^{-1}\,cm^{-1}$, for HtrA1-prot 5840 $M^{-1}\,cm^{-1}$. HtrA1 does not contain any tryptophan residues and it was shown that this can result in more than 10% error in the computed extinction coefficient.

3.2.2.4 *Electroblotting of proteins to PVDF membranes for N-terminal sequencing*

After SDS polyacrylamide gel electrophoresis proteins were transferred to a PVDF (polyvinylidene diflouride) membrane (Amersham Biosciences) for subsequent N-terminal sequencing or Western blots. Transfer was carried out at 100 mA till 25 V were reached for approx. 1.5 h using a semi-dry blotting apparatus at room temperature in transfer buffer. For N-terminal sequencing, the membrane was stained in staining solution for one minute and afterwards destained in water for 15

min. Then the membrane was air-dried so that the blotted bands became visible. They were cut for N-terminal sequencing.

Transfer buffer:	50 mM Tris, 380 mM glycine, 0.1% SDS, 20% methanol
Staining solution:	Amido black solution

3.2.2.5 *Western Blot*

After separating the proteins according to their molecular mass by SDS-PAGE (3.2.2.1) and electroblotting of the proteins to a PVDF membrane (3.2.2.4) the membrane was blocked with blocking solution for 1 h at RT or 4°C over night. The primary antibody antipenta-His (mouse) was diluted 1:1000 in antibody solution (3% BSA in TBS) and the blot was incubated with shaking over night at 4°C or 1 h at RT. After washing three times with TBST for 1 h, the secondary antibody, anti-mouse HRPO (diluted 1:15000 in 5% milk powder in TBS) was incubated shaking for 2 hrs at 4°C. Thereafter the blot was washed three times with TBST and finally developed for horseradish peroxidase (HRPO) activity: The blot membrane was incubated for 1 min in a 1:1 solution of stable peroxide and Luminol/Enhancer (Super Signal West Pico Chemiluminescent substrate, Pierce). The excess reagent was drained off and the blot was transferred into a film cassette wrapped in plastic foil. The blot was overlaid with an autoradiographic film (Hyperfilm ECL, Amersham Biosciences) in a dark chamber and exposed for 2 sec up to 2 min. The film was afterwards developed in a developer.

Blocking buffer:	3% BSA, 1 mM EDTA, 0.05% Tween 20, 1:1000 20% NaN_3
TBS(T):	10 mM Tris pH 7.5, 150 mM NaCl, (0.05% Tween 20)

3.2.2.6 *Lipid binding assay*

Lipid binding of ΔN-HtrA1 and HtrA1-prot was performed as follows. Brain lipid extracts (Sigma, Folch fraction I) were suspended in 140 mM NaCl, 50mM Hepes-NaOH pH 7.4 and stock solutions of 1mg/ml or 4 mg/ml were made. The proteins with a concentration of 0.1 mg/ml were incubated for 15 min at 37°C with lipid concentrations 0.02, 0.05, 0.1, 0.2, 0.5, 1.0, 1.5 and 2 mg/ml in a final assay volume of 100 µl. 20 µl were taken as loading control and the samples were centrifuged for 30 min at 42´000 rpm and 4°C. After the supernatant was removed and the pellet had been resuspended with an equivalent volume of 80 µl buffer, 20 µl samples from supernatant, pellet and loading control were analysed by SDS–PAGE.

3.2.2.7 *Purification of full length HtrA1, full length HtrA1$_{S328A}$ and NT-HtrA1*

After expression, cells were harvested by centrifugation (4000 rpm), resuspended in 100 ml of buffer A and 2 ml DNAse I (1 mg/ml) was added. Otherwise the pellet was too viscous to be resuspended. Subsequently the cells have been disrupted by sonication on ice. From this point on, all steps of protein purification were performed at 4°C. The lysate was centrifuged (19´000 rpm, 40 min) and the supernatant was loaded on a Ni-NTA column (Qiagen) equilibrated with buffer B. The column was washed with buffer B and subsequently with stepwise increasing imidazole concentrations, namely 12% buffer C (30 mM imidazole) and 20% buffer C (50 mM imidazole) to remove unspecific bound proteins. HtrA1 was eluted with 60% (150 mM imidazole). Eluted fractions were analysed by SDS-PAGE. Subsequently the protein was concentrated with a concentrator (Vivaspin, Amicon, cutoff 50´000 kDa) and desalted with a PD 10 column in buffer B. The elution fraction was digested with PreScission protease (GE Healthcare) to remove the TrxA-tag over night at 4°C (1 unit protease pro 100 µg protein). This step was not required for the wild type protein as it underwent self cleavage and thus the TrxA-tag was removed after NiNTA purification. After concentrating the protein to 2ml the sample was applied with 1ml/min to a Superdex 200 26/60 column (GE Healthcare) to separate the cleaved tag and the PreScission protease from HtrA1. Gelfiltration fractions (2 ml fractions) were combined according to their elution volumes for trimeric HtrA1 (≈ 160 ml). The purified protein was concentrated using Vivaspin concentrators (Vivaspin, cut-off 30 kDa) to approx. 4 mg/ml. HtrA1$_{S328A}$ was taken for crystallization.

Buffer A:	100 mM NaH_2PO_4 pH 7.5
	300 mM NaCl
Buffer B:	50 mM NaH_2PO_4 pH 7.5
	150 mM NaCl
Buffer C:	50 mM NaH_2PO_4 pH 7.5
	150 mM NaCl, 250 mM Imidazole
Buffer D:	10 mM HEPES/NaOH pH 7.5
	50 mM $(NH_4)_2SO_4$

3.2.2.8 *Purification of ΔN-HtrA1, ΔN-HtrA1$_{S328A}$, HtrA1-prot and HtrA1-prot$_{S328A}$*

Cell were harvested, sonicated, centrifuged and purified with a NiNTA and SEC mainly as described for the full *length* protein. The buffers for NiNTA contained Tris instead of phosphate and additionally 5 mM ß-Mercapthoethanol (ß-ME). The NiNTA column was washed only with 30 mM imidazole to remove unspecific bound proteins. After NiNTA, the protein was concentrated to 2 ml and loaded to a Superdex-200 prep grade column (GE Healthcare) equilibrated with buffer D. Fractions containing trimeric HtrA1 were combined and either concentrated to approx. 40 mg/ml for ΔN-HtrA1 or 20 mg / ml for HtrA1-prot or taken for methylation.

Buffer E: 100 mM Tris/HCl pH 7.5, 150 mM NaCl, 5 mM ß-ME

Buffer F: 100 mM Tris/HCl pH 7.5, 150 mM NaCl, 5 mM ß-ME, 250 mM Imidazol

3.2.2.9 *Methylation*

Screening with commercially available screens which sample a wide range of crystallization space is the first choice when crystallizing proteins as in many cases this approach was described to be successful. Proteins which fail to crystallize can be chemically modified to facilitate crystallization. Surface engineering of proteins by chemical modification offers a radical approach to reduce surface entropy. Reductive lysine methylation is one of the possibilities and was described as a simple, inexpensive and efficient rescue strategy by Walter *et al.* 2006 for proteins which failed to crystallize. The effect of methylation on the physico-chemical properties of these proteins are complex as pI, solubility and oligomeric state can be influenced (Walter *et al.* 2006).

Purified ΔN-HtrA1 protein (1 mg/ml) was incubated for 2 hrs with 20 µl 1 M ABC (Boran dimethylamine complex, Sigma) solution and 40 µl 1 M formaldehyde solution per mg protein on ice. After adding the same amount of ABC and formaldehyde solution the mixture was incubated again for 2 hrs. Finally 10 µl ABC solution was added and the protein was incubated for 20 hrs at 4°C.

The methylation reaction was stopped by adding 1 ml of 1 M Tris-HCl (pH 8.8) and a second size exclusion chromatography on a Superdex-200 in buffer D to yield a homogeneous fraction. Finally, the protein was concentrated to 30-40 mg/ml with Vivaspin concentrators (Vivaspin, cutoff 30 kDa) and taken for crystallization or biochemical assays.

3.2.2.10 *N-terminal sequencing*

For N-terminal sequencing the protein was loaded to an SDS-PAGE, separated and blotted to a PVDF membrane. The degradation band was cut and sended to Alphalyse in Denmark. The analysis was performed on an ABI Procise 494 sequencer. The procedure determines the amino acid sequence of proteins by Edman procedure.

3.2.2.11 *Mass spectrometry*

Electrospray-ionization mass spectrometry (ESI-MS) was carried out on purified samples of full length HtrA1 and ΔN-HtrA1. The analyses were performed at the IMP in Vienna, in the group of Karl Mechtler.

3.2.2.12 *Size Exclusion Chromatography (SEC)*

Size exclusion chromatography relies on the fact that molecules in solution are separated by size as they pass through a column packed with a chromatographic medium. The matrix consisting of microscopic beads with pores and internal channels function as a separation medium. Relatively small molecules can diffuse into the gel whereas large molecules will be prevented by their size from diffusing into the gel and are thus confined to the solution. Thus gel filtration displays a method that can be applied to further purify proteins and to determine the molecular mass of a molecule in order to characterize it.

A calibration curve for molecular mass determination was set up as described. A gel filtration standard (BioRad) was used to determine the elution volumes (V_E) of the following molecular mass standards: thyroglobulin (670 kDa), γ-globulin (158 kDa), ovalbumin (44 kDa), myoglobin (17 kDa) and vitamin B_{12} (1.3 kDa). The total volume of the column (V_T) was calculated according to its length and diameter. Blue Dextran was used to determine the void volume of the column. The K_{AV} value for every molecular mass standard was calculated: $K_{AV} = (V_E - V_0) / (V_T - V_0)$.

The K_{AV} value for the molecular mass standards was then plotted against the logarithm of their molecular mass and the points were fit to a linear equation. For proteins with unknown molecular mass, the K_{AV} value was determined and the corresponding molecular mass was calculated from the calibration curve. The K_{AV} value has the advantage that it is pressure independent. The analyses were carried out on a SMART-system (Pharmacia).

The molecular mass of full length HtrA1, ΔN-HtrA1 and HtrA1-prot in solution was determined by analytical gel filtration chromatography on a Superdex-200 PC 3.2/30 and Superdex-200 10/300

column (Pharmacia). The columns were equilibrated with 50 mM ammonium sulphate, 10 mM HEPES/NaOH, pH 7.5 at 4°C or RT. Protein samples with a concentration of about 5mg/ml were applied to the column with 80µl/min for SD 200 PC 3.2 and 0.8 ml for SD 200 10/300. For SEC SD200 26/60 during purification of HtrA1 refer to 3.2.2.7.

To follow the complex formation of trimeric ΔN-HtrA1$_{S328A}$ with citrate synthase, 5 µl of 110 µM ΔN-HtrA1$_{S210A}$ were incubated with 15 µl of 170 µM citrate synthase in 100 mM Tris-HCl (pH 7.5, 8, 8.5 or 9), 150 mM NaCl for 15 min at 42°C prior to injection on a Superdex 200 (PC 3.2/30; GE Healthcare). Trimeric ΔN-HtrA1$_{S328A}$ and CS were used as a control. Runs were fractionated in parallel (100 µl fractions) and 10 µl samples were taken to check the content on SDS-PAGE. The experiment was done in addition for HtrA1-prot$_{S328A}$.

To follow the complex formation with denatured lysozyme 5 µl of 110 µM ΔN-HtrA1$_{S210A}$ were incubated with 0.5 µl of 7 M lysozyme in 100 mM Tris-HCl (pH 8 or 9), 150 mM NaCl, 40 mM fresh DTT for 10 min at 42°C prior to injection on a Superdex 200 (PC 3.2/30; GE Healthcare). The final assay volume was 30 µl. Lysozyme was denatured and unfolded over night in 4 M urea, 40 mM DTT. Trimeric ΔN-HtrA1$_{S328A}$ and lysozyme were used as a control. Runs were fractionated in parallel (100 µl fractions) and 10 µl samples were taken to check the content on SDS-PAGE.

3.2.2.13 *Dynamic Light Scattering (DLS)*

DLS was carried out using a DynaPro-801 (Protein-Solutions Inc.) molecular sizing instrument. A 50 µl sample of HtrA1$_{S328A}$ with a concentration of about 1mg/ml in 10 mM HEPES/NaOH, pH 7.5 was given into a 12 µl chamber quartz cuvette. The measurements were performed at 20°C. The data were analysed using the Dynamics 4.0 software (Protein-Solutions Inc.) as described by Moradian-Oldak *et al.* (1998) (Moradian-Oldak *et al.* 1998).

3.2.2.14 *Resorufin-labeled casein assay*

The proteolytic activity of HtrA1 and its derivatives was determined with resorufin-labeled casein (Roche, Germany). Fifteen microliters of 0.4% (w/v) resorufin-labelled casein was added to 100µl incubation buffer containing approximately 1 µM HtrA1. The mixture was incubated at 37°C for several hours. The reaction was stopped by precipitation of casein with 480 µl 10% (w/v) TCA. Samples were again incubated for 10 min. at 37°C and subsequently centrifuged (10 min, 10000 x g, RT). 400 µl of the supernatant was mixed with 600 µl 1 M Tris/HCl, pH 8.8 to determine the absorbance at 574 nm. A sample without HtrA1 was used as a blank.

Incubation buffer:	100 mM Tris/HCl pH 7.5
	100 mM NaCl

3.2.2.15 *ß-Casein degradation assay*

To follow the degradation of the model substrate ß-Casein 20 µM ΔN-HtrA1 or HtrA1-prot were incubated with 170 µM casein in 100 mM Tris-HCl pH 8.0 at 37°C. At certain time points the reaction was stopped by adding 2xSDS loading buffer to take aliquots. Subsequently, the aliquots were incubated for 5min at 95°C and analysed by SDS–PAGE. ΔN-HtrA1 and ß-Casein were detected by Coomassie stain. In parallel the degradation of ß-Casein was follwed in the presence of 100 µM peptide KKKDSRIWWV and incubating all three components in the same degradation buffer at 37°C.

3.2.2.16 *pNA-assay*

Serine proteinase activity of the enzyme was measured by the release of p-nitroanilidine (pNA) from substrates VFNTLPMMGKASPV-pNA and monitored by spectrophotometry at 405 nm. The activity of ΔN-HtrA1 was measured in 100 µl reaction mixtures containing 10 µM ΔN-HtrA1, 100 mM Tris-HCl (pH 8 or 8.5) and 150 mM NaCl. The samples were preincubated for 10 min at 37°C, then the chromogenic substrate was added to a final concentration of 500 µM, and the increase in the absorbance at 405 nm and 37°C was measured continuously every minute with a fluorescence 96-well plate reader (BioTek). The same assay conditions were performed at 42°C to measure the activity in the presence of citrate synthase, which was added prior to the 10 min incubation step with a final concentration of 20 µM.

3.2.2.17 *pNA-assay in the presence of peptides*

Cleavage assays concerning the influence of a certain peptide on the protease activity were performed by preparing a solution in incubation buffer (3.2.2.16) with a final concentration of 10 µM HtrA1 and 5 to 250 µM of the peptide. Again, reference as well as blank samples were prepared containing no peptides or no HtrA1, respectively. All the samples were preincubated for 10 min. at 37°C, then 500 µM pNA substrate was added and the proteolytic activity was determined as described under 3.2.2.16. Every sample, the probe with the corresponding inhibitor as well as the reference was prepared three times. Average absorption values for the probe and the reference samples were calculated and the remaining activity of the inhibited probe was related to the reference.

The specific activity for HtrA1 was calculated using Lambert-Beer: $\Delta E = \epsilon_{mol} \times c \times d$ with d = 0.3 cm (corresponding to the height of the liquid in the 96 well plate), $\epsilon_{mol} = 8800\ M^{-1} \times cm^{-1}$ as the extinction coefficient of the pNA and ΔE defined as the slope at the steepest part of the curve.

3.2.2.18 *pNA-assay in the presence of unfolded citrate synthase*

Peptidase activity of ΔN-HtrA1 was measured in 100 µl reaction mixtures containing 10 µM ΔN-HtrA1 or HtrA1-prot and 20 µM citrate synthase in 100 mM Tris-HCl (pH 8 or 8.5) and 150 mM NaCl. The samples were preincubated for 10 min at 42°C then 500 µM pNA was added. The assay was done under the same conditions as described in 3.2.2.16 but at 42°C to measure the activity in the presence of citrate synthase.

3.2.2.19 *Inhibition of ΔN-HtrA1 with DPMFKLboroV peptide*

25 µM wild type protein was incubated with increasing amounts of the inhibitor peptide in 0.1 M Tris pH 8.5, 0.1 M NaCl. The assay volume was 100 µl. After 30 min incubation at 37°C, 160 µM ß casein was added and 5 µl samples were taken after 10 min for SDS-PAGE.

3.2.2.20 *Degradation of model substrates*

The degradation of substrate proteins by ΔN-HtrA1 and HtrA1-prot was analyzed by incubating a solution containing 80 µM HtrA1 in 100 mM Tris-HCl (pH 8.5), 100 mM NaCl with 7 mg/ml CS, or 5 mg/ml MDH at 43°C. Samples were taken at certain time points and mixed with an equal volume of 2x SDS loading dye to check the reaction on SDS-PAGE. After 3 hrs undigested proteins were removed by precipitation with six volumes of cold acetone. After incubation for 12 hrs at −20°C, samples were centrifuged for 30min at 4°C and 20,000 ×***g***. The pellet was discarded, and the acetone was removed from the supernatant in a SpeedVac. The pellet was resuspended in H_2O. Peptides generated by ΔN-HtrA1 and HtrA1-prot were subjected to sequencing by mass spectrometry on a hybrid linear ion trap/Fourier transform ion cyclotron resonance mass spectrometer (LTQ-FT Ultra, (ThermoFisher). For peptide identification, a database of all respective substrate proteins was generated, and the identified masses were searched against this database. The analysis was performed with the probability-based MASCOT software suite, version 2.2.0 (Matrix Science) without specifying any cleavage specificity.

3.2.2.21 *Analysis of degradation products by mass spectrometry*

The analyses of the samples were carried out by the service department mass spectrometry at the IMP in the group of Karl Mechtler. Briefly, the degradation products were separated by reversed-phase chromatography and subsequently applied to a Reflex III, MALDI-TOF mass spectrometer (Bruker Daltonics). Afterwards, individual peptides could be identified according to their molecular mass. The analyses of the raw mass spectrometry data were performed with Xcalibur mass spectrometry data system software (Thermo Electron Corporation).

3.2.2.22 *Isothermal Titration Calorimetry*

ITC is a thermodynamic technique that directly measures the heat released or absorbed during a biomolecular binding event. Measurement of this heat allows accurate determination of binding constants (K_B), reaction stoichiometry (n), enthalpy (ΔH) and entropy (ΔS), thereby providing a complete thermodynamic profile of the molecular interaction in a single experiment.

The thermodynamic values of the interaction between different constructs of HtrA1 and different peptides were determined by isothermal titration calorimetry (MCS-ITC; Microcal). All experiments were conducted in overflow mode at 30°C. 30 µM solution (1.4 ml) of ΔN-HtrA1 or HtrA1-prot were placed in the temperature-controlled sample cell and titrated with the peptide (300 µM), that was loaded in the 300 µL mixing syringe. For all experiments, 10 mM Hepes buffer, pH 7.5 supplemented with 50 mM $(NH_4)_2SO_4$ was used as the buffer. Injections of 10 µL of peptide were dispensed into the sample cell using a 120 sec equilibration time between experiments and stirring at 300 rpm. Control experiments using the identical experimental setup were carried out in order to measure and correct the heat of dilution. Ultimately, the data were analyzed using ORIGIN software following the instructions of the manufacturer.

3.2.3 Crystallographic methods

3.2.3.1 *Protein crystallization*

ΔN-HtrA1 and ΔN-HtrA1$_{S328A}$:

For initial surveys of crystallization conditions, standard screening kits purchased from Hampton Research (USA) and Jena Bioscience were used, using a Cartesian Roboter or a Phenix Roboter. Therefore HtrA1$_{S328A}$ at approximately 30 mg/ml was used with typically 0.1 µl or 0.2 µl of protein

solution mixed with 0.1 µl of reservoir solution set up as sitting-drop vapour-diffusion experiments using cryschem plates (Charles Supper Company, Massachusetts) with 500 µl of reservoir solution at 4°C and 19°C, respectively. The initial condition consisting of 1.0 M $LiSO_4$, 0.1 M sodium citrate pH 5.8, 0.5 M $(NH_4)_2SO_4$ was subsequently refined by a systematic variation of buffer, pH, drop ratio and by addition of certain additives to the drop mixture.

ΔN-HtrA1$_{S328A}$ (SeMet) and ΔN-HtrA1(SeMet):

Crystals of HtrA1$_{S328A}$(SeMet) were grown using sitting drops equilibrated against a reservoir of 1.0 M $LiSO_4$, 0.1 M sodium citrate pH 5.6 to 6.3, 0.5 M $(NH_4)_2SO_4$. Drops were set up with 2 µl HtrA1 (SeMet) (30 mg/ml), and 1 µl or 2 µl reservoir solution.

ΔN-HtrA1 + Inhibitor:

Crystals of wildtype ΔN-HtrA1 or ΔN-HtrA1(SeMet) were incubated with 2 mM (f.c.) of the inhibitor DPMPKLV-Boro for 30 min at ice, before setting up the co-crystallization trials. They were grown using sitting drops equilibrated against a reservoir of 1.0 M $LiSO_4$, 0.1 M sodium citrate pH 5.6 to 6.3, 0.5 M $(NH_4)_2SO_4$. Drops were set up with 2 µl HtrA1-Inh (30 mg/ml), and 1 µl reservoir solution.

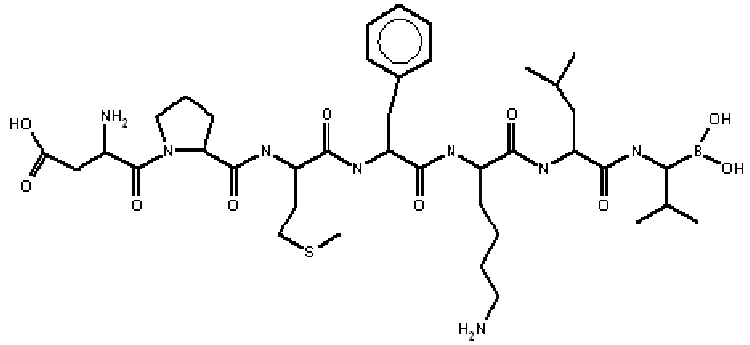

Fig. 3.2 DPMPKLV-Boro
Depicted is the peptide inhibitor used for co-crystallization trials. The inhibitor molecule is composed of a peptide of seven amino acids and a boronic acid group fused at the C-terminus. The drawing was made with the program Chemograph.

HtrA1-prot:

Crystallization of HtrA1prot was done following the same procedure described for ΔN-HtrA1$_{S328A}$ first setting up initial screens and subsequent refinement. Big crystals appeared after one day in several conditions. Some of them have been refined. One finally condition for crystals taken for data collection experiments and structure solution contained 2.0 M ammonium sulfate and 0.1 M sodium acetate pH 4.6.

3.2.3.2 *Improvement of diffraction properties - Seeding*

Crystals of ΔN-HtrA1 with bound inhibitor were used for seeding the following way in order to improve their diffraction properties. After crystallization at room temperature, a single crystal was fished and crushed in 50 µl reservoir solution. The seeding solutions were prepared using the Seed Bead Kit from Hampton Research. Dilutions were prepared from 10^{-1} to 10^{-6}. Drops were set up using the Oryx Robots with 1 µl HtrA1 in complex with the inhibitor, 1 µl reservoir solution and 0.3 µl seeding solution. Crystal grew for four weeks and were then flash frozen by plunging into liquid nitrogen using 1.8 M $LiSO_4$ as a cryoprotectant and maintained at ~100 K in a nitrogen gas stream during data collection.

3.2.3.3 *Data collection and data processing*

Single crystals were mounted in Hampton Research Cryo loops of appropriate size, flash frozen to 100K in a cold nitrogen-gas stream and subjected to X-ray diffraction. Before the crystals were transferred to cryobuffer for several seconds prior to flash-freezing in order to avoid ice rings and crystal damage due to cooling. Data were collected at beamline ID14-4 at the ESRF (Grenoble, France) or at beamline X06SA at the SLS (Zurich, Swiss).

For MAD experiments, prior to data collection an X-ray fluorescence spectrum of the respective crystal was recorded in order to determine the peak, inflection and remote wavelength corresponding to the anomalous scatterer present in the crystal. After recording and processing a test oscillation image, the angle range which is necessary to achieve an optimal completeness was determined by using the program STRATEGY (Leslie, 1992). The most precise anomalous differences are obtained by collecting the so-called Friedel mates at inverse beam geometry. For this purpose, for every wavelength a second data set was collected after rotating the crystal by 180° corresponding to the first starting value.

All diffraction data were processed and scaled using the programs DENZO, SCALEPACK (Otwinowski and Minor, 1997) and HKL2000 or XDS. The indexed intensities were converted and reduced to structure factors using the program TRUNCATE from the CCP4 program suite (Bailey, 1994).

Cryobuffer ΔN-HtrA1: 1.8 M $LiSO_4$, 0.1 M Na-citrate pH 6.0, 0.6 M $(NH_4)_2SO_4$

Cryobuffer for HtrA1-prot: 0.1 M Na-acetate pH 4.6 and 2 M $(NH_4)_2PO_4$, 20% Glycerol

3.2.3.4 *Structure solution*

ΔN-HtrA1$_{S328A}$:

The structure was determined by molecular replacement using the program Phaser of the CCP4 package (CCP4, 2002) and the protease domain (residues 140 - 340) of human HtrA2 (Protein Data Bank ID 1LCY) as a search model. Electron density maps based on the coefficients 2Fo-Fc and 3Fo-2Fc were calculated from the phases of the initial model. The resulting maps were used to build atomic models in O (Jones *et al.* 1991). Refinement and model rebuilding proceeded smoothly via rigid body, positional, and later B factor optimization in CNS (Brunger *et al.* 1998). The entire structure was checked using simulated annealing composite omit maps. Some protein segments including residues 158 – 160, 301 – 314 (Loop L3) and 371 - 480 (PDZ domain) were hardly visible or invisible in these maps and were therefore omitted from the model. The refined HtrA1$_{S328A}$ structure was used to solve the structure of the inhibitor complex of HtrA1.

ΔN-HtrA1 + Inhibitor

A complete dataset for the HtrA1 inhibitor complex was measured at the Swiss Light Source (SLS, Beam line X06SA) at λ = 0.9724 Å using a Pilatus detector (Dectris). The crystals also belonged to spacegroup H 3 with slightly different cell constants of a = 105.965, b = 105.965, c = 118.336. During refinement of the HtrA1 inhibitor complex, clear electron density developed for one inhibitor molecule within the active site of the protein. In contrast to ligand-free HtrA1, the entire protease domain was well defined. Especially the proteolytic site that underwent pronounced conformational remodeling was carefully inspected. In these maps, residues 158 - 159 and 371 - 480 had to be omitted from the model due to high flexibility.

As the crystals of HtrA1-Inh were nearly isomorphous to the HtrA1$_{S328A}$ crystals, the coordinates, constructing the asymmetric unit of the HtrA1$_{S328A}$ structure were used to calculate an initial rigid-body refinement, using data from 20 – 3.2 Å. After this procedure, both R_{work} and R_{free} dropped well below 40%.

HtrA1-prot

The structure was determined by molecular replacement using the program Phaser of the CCP4 package (CCP4, 2002) and the protease domain (residues 140 - 340) of human HtrA2 (Protein Data Bank ID 1LCY) as a search model. Electron density maps based on the coefficients 2Fo-Fc and 3Fo-2Fc were calculated from the phases of the initial model. The resulting maps were used to build atomic models in O (Jones *et al.* 1991). Refinement and model rebuilding proceeded smoothly via rigid body,

positional, and later B factor optimization in CNS (Brunger *et al.* 1998). The entire structure was checked using simulated annealing composite omit maps. Crystals of the protease domain belonged to the tetragonal spacegroup $P4_32_12$ with cell constants a = 153.671, b = 153.671, c = 89.835 containing three molecules per asymmetric unit. Protein segments including residues 158 – 160, 301 – 314 and 365 - 373 were hardly visible or invisible and were therefore omitted from the model.

3.2.3.5 *Model building and refinement*

The program O (Jones *et al.* 1991) was used for model building. For $HtrA1_{S328A}$ and HtrA1-Inhibitor energy-restrained crystallographic refinement was carried out with maximum likelihood algorithms implemented in CNS (Brunger *et al.* 1998), using the protein parameters of Engh and Huber (1991) (Engh and Huber, 1991). Bulk solvent, overall anisotropic B-factor corrections and non-crystallographic (NCS) restraints were introduced depending on the behaviour of the free R index. Refinement proceeded in several cycles, which were interrupted for manual rebuilding with the program O. The stereochemistry of the model was validated with PROCHECK (Laskowski *et al.* 1993).

3.2.3.6 *Graphical representations and sequence alignments*

Graphical presentations as well as surface and electrostatics calculations were prepared with the program PyMOL (DeLano 2004). Initial sequence alignments were made with ClustalW (http://www.ch.embnet.org/software/ClustalW.html) and presentations of sequence alignments were made with ESpript (Gouet *et al.* 1999).Secondary structure predictions were made with the program HHPred (http://toolkit.tuebingen.mpg.de/hhpred).

4 Results

4.1 Purification of HtrA1

4.1.1 Purification of full length HtrA1

HtrA1 consists of three different domains, an N-terminal domain with unknown function, a serine-protease domain and one C-terminal PDZ domain (Clausen *et al.* 2002). The N-terminal region of HtrA1 contains 18 cysteines which potentially form several disulfide bonds and may be necessary for proper folding of the protein. Expression and purification of the deletion construct containing the protease- and PDZ domain was established in *E. coli* as described in 4.1.2. So far, it has been possible to express the full length HtrA1 in an eukaryotic expression system (ProteaImmun, Berlin). This expression system showed limitations as the amount of purified protein was not sufficient for crystal trials. Eucaryotic expression systems are nevertheless beneficial if posttranslational modifications like disulfide bond formations are needed as the cytoplasm of *E. coli* is reducing and does not allow S-S bond formation. This may be the reason why so far any attempt to express HtrA1 in an *E. coli* expression system has failed.

Several strategies were performed to express HtrA1 in *E. coli*. Besides cloning of different tags which could enhance the solubility of the protein, different bacterial strains and the secretion to the periplasm of *E. coli* were tested for expression. Finally the expression of the full length HtrA1 in fusion with a Thioredoxin-tag (TrxA-tag) in *E. coli* Origami B cells has been successful (see 3.2.2.7 for cloning strategy) and is described below.

The full length protein as well as the N-terminal domain (NT-HtrA1) of HtrA1 both without the signal sequence (residues 1-21) were expressed and purified. The purification included NiNTA affinity chromatography and size exclusion chromatography (SEC). After loading the cell lysate to the NiNTA column washing with a stepwise increasing imidazole concentration removed unspecific bound proteins. Loading the fractions on a SDS-PAGE showed a 72 kDa protein in the elution fraction which

corresponds to the expected size of HtrA1 in combination with the TrxA-tag. Figure 4.1 gives an example of the NiNTA chromatography profile.

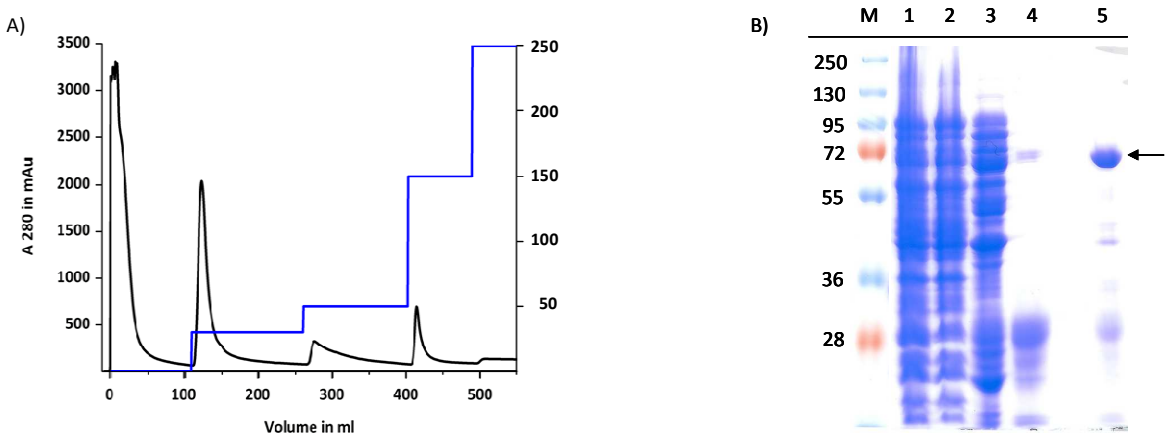

Fig. 4.1 NiNTA purification of HtrA1$_{S328A}$
A) NiNTA chromatography for HtrA1$_{S328A}$. Increasing imidazole concentrations are indicated. Fractions are loaded on a SDS-PAGE shown in B) following Coomassie blue staining. B) Lane 1 whole cells, 2 load, 3 flow through, 4 wash I, 5 elution with 150 mM imidazole. The arrow indicates HtrA1 in fusion with a TrxA-tag with the expected size of 72 kDa.

After NiNTA the 150 mM imidazole elution fraction was buffer exchanged into buffer B (without imidazole) and concentrated to 5 ml. The TrxA-tag was cleaved with PreScission protease (GE Healthcare) over night at 4°C. Samples were taken at different time points to monitor the cleavage. Subsequently, SEC was performed on a Superdex 200 column to separate the TrxA-tag and the PreScission protease from HtrA1. The SEC profile is shown below.

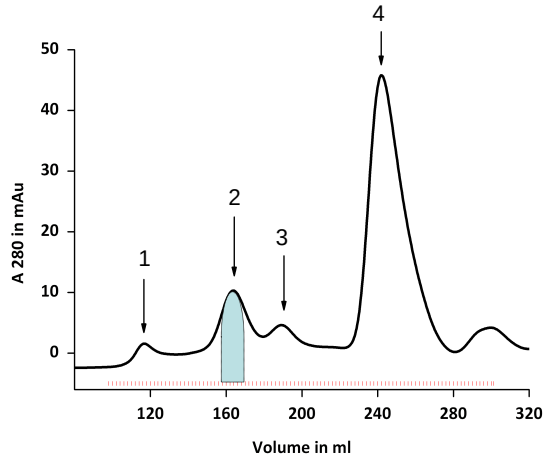

Fig. 4.2 SEC profile of full length HtrA1$_{S328A}$
SEC was performed after cleaving the TrxA-tag with PreScission protease. The protein was concentrated and injected to a SD 200 26/60 column via a 2 ml loop. 2 ml fractions were collected and analysed by SDS-PAGE. Four peaks can be distinguished. Peak 1 elutes in the void volume, peak 2 corresponds to trimeric HtrA1, peak 3 contains PreScission protease and peak 4 the cleaved TrxA-tag.

Four peaks were detected on SEC and loaded on a SDS-PAGE. Figure 4.3 shows that HtrA1 was cleaved yielding a 51 kDa protein corresponding to the expected size. PreScission protease as well as the tag elute as single peaks with a molecular weight of 48 kDa and 17 kDa, respectively.

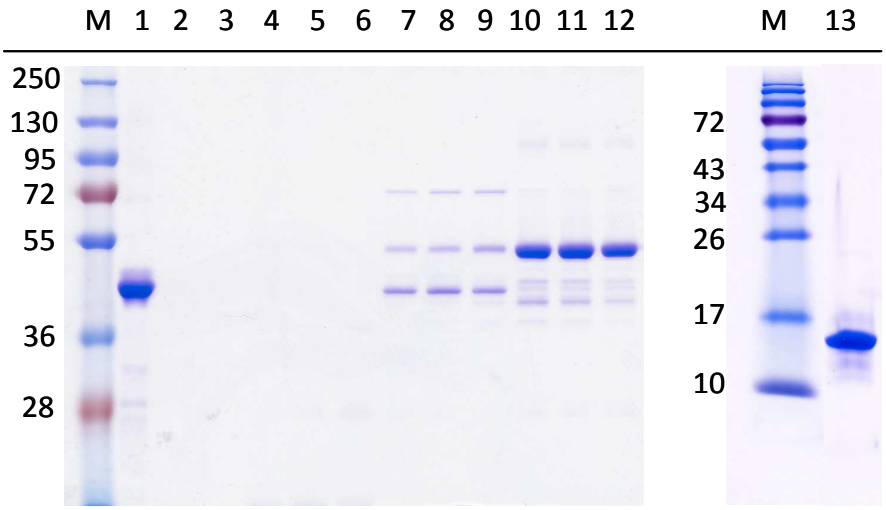

Fig. 4.3 SDS PAGE of SEC fractions
Fractions of SEC were loaded on a SDS-PAGE following Coomassie blue staining: 1 (control) PreScission protease (48 kDa) from GE Healthcare, 2-6 peak 1 (void), 7-9 peak 3 (PreScission), 10-12 peak 2 (corresponding to HtrA1, 51 kDa), 13 peak 4 (TrxA-tag, 17 kDa).

SEC showed that $HtrA1_{S328A}$ forms a trimer in solution and is about 95% pure after the two step purification. The TrxA-tag is cleaved efficiently after 2 hrs incubation at 4°C (not shown). The protein was taken for initial crystallization trials but so far no crystals could be obtained.

The wild type protein was purified according to the same protocol described for the inactive mutant but showed degradation during NiNTA chromatography (Fig. 4.4). The three degradation bands were identified by mass spectrometry to be HtrA1. Therefore, the wild type protein seems to undergo auto degradation. Cleavage by endogenous proteases could be excluded because the same purification protocol was applied for the inactive and the active mutant and degradation would occur also for the inactive mutant. All cleavage sites lie within the region between the N-terminal domain and the protease domain, yielding constructs of around 38 to 45 kDa consisting of the protease and the PDZ domain as shown in figure 4.4.

In order to map the cleavage sites all three bands of the wt protein (Fig. 4.4) were cut out from the gel and digested with trypsin, chymotrypsin and subtilisin and subjected to mass spectrometry analysis. One cleavage site could be identified with this method and was confirmed by N-terminal sequencing as described below.

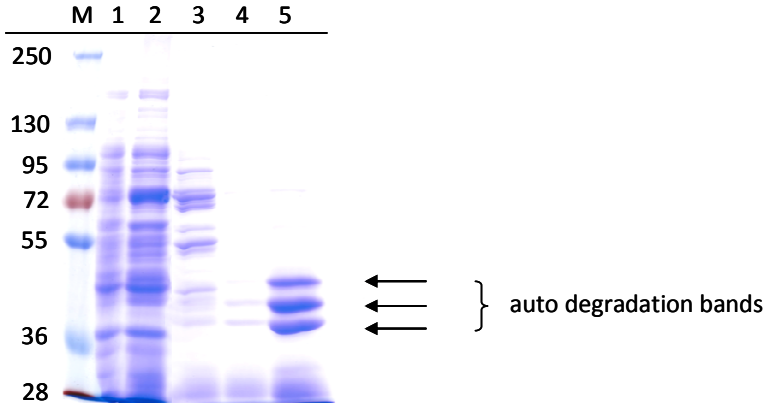

Fig. 4.4 NiNTA fractions of wt HtrA1
Samples were taken after different steps during NiNTA chromatography and subjected to SDS-PAGE following Coomassie blue staining. Lane 1 shows uninduced cells, lane 2 load, lane 3 wash I, lane 4 wash II, lane 5 elution with 150 mM imidazole. Arrows indicate self cleavage products of wild type HtrA1.

4.1.1.1 *Folding status of HtrA1*

To confirm the folding of full length HtrA1 and the formation of disulfide bonds, reduced and non reduced protein samples were analysed by SDS-PAGE. Figure 4.5 shows that the reduced form of HtrA1 displays a different mobility on a SDS-PAGE compared to the non reduced protein. As disulfide bond formation takes place the protein is likely to be folded. To further approve the the folded state of HtrA1 different experiments could be considered and are discussed under 5.1.

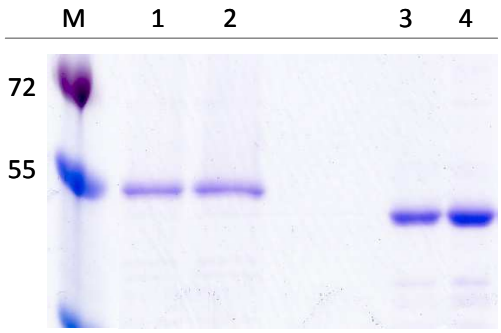

Fig. 4.5 Reduced and not reduced samples of HtrA1$_{S328A}$ on SDS-PAGE
Samples were mixed 1:1 with 2xLoading buffer either with or without DTT, boiled at 95°C for 5 min and subjected to SDS-PAGE following Coomassie blue staining. Lane 1 and 2 show DTT-reduced HtrA1. Lane 3 and 4 show not reduced HtrA1 running faster on SDS-PAGE.

4.1.2 Purification of ΔN-HtrA1 and ΔN-HtrA1$_{S328A}$

4.1.2.1 *Design of deletion constructs*

In order to crystallize HtrA1 and assess its biochemical properties, deletion constructs of HtrA1 were designed taking into consideration that full length HtrA1 did not crystallize and additionally undergoes auto degradation (see 4.1.1). One strategy for successful crystallization is to clone only

stable parts of the protein and to shorten the constructs at the N- or C-termini. Furtherrmore auto degradation leads to a heterogeneous protein composition, usually making protein crystallization impossible (Ferré-d'Amaré and Burley, 1994).

Originally the gene was expressed and purified from pSG7 or pSG13 (Grau *et al.* 2005) which did not express the N-terminal domain of HtrA1 (residues 1 to 139). The expression from these vectors which are derivatives of pQE60 (Qiagen) yielded only small amounts of HtrA1 but high amounts of the Lac repressor protein (LacI). LacI was found to unspecifically bind to Ni-columns and was purified instead of HtrA1. This was due to the fact that the monomeric size of LacI with 38 kDa is the same as for the expressed HtrA1 construct and the formation of the tetramer could not be distinguished from a trimer of HtrA1 on SEC. Different purification procedures were tried including a Hydroxylapathite column, a MonoQ, DEAD column, Heparin columns and others. Using the pET vecter expression system (pET21d) instead yielded a much higher overexpression of HtrA1 and thus facilitated a proper enrichment of the protein. PCR amplification and cloning of HtrA1 into pET21d expressed a C-terminal His_6-tagged protein in *E. coli* BL21 (DE3) cells (3.2.2.8). Nevertheless, this protein still showed auto degradation and the design of other deletion constructs was necessary.

The auto cleavage site could be verified by N-terminal sequencing (4.1.2.2) and gave rise for the first construct. The design was furthermore based on a secondary structure prediction with HHPred for HtrA1 as shown in Fig. 4.6 and alignments with DegP and DegS the bacterial homologs. Finally three constructs were cloned and expressed as shown in the Fig. 4.6.

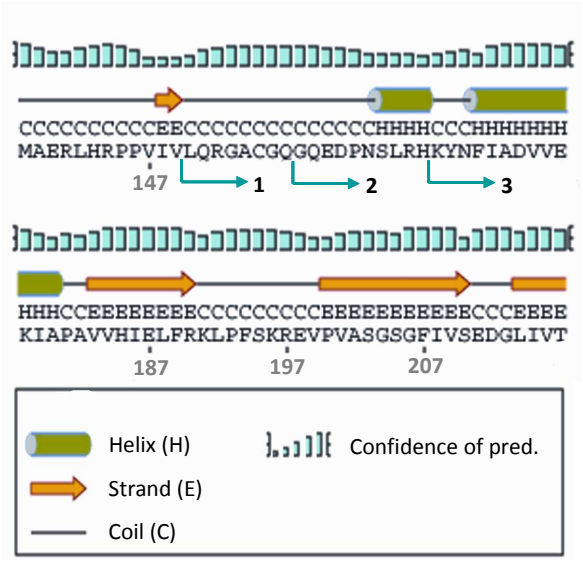

Fig. 4.6 Designing deletion constructs for expression in *E. coli*
Secondary structure prediction for HtrA1 was made with HHPred and is indicated above the amino acid sequence for HtrA1. Arrows indicate starting points of the constructs taken for cloning and expression in *E. coli*. Construct 1 marks the self cleavage site identified by N-terminal sequencing, construct 2 is based on the predicted secondary structure for HtrA1, construct 3 is based on a sequence alignment and the secondary structure of DegS.

All constructs were cloned and expressed but only construct 2, later referred to as ΔN-HtrA1, could be successfully purified and concentrated for crystallization trials and is discussed in the following sections of this work. Construct 3 was unstable and precipitated after NiNTA purification. From the structure solved during this work it became obvious that Tyr169, Phe171 and in addition the N-terminal half of the α-helix including Leu165 and Arg166 are important to mediate trimer formation of HtrA1. It has been therefore concluded that the assembly of the trimer was disrupted and HtrA1 was not stable as a monomer in solution.

4.1.2.2 *N - terminal sequencing*

Wildtype HtrA1 undergoes self cleavage which could interfere with crystal growth. Therefore it was necessary to map the cleavage sites to express a stable construct. After SDS-PAGE, ΔN-HtrA1 was blotted to a PVDF membrane, the degradation band cut out from the membrane and subsequently analyzed by N-terminal sequencing. The analysis has been carried out at Alphalyse in Denmark. The sequence of the first N-terminal residues is L-Q-A/R-A-A-Q, which could correspond to the N-terminal residues L-Q-R-G-A of HtrA1. A protein starting at these residues would correspond to a 36 kDa fragment and it was assumed that the cleavage occurs between Val149 and Leu150. This is in good agreement with results showing that HtrA1 has a preference for small hydrophobic residues such as valine and leucine at the P1 site (Fig. 4.22).

4.1.2.3 *Purification*

The wild type ΔN-HtrA1 and the inactive mutant ΔN-HtrA1$_{S328A}$ were purified the same way. The overexpression and purification of the proteolytically inactive variant of HtrA1 was indistinguishable from that of the wild type.

The purification procedure involved Ni-NTA affinity and size exclusion chromatography (SEC) and a more than 95% pure protein as estimated from SDS-PAGE was obtained after this two-step purification protocol (Fig. 4.8 B). In the first step, the His-tagged ΔN-HtrA1 was bound to a NiNTA column (Amersham) applying the whole cell lysate. The column was washed with a buffer containing 30 mM imidazole and HtrA1 was finally eluted with 150 mM imidazole (Fig. 4.7). Fractions containing the 150 mM elution step were collected, concentrated and further purified by SEC or taken for methylation. The protein yield at this stage was approx. 8 mg from 1 l culture.

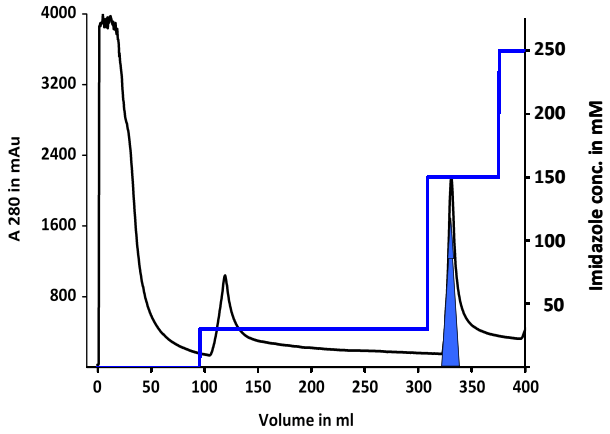

Fig. 4.7 Ni-NTA elution profile of His_6-tagged wt ΔN-HtrA1
The corresponding imidazole concentrations are indicated in the elution profile. The collected fractions were loaded on a 12% SDS-PAGE gel (see figure 4.8). The elution fraction depicted in blue was collected for the next purification step.

Size exclusion chromatography was performed on a Superdex 200 prep grade gel filtration column. The resulting gel filtration profile showed a small aggregation peak eluting in the void volume of the column (P1) and two peaks corresponding to HtrA1 (Fig 4.8 A). The molecular mass of the third peak was according to the calibration of the column 120 kDa, which corresponds to a trimer of ΔN-HtrA1. SDS-PAGE analysis of this peak fractions indicated that the protein preparation was > 95% pure (Fig. 4.8 B) for both the wild type and the SA mutant. The collected P3 fractions yielded 30 mg of highly pure protein which was subsequently used for further experiments. Strikingly, the wild type protein with the N-terminal deletion did not show self cleavage any more and was taken for crystallization. The protein was concentrated for biochemical assays or further treated by methylation (4.1.2.4).

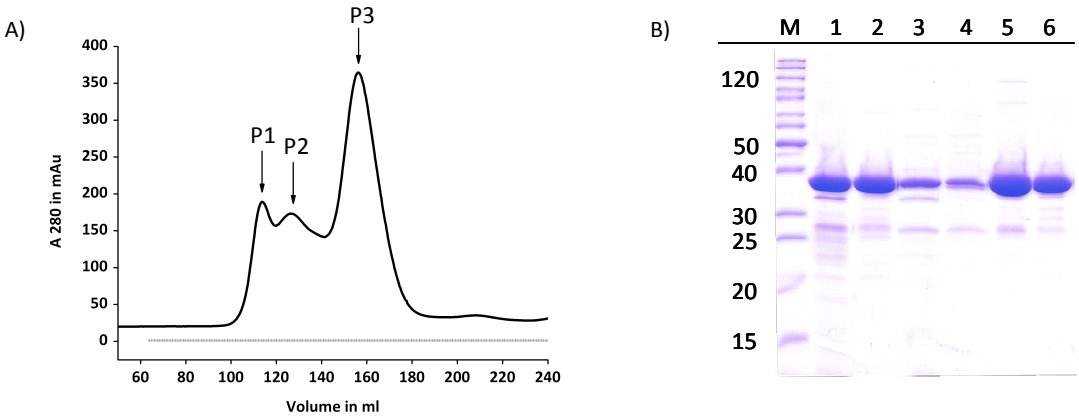

Fig. 4.8 SEC elution profile and SDS-PAGE of ΔN-HtrA1 purification
A) 150 mM elution peak from Ni-NTA column was concentrated and applied over a 2ml loop to a Superdex 200 26/60 column (GE Healthcare) equilibrated with 10 mM HEPES pH 7.5, 50 mM $(NH_4)_2SO_4$. Indicated fractions were analysed by SDS-PAGE (right). P3 fractions were pooled separately, concentrated and stored at -80°C. B) SDS-PAGE shows in lanes 1 and 2 ΔN-$HtrA1_{S328A}$ after NiNTA and SEC, respectively. Lanes 3 to 6 show wild type ΔN-HtrA1: in 3 P1, in 4 P2, in 5 P3 after SEC and in 6 after NiNTA purification.

4.1.2.4 *Methylation*

For successful crystallization methylation of lysine residues of ΔN-HtrA1 and ΔN-HtrA1$_{S328A}$ was necessary. Methylation of lysines leads to decreased solubility of the protein and was first described by Walter *et al.* 2006. The trimeric peak fraction of ΔN-HtrA1 was taken directly after SEC and incubated with formaldehyde and ABC solution as described in 3.2.2.9. After stopping the reaction the protein was concentrated to 2 ml and injected to a Superdex 200 column. The protein eluted as one single peak from the column. The elution volume and the mass of the protein judged from SDS-PAGE were slightly higher than for the unmethylated protein indicating that methylation was successful. As shown in 4.4 the methylated protein retained proteolytic activity.

4.1.3 Purification of the protease domain of HtrA1 (HtrA1-prot)

Purification of the protease domain of HtrA1 was performed mainly as described for ΔN-HtrA1. The construct was designed based on the ΔN-HtrA1 deletion construct. The two-step purification yielded > 95% pure protein as judged by SDS-PAGE. SEC on a SD 200 26/60 column showed an elution peak in the void volume of the column and one peak at 202 ml corresponding to a dimer or a trimer of HtrA1-prot. To verify the oligomeric state of the protease domain analytical SEC on a Superdex 75 was performed. The result is shown in figure 4.10 and confirms that HtrA1-prot forms a trimer in solution.

4.1.4 Purification of selenomethionine substituted ΔN-HtrA1

The proteins ΔN-HtrA$_{S328A}$(SeMet) and ΔN-HtrA1(SeMet) were expressed in methionine auxotroph B834 cells. The expression in minimal-medium and B834 cells was slower but yielded comparable amounts with 10 mg/l as for the expression in LB media. ΔN-HtrA1$_{S328A}$(SeMet) and ΔN-HtrA1(SeMet) were purified as decribed in 4.1.2.3 for the not selenomethionine substituted protein. SEC showed a distinct peak for a higher oligomeric species and was analysed by SDS-page. The P2 peak fraction contained highly pure HtrA1 and an additional band of approx. 35 kDa. Mass spectrometry analysis identified this band as the outer membrane protein A (OmpA) from *E. coli* (4.1.4.1). Fractions containing only the trimer of HtrA1 (P3) were pooled and used for methylation and crystallization.

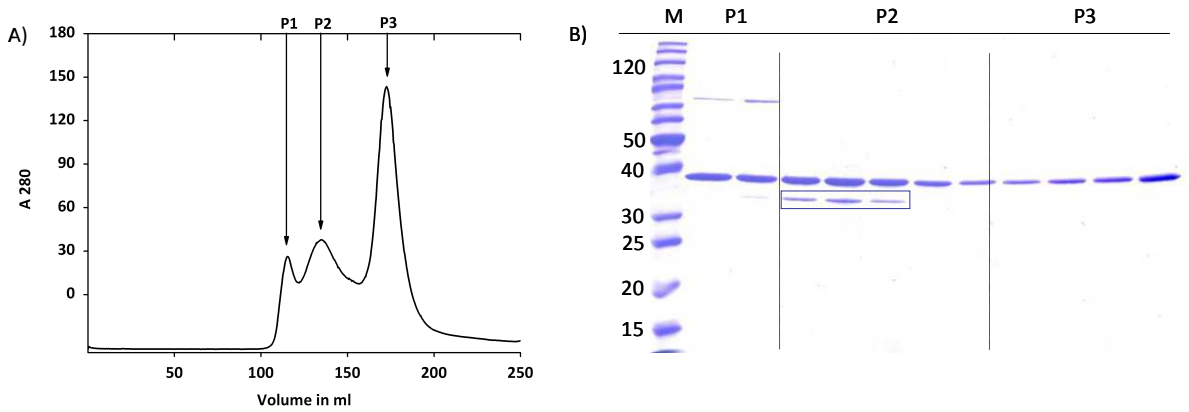

Fig. 4.9 SEC profile and SDS-PAGE for selenomethionine substituted ΔN-HtrA1
A) SEC profile showing three peaks which were loaded to an SDS-Page shown in B. B) Peak1 (P1), peak2 (P2) and peak3 (P3) are loaded to an SDS-PAGE. The elution volume of P3 corresponds to a trimer of HtrA1.Peak2 shows beside HtrA1 one additional band around 35 kDa. The band was cut and identified by mass spectrometry as OmpA from *E. coli*.

4.1.4.1 *Mass Spectrometry*

To confirm the identity of the purified proteins mass spectrometry was performed. The SA mutant of the full length HtrA1 and ΔN-HtrA1 were both identified by mass spectrometry in the group of Karl Mechtler in the IMP in Vienna. The protein bands were cut from SDS-PAGE and digested with trypsin. The obtained peptides were than searched against the *E. coli* and the human proteom.

SEC showed for wt HtrA1 and $HtrA1_{S328A}$ protein three different peaks and analysis of the second peak which could correspond to a higher oligomer of HtrA1 SDS-PAGE analysis clearly revealed two distinct bands with an estimated molecular weight of 38 kDa and approx. 30 to 35 kDa (Fig. 4.9). The upper band corresponds to the HtrA1 protein whereas the lower band resulted in the identification of the *E. coli* porin OmpA which runs with a molecular mass of 35 kDa if unfolded and 30 kDa if folded. That HtrA1 co-purifies with bacterial OmpA is interesting as for the bacterial homolog DegP it was shown to bind folded OMP´s forming 12meric or 24meric particles (Krojer *et al.* 2008). This result indicated that HtrA1 is able to form higher oligomeric complexes (see below).

4.2 Oligomeric state of HtrA1 in solution

4.2.1 Oligomeric state of HtrA1-prot

The oligomeric state of HtrA1-prot could not be distinguished between a dimer and a trimer after SEC on a SD 200 26/60. Thus analytical SEC on a SD 75 10/300 has been performed. From this column the protein elutes at 10.1 ml as a single peak. The calculated protein size for this volume is 67 kDa which is similar to the expected size of a trimer with 75 kDa. Additional the observed trimeric state of full length HtrA1 and ΔN-HtrA1 after preparative SEC (Fig. 4.2 and Fig. 4.8) could be confirmed for both proteins in analytical SEC (data not shown).

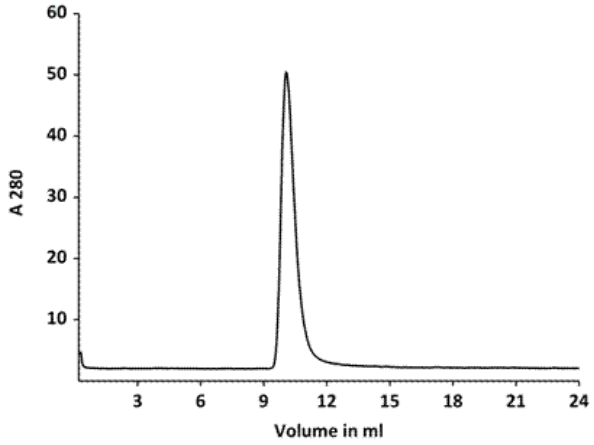

Fig. 4.10 Chromatogram HtrA1-prot$_{S328A}$
HtrA1-prot was subjected to a SD 75 10/300 column. It eluted as a single peak with an elution volume of 10.1 ml which corresponds to a trimer of the protease domain.

4.2.1.1 *Oligomerization in the presence of unfolded substrates*

As the bacterial homolog DegP is activated by forming higher oligomeric complexes with substrates, namely 12- or 24mers, this function was also investigated for HtrA1. HtrA1 cleaves unfolded substrates like chemically denatured lysozyme and heat denatured citrate synthase (CS). These two substrates were incubated with ΔN-HtrA1$_{S328A}$ and subjected to size exclusion chromatography. In figure 4.11 A the chromatogram is shown for the incubation with citrate synthase. Three peaks can be clearly distinguished. Both proteins were additionally injected alone to the column to determine their elution volume which facilitates the correct assignment of the peaks in the elution profile of ΔN-HtrA1 incubated with CS. Peak 2 contains trimeric ΔN-HtrA1 (elution volume 1.33 ml) and peak 3 citrate synthase (elution volume 1.54 ml). Peak 1 (elution volume 1.1 ml) contains both HtrA1 and CS

suggesting that HtrA1 forms a higher oligomeric species when incubated with unfolded substrates. To verify this result peak 1 was collected and reinjected to the column showing the same elution volume (data not shown) indicating the formation of a stable complex. It could be furthermore shown that the oligomer formation is pH dependent as the switch was more prominent at pH 9 than at pH 7.5 or 8.5.

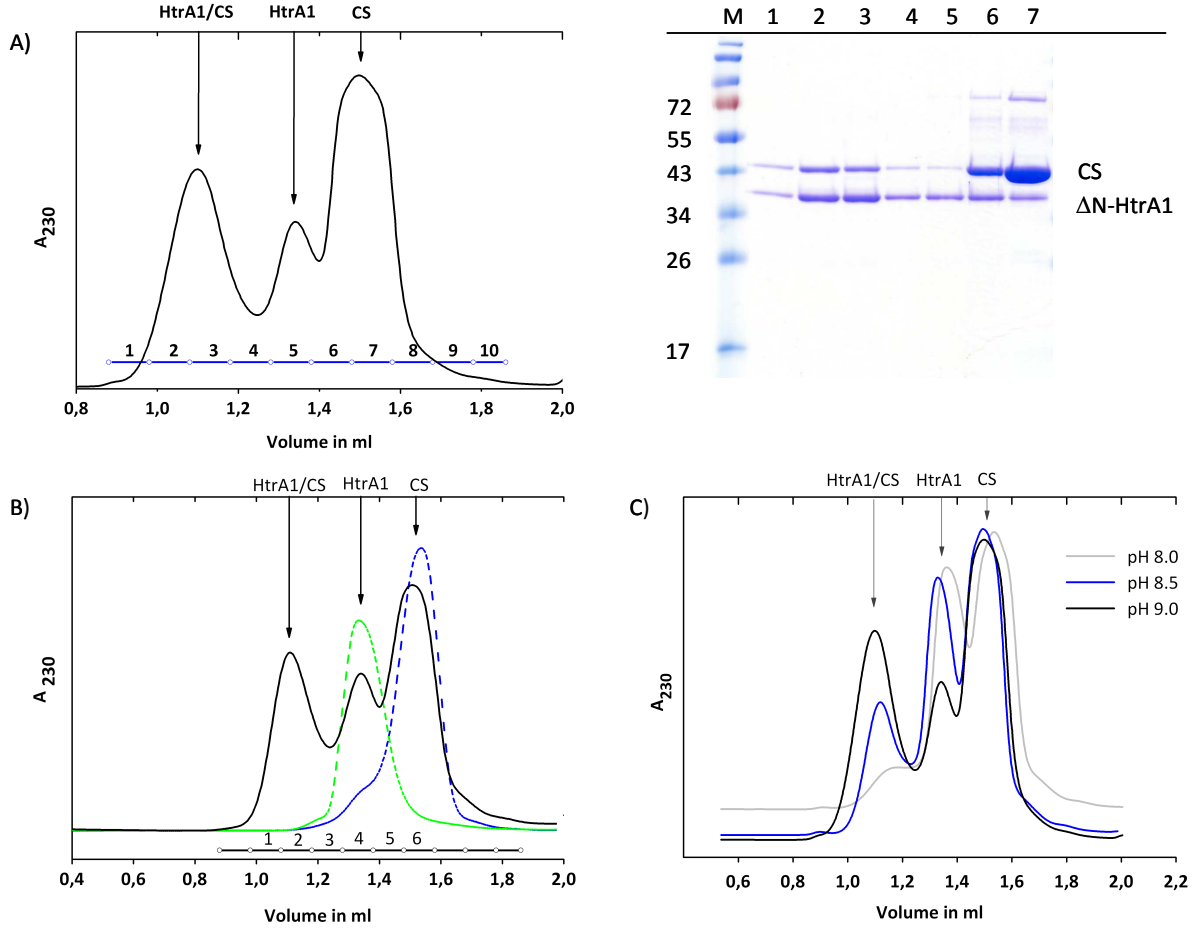

Fig. 4.11 SEC for ΔN-HtrA1$_{S328A}$ incubated with unfolded citrate synthase at pH 9
A) ΔN-HtrA1$_{S328A}$ was mixed with CS, incubated for 10 min at 42°C and injected to a SD 200 PC 3.2 Three peaks are labelled and fractions indicated were loaded on a SDS-PAGE. Fraction 2 and 3 show co-elution of HtrA1 and CS, fractions 4 and 5 show HtrA1 (trimer), fractions 6 and 7 show CS. B) Overlay of normalized elution profiles of ΔN-HtrA1 after incubation at 42°C (green dotted line) and CS (blue dotted line) if injected separately to SEC. Both elute as a single peak. C) PH dependent oligomer formation is shown. Black curve shows oligomer formation at pH 9.0, blue curve at pH 8.5 and grey curve at pH 8.

In a control reaction HtrA1 was incubated alone at 42°C or HtrA1/CS at 37°C and no complex formation could be determined by SEC which is consistent as CS starts to unfold at 42°C but is folded at 37°C. These data indicate that the HtrA1 trimer is transformed into a larger multimer in the presence of unfolded substrate. It can only be speculated if this multimer corresponds to a defined particle of HtrA1, e.g. a 12mer, or if HtrA1 is clustering around unfolded substrates.

The complex formation was additionally investigated for unfolded, denatured lysoyzme (Fig. 4.12) also showing a shift on SEC. No single peak for HtrA1 remained, as seen for the incubation with unfolded CS (Fig. 4.11 A), indicating that ΔN-HrA1 completely shifted into the oligomeric species. The complex fraction showed co-elution of both proteins as judged by SDS-PAGE (not shown). The elution fraction was taken for negative stain electron microscopy (Fig. 4.12). As judged from the picture the fraction reveals homogenous particles with a diameter of approx. 120 Å.

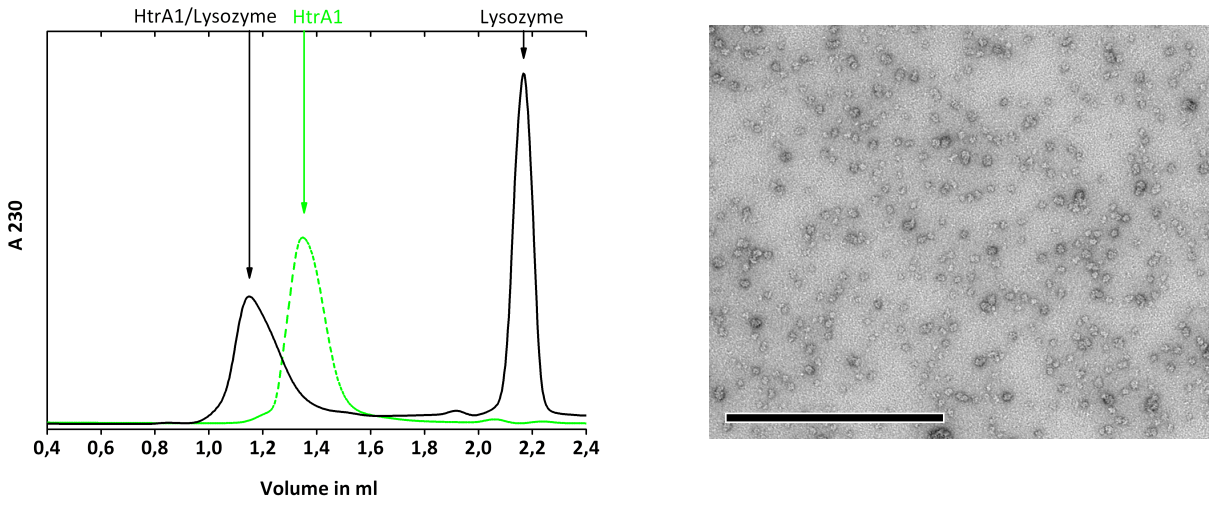

Fig. 4.12 SEC of ΔN-HtrA1 incubated with Lysozyme and negative stain of complex fraction
ΔN-HtrA1$_{S328A}$ was mixed with lysozyme, incubated for 10 min at 37°C and injected to a SD 200 PC 3.2. The peak containing HtrA1 and lysozyme was taken for negative stain. The green dotted line indicates the normalized elution volume of HtrA1 as a trimer if injected to the column separately without unfolded substrate. Electron microscopy revealed a homogeneous fraction showing defined particles with a diameter of approx. 120 Å. The scale bar refers to 100 nm.

Strikingly CS incubated at 42°C for 10 min and denatured lysozyme incubated at 37°C for 10 min precipitated as visible to the naked eye which could be prevented by the addition of HtrA1. Thus HtrA1 seems to prevent formation of aggregates and has the ability to keep unfolded proteins.

The formation of complexes with OmpA and ß-casein was also possible, nevertheless these complexes were not as stable as with CS or lysozyme as they could not be reinjected to the column without falling apart (data not shown).

Figure 4.13 shows that similarly to ΔN-HtrA1 HtrA1-prot does form a higher oligomer species. HtrA1-prot elutes with 1.51 ml, CS with 1.54 ml. Therefore the two peaks overlap and it can not be concluded that all of the protease shifts. As checked by SDS-Page both peaks contain both proteins indicating that not all of the protease shifts into the oligomeric species. The occurrence of the higher order oligomer suggests that the PDZ domains are not required to trigger HtrA1 assembly in multimers and should not be part of the newly formed multimeric interfaces.

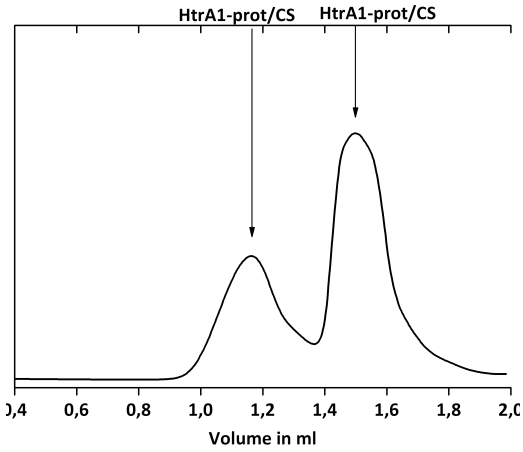

Fig. 4.13 SEC of HtrA1-prot incubated with unfolded citrate synthase at pH 9
HtrA1-prot was mixed with CS, incubated for 10 min at 42°C and injected to a SD 200 PC 3.2. Two peaks occur which contain both HtrA1-prot and CS as labelled above and checked by SDS-Page.

The complex fraction was re-applied to the column showing again the complex fraction but in addition a peak at around 1.5 ml corresponding either to HtrA-prot, CS or both (data not shown). This indicates that the complex is not as stable as for ΔN-HtrA1 as it tends to fall apart and points to a stabilizing effect of the PDZ domain or a function in binding substrates.

4.2.2 Dynamic light scattering

Dynamic light scattering was employed as a second method to determine the apparent molecular weight of ΔN-HtrA1$_{S328A}$ alone and in complex with citrate synthase in solution and additionally for HtrA1-prot. As the underlying physical principle is different to size-exclusion chromatography, the results should support the reliability of the previously determined molecular weights and should give an indication how likely the proteins will crystallize. Measurements for HtrA1 and complexed HtrA1 were carried out at 19°C and further processed with the program Dynamics 4.0 (Protein-Solutions Inc.) with the following results:

Tab. 4.1 Dynamic light scattering

Parameter	HtrA1$_{S328A}$	HtrA1$_{S328A}$ + CS		HtrA1-prot
R_H(nm)	4.81	3.30	9.62	3.80
MW (kDa)	133	55	673	77
C_P/R_H (%)	13.0	8.7	14.8	13.7
Baseline	1.002	1.001	1.001	1.001
SOS	14.87	15.62	15.62	17.81

Tab. 4.1 Dynamic light scattering R_H: hydrodynamic radius, MW: molecular weight, C_P/R_H: polydispersity index, C_P: standard deviation of R_H, SOS: sum of squared

The interpretation and the use of the statistical parameters as calculated by Dynamics 4.0 are given below. The values have been adapted from the DynaPro-801 Operator Manual:

Tab. 4.2 Interpretation and use of the statistical parameters as calculated by Dynamics 4.0 (Protein Sol. Inc.)

Parameter	Interpretation
Baseline	
0.977-1.002	Monomodal distribution
1.003-1.005	Bimodal distribution
>1.005	Bimodel/multimodal distribution
Sum of Squared (SOS)	
1.000-5.000	Low noise, negligible error
5.000-20.000	Background error owing to noise, low protein concentration or a small amount of polydispersity
>20.000	High noise/error owing to high polydispersity in size distribution (aggregation), irregular solvent
Polydispersity	Note: this parameter should be used for monomodal distribution only
C_P/R_H *<15%*	Monodisperse solution, likely to crystallize
C_P/R_H *<30%*	A moderate amount of polydispersity, possible to crystallize
C_P/R_H *>30%*	A significant amount of polydispersity, less likely to crystallize

Tab. 4.2 R_H: hydrodynamic radius, MW: molecular weight, C_P/R_H: polydispersity index, C_P: standard deviation of R_H, SOS: sum of squared

HtrA1-prot and ΔN-HtrA1 alone and in complex with CS show a monomodal distribution and a monodisperse solution. They can therefore be considered to crystallize which was tried for ΔN-HtrA1 and HtrA1-prot successfully. Furthermore the calculated molecular weight is close to the expected mass of 120 kDa for a ΔN-HtrA1 trimer and 75 kDa for a HtrA1-prot trimer. Analysis of samples containing ΔN-HtrA1 and CS showed two peaks in the corresponding graph (not shown). The values in the table show that the smaller peak could correspond to not complexed CS (free substrate) as the calculated MW is 55 kDa and therefore similar to a monomer of CS (45 kDa). The 673 kDa peak could correspond to a higher oligomeric particle of HtrA1 formed upon substrate binding. The mass for a HtrA1 12-mer is approx. 440 kDa suggesting that roughly 4 CS monomers would be bound to HtrA1.

4.3 Isothermal Titration Calorimetry (ITC)

PDZ domains are protein-protein interaction modules which bind the C-termini of target proteins. So far only little is known about peptides binding to the PDZ domain of HtrA1 and about the consequences for proteolytic activity. For the bacterial homologs like DegS and DegP it is known that binding of peptides to the PDZ domains can alter proteolytic activity or is necessary to activate the protease. For HtrA1 it was shown using phage-displayed peptide libraries that hydrophobic peptides with a broad range bind to the PDZ domain of HtrA1 (Runyon *et al.* 2007) and it was proposed that binding of peptides to the PDZ may alter proteolytic activity (Runyon *et al.* 2007). In order to identiy peptides binding to the PDZ domain of HtrA1 and to determine their binding affinity, ITC measurements with several candidate peptides were done. Candidates were chosen with regards to published data by Runyon *et al.* and known preferences from the bacterial homologs DegS and DegP (Hasselblatt *et al.* 2007, Krojer *et al.* 2008). The following peptides were tested and binding affinities determined if possible:

Tab. 4.3 Peptides tested in ITC and their calculated binding constants

Peptide	K_d (μM)
TPVFNTLPMMGKASPV (1637)	Nd
SPMFKGVLDMMYGGMRGYQV (2049, DegP ligand)	nd *
FANQHLCGSHLVEA (2327, HtrA1-pNA peptide)	nd *
HLVEALDMMYGGMRGYQF (2356, DegP ligand)	nd *
KKKKCQYYFV (2358)	181
KKKKDSRIWWV (2359)	21
QVVATATFRF (2371, DegS ligand)	nd *
DNRDGNVYQV (2377, DegS ligand)	nd
DNRDGNVFRF (2379, DegS ligand)	nd
DNRDGNVWWF (2380, DegS ligand)	nd
KGIKDVVTQPQA (2677)	nd

Tab. 4.3 ITC buffer contained 10 mM Hepes, pH 7.5 and 50 mM ammonium sulphate.
nd = not detectable, * indicates that 3% DMSO was necessary to dissolve the peptide

All peptides were used in a concentration of 300 µM and ΔN-HtrA1 with 30 µM. Four peptides (2049, 2356, 2327 and 2371) had to be dissolved in 3% DMSO to be solubilized (Tab. 4.3). To measure the affinity to HtrA1 the protein solution had to contain 3% DMSO. It can not be excluded that DMSO interfered with peptide binding and therefore no affinity could be measured.

Peptide 2359 was soluble in buffer without DMSO and was determined to bind with a K_D of 13.4 µM to ΔN-HtrA1. Subsequently the binding was furthermore tested for the methylated protein which showed comparable binding of the peptide with a K_D of 21 µM and demonstrated that methylation does not impair binding of peptides to HtrA1.

To clarify if the binding occurs to the PDZ domain and/or the protease domain of HtrA1, ITC was performed with HtrA1-prot. No binding could be observed in a µM range. The binding may occur in mM range but can not be determined with ITC due to the limitations in ITC which allows to measure affinities in µM range.

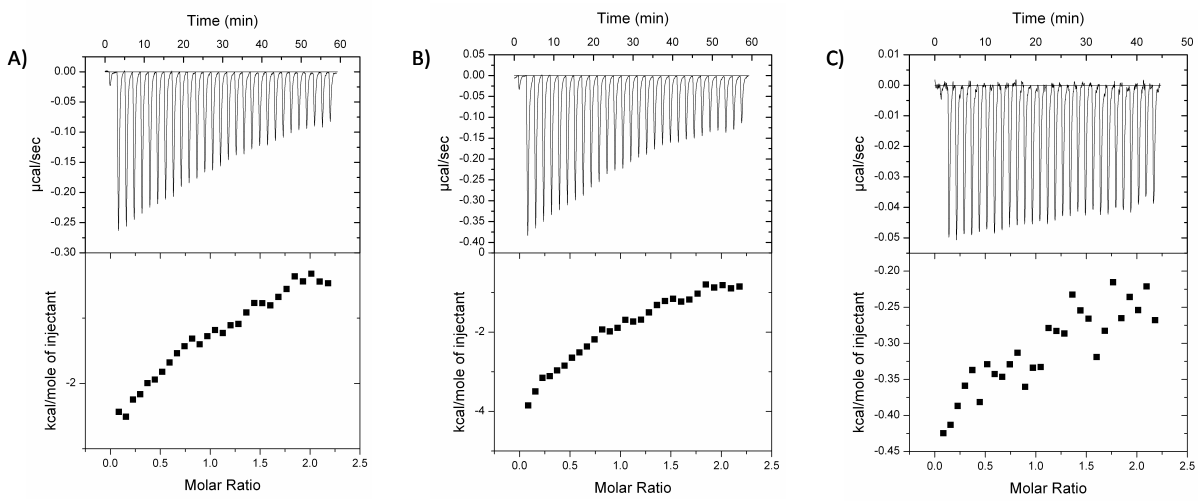

Fig. 4.14 ITC measurements with KKKDRSIWWV

A) 300 µM peptide was injected into the cell containing 30 µM ΔN-HtrA1$_{S328A}$. B) 300 µM peptide was injected into the cell containing 30 µM methylated ΔN-HtrA1S328A. C) 300 µM peptide was injected into the cell containing 30 µM HtrA1-prot$_{S328A}$. For evaluations the number of binding sites was fixed to N = 1; Kd = 1/K.

It would be interesting to evaluate the activation mechanism of HtrA1 as so far little is known. In analogy to the bacterial HtrAs the identified peptide which binds to the PDZ domain of HtrA1 would be a good candidate to further test the ability of this candidate peptide to activate HtrA1 (4.4.4) and /or to stabilize the PDZ domain in co-crystallization trials (4.7.4.2). Taken together the peptide KKKDSRIWWV is the first candidate for a peptide found via ITC to bind to the PDZ domain of HtrA1. It

would be interesting to do additional binding studies with the isolated PDZ domain of HtrA1 to confirm the results. Furthermore substitutions of amino acids at the C-terminus of the peptide would highlight the important residues for binding and would provide a detailed view into the binding mode.

4.4 Proteolytic activity of HtrA1

To characterize the proteolytic activity of HtrA1 ß-casein cleavage assays as well as assays with a chromogenic pNA-substrate were carried out. All assays were done with ΔN-HtrA1 and HtrA1-prot.

4.4.1 ß-Casein degradation

Time dependent degradation of ß Casein was followed on SDS-PAGE. Both HtrA1 variants degraded ß-casein highly efficient within 2 min (Fig. 4.15). The assay showed that the protease domain on its own retained proteolytic activity and can be considered to be as active as the wild type protein. This is in contrast to *E. coli* DegP and DegS, where the PDZ domain influences catalytic activity. The PDZ domain of HtrA1 seems to be dispensable for enzymatic activity. Despite the fact that full length casein is degraded equally fast, the subsequent cleavage of the casein degradation products is significantly faster with PDZless HtrA1 (Fig. 4.15).
The degradation products occurring in the ß-casein assay are similar for both HtrA1 variants, showing no influence of the PDZ domain on the overall size of the products.

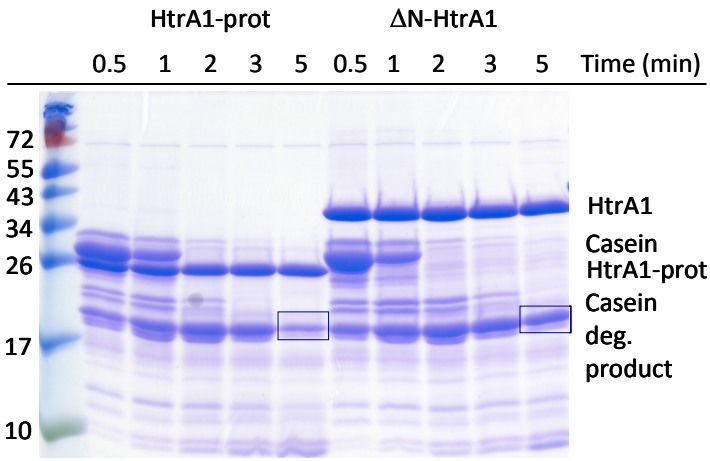

Fig. 4.15 ß-casein degradation by ΔN-HtrA1 and HtrA1-prot
Time dependent degradation of ß-casein was followed on SDS-PAGE showing that the substrate is efficiently degraded by HtrA1. 10 µM HtrA1 was incubated with 170 µM ß-casein at 37°C for the time points indicated and subjected to SDS PAGE followed by Coomassie blue staining. Blue boxes mark degradation products which occure during cleavage and are faster processed with HtrA1-prot.

To test if methylated ΔN-HtrA1 retained proteolytic activity this assay was performed in comparison to non-methylated ΔN-HtrA1. Methylated HtrA1 shows slightly decreased activity (Fig. 4.16). It can be concluded that methylation does not alter the activity towards ß-casein. Further tests were done with pNA as substrate as shown in 4.4.2. As expected, the methylated variant of ΔN-HtrA1 runs slightly higher in SDS-PAGE underlining that methylation occured.

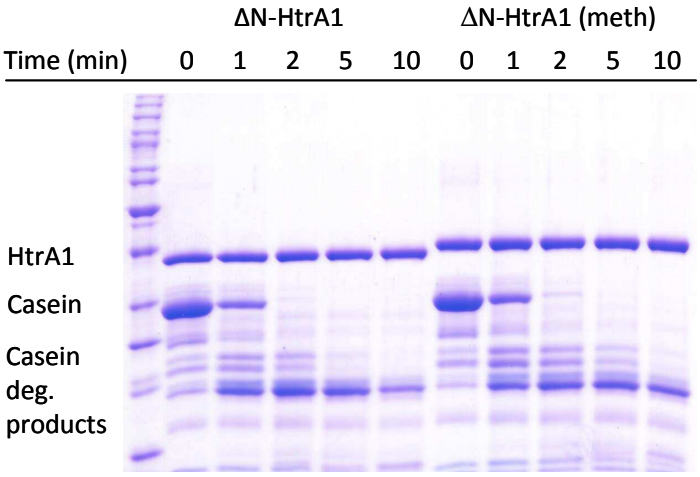

Fig. 4.16 Comparison of ß-casein degradation for methylated and not methylated ΔN-HtrA1
10 µM HtrA1 was incubated with 170 µM ß-Casein and samples were incubated for the time points indicated and loaded on SDS-PAGE followed by Coomassie blue staining. The methylated (meth) protein runs slightly higher due to methylated lysines. ß-Casein is degraded equally fast.

4.4.2 pNA – Assays

ß-casein assays have limitations because continuous measurements are not possible and analysis by SDS-PAGE is error prone. To overcome the disadvantages and to have the possibility to calculate specific activities of HtrA1 a pNA assay was established. Serine proteinase activity of the enzyme was measured by the release of p-nitroanilidine (pNA) from a peptide substrate. Several pNA´s available were tested and two could be taken for final measurements as they were processed by HtrA1. VFNTLPMMGKASPV-pNA was derived from the DegS substrate RseA and AC-FANQHLCGSHLVEA-pNA was derived from insulin-ß chain. Increasing release of pNA was monitored by spectrophotometry at 405 nm.

The pNA assays with the synthetic substrates shows that the rate of the degradation is affected slightly by deleting the PDZ domain suggesting that the PDZ domain does not contribute significantly to the enzymatic activity of HtrA1.

In figure 4.17 a pNA assay is shown for the wt of ΔN-HtrA1, methylated ΔN-HtrA1 and HtrA1-prot with the substrate VFNTLPMMGKASPV-pNA. The methylated protein as well as the HtrA1-prot showed decreased activity towards the substrate. After 60 min the absorbance at 405 nm is approx. 0.28 for ΔN-HtrA1 and 0.2 for methylated ΔN-HtrA1 and for HtrA1-prot.

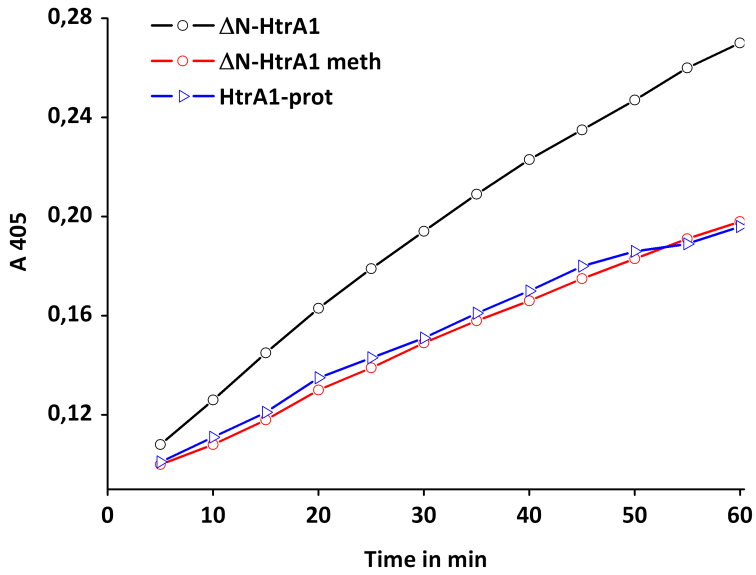

Fig. 4.17 pNA assay for different variants of HtrA1
10 µM wt ΔN-HtrA1, methylated ΔN-HtrA1 and HtrA1-prot were incubated with 500 µM pNA-substrate at 37°C. The absorbance at 405 nm was measured continuously and plotted against the time.

4.4.3 Inhibition of HtrA1

To test if the proteolytic function of HtrA1 can be inhibited, several boronic acid-based or chloro methyl ketone-based inhibitors were tested in ß-casein and pNA assays as they were describe as potential serine protease inhibitors (Kettner and Shenvi 1984). Inhibition could be observed by the use of the boronic acid derivative DPMFKLboroV as an inhibitor in a ß-casein degradation assay. At 10 fold molar excess inhibition could be observed as judged by SDS-PAGE (Fig. 4.19). Complete inhibition was achieved in the presence of a 42 fold molar excess of the inhibitor (not shown). The assay was carried out with methylated protein as an identified inhibitor should be taken for co-crystallization. The tested CMK inhibitor did form aggregates with HtrA1 (data not shown) and was therefore not considered for co-crystallization trials.

Taken together the peptide inhibitor was identified as one potent inhibitor and was subsequently tested for co-crystallization.

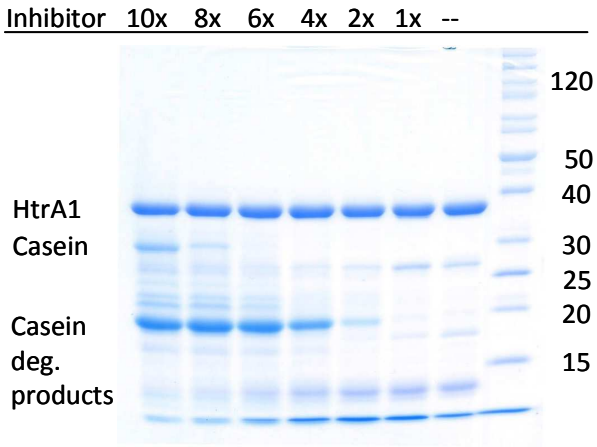

Fig. 4.18 Inhibition of ΔN-HtrA1 with DPMFKLboroV peptide
ΔN-HtrA1 was incubated with increasing amounts of the peptide inhibitor at 37°C. Molar ratios are indicated. Samples were taken after 10 min and subjected to SDS PAGE followed by Coomassie blue staining

4.4.4 Proteolytic activity in the presence of the peptide KKKDSRIWWV

The ligand KKKDSRIWWV (identified by ITC) was tested in ß-casein and pNA assays for the ability to activate HtrA1. Both assays show a minor activation of HtrA1. The activated wt protein degrades ß-casein completely within 8 min while the wt protein without peptide needs more than 10 min (Fig. 4.19). Although full length ß-casein is degraded equally fast with or without peptide, the regulatory effect can be seen for the occurring degradation products (see blue box on SDS-PAGE). Here the accelerated degradation is obvious when the peptide is added.

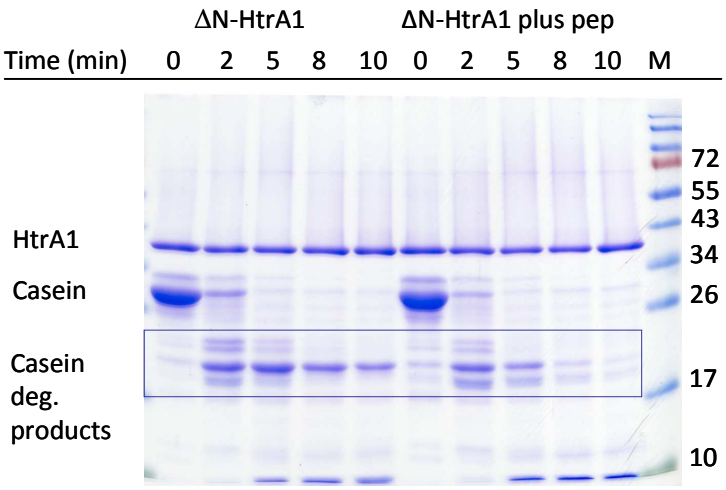

Fig. 4.19 Activation of ΔN-HtrA1 by KKKDSRIWWV
Incubation of ΔN-HtrA1 with peptide KKKDSRIWWV activates degradation of ß-casein. ß-casein was incubated with 10 µM HtrA1 with and without KKKDSRIWWV. Samples were taken at the time points indicated and subjected to SDS-PAGE following Coomassie blue staining.

The result is similar to the observed result for PDZless HtrA1 (Fig.4.16) which is degrading casein degradation product significantly faster. Activated ΔN-HtrA1 seems to act similar to PDZless HtrA1 (Fig. 4.16). The same assay was performed for HtrA1-prot, but no activation could be determined (data not shown).

A possible activation with the peptide KKKDSRIWWV was also investigated in a pNA assay. The assay was performed with different peptide concentrations ranging from 5 µM to 250 µM as the Kd of the peptide was determined determined to be 13.4 µM. 5 µM peptide is able to increase ΔN-HtrA1 activity up to 30% (Fig. 4.21) and ΔN-HtrA1 activity with 20% but did not activate HtrA1-prot. Higher peptide concentration than 10 µM did show only minor activation effects which could be explained with the reduced solubility of the peptide.

Based on this assay the specific activity of HtrA1 could be calculated as indicated in the following table:

Tab. 4.3 Specific activities of ΔN-HtrA1 and HtrA1-prot

	ΔAbs = m	**Δc/min**	**Kcat (µM x min^{-1})**	**spec. activity (pmol x min^{-1} x mg^{-1})**
ΔN-HtrA1	0,0036	1,36E-06	1,36	**37,06**
ΔN-HtrA1 + 5 µM pep	0,0047	1,78E-06	1,78	**48,38 (30%)**
ΔN-HtrA1 + 10 µM pep	0,0043	1,63E-06	1,63	**44,10**

	ΔAbs = m	Δc/min	Kcat (µM x min^{-1})	spec. activity (pmol x min^{-1} x mg^{-1})
ΔN-HtrA1 + 20 µM pep	0,0044	1,67E-06	1,67	**45,20**
ΔN-HtrA1 + 50 µM pep	0,0036	1,36E-06	1,36	**37,01**
ΔN-HtrA1 (meth)	0,002	7,58E-07	0,76	**19,94**
ΔN-HtrA1 (meth) + 5 µM pep	0,0024	9,09E-07	0,91	**23,92 (20%)**
HtrA1-prot	0,0023	8,71E-07	0,87	**34,99**
HtrA1-prot + 5 µM pep	0,0024	9,09E-07	0,91	**36,51**

Abs = absorbance, ΔAbs = m; Δc = ΔAbs / (8800 M^{-1} x cm^{-1} x 0.3 cm); Kcat = Δc x 106, specific activity in pmol= Δc/molecular mass (Da) x 1012 pep = KKKDSRIWWV

In contrast to ΔN-HtrA1, HtrA1-prot can not be activated with the peptide. This is in agreement with the observed ITC data which showed binding of the peptide only in presence of the PDZ domain. And with the ß-casein assays which did not show activation for HtrA1-prot when incubated with the peptide. Taken together these data imply an allosteric regulatory role for the PDZ domain concerning the activity of HtrA1.

4.4.5 Activation through oligomerization in the presence of model substrates

As shown in 4.2.1.1 there are indications that HtrA1 is able to oligomerize in the presence of unfolded substrate. Thus the influence of the presence of unfolded substrates on the proteolytic activity of HtrA1 was studied in a pNA assay. The assay was performed at 42°C as citrate synthase starts to aggregate at this temperature. The specific activity for HtrA1 was calculated at the steepest part of the curve shown in figure 4.20. ΔN-HtrA1 can be activated 2.7 fold when the release of pNA is measured in the presence of unfolded CS (Fig. 4.20 A). Consistently with the observed data from SEC HtrA1-prot can also be activated by binding unfolded substrates in the same order of magnitude. Interestingly no activation could be observed if the assay was performed in pH 7.5, a condition were no multimer can be observed in SEC (Fig. 4.12 C) and HtrA1 shows very low proteolytic activity (data not shown).

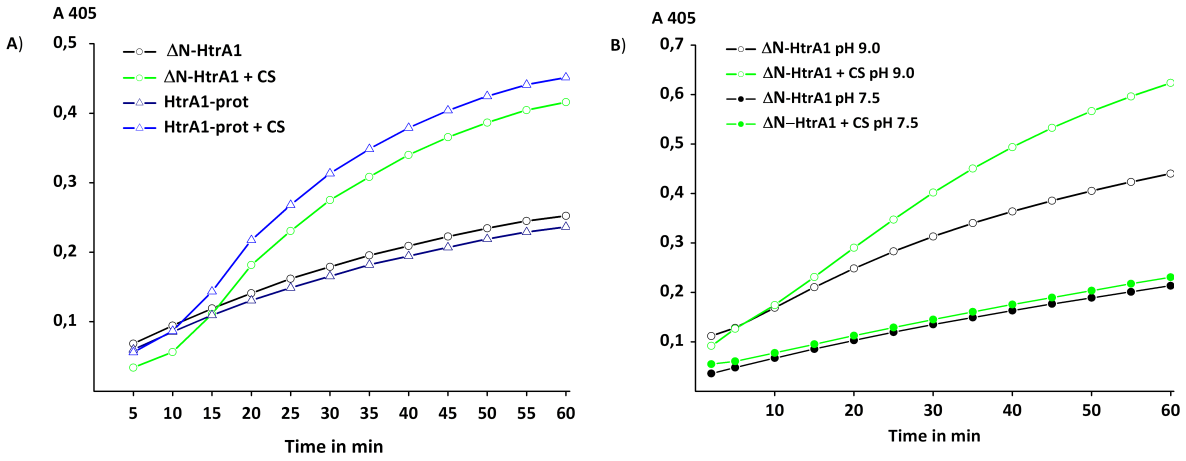

Fig. 4.20 pNA assay in presence of unfolded substrate citrate synthase
A) Activation of ΔN-HtrA1 and HtrA1-prot by unfolded citrate synthase is shown. Specific activity of ΔN-HtrA1 or HtrA1-prot was determined using VFNTLPMMGKASPV-pNA as a substrate in the presence and absence of heat denatured citrate synthase at 42°C. B) No activation was observed if the assay was performed at pH 7.5.

From the assay it can be speculated that oligomerisation might be a mechanism of activation independent of the PDZ domain as both variants show increased activation.

4.5 Complete digests of model substrates

4.5.1 Complete digests of citrate synthase and malate dehydrogenase

In order to identify the specificity of HtrA1 complete substrate digests heat denatured malate dehydrogenase (MDH) and heat denatured citrate synthase (CS) were performed. To reveal the identity of the peptide products they were analysed by mass spectrometry. Substrates were added in excess amounts and the reaction was incubated for 4 hrs or over night and followed in parallel by SDS-PAGE (not shown). Not digested substrate and HtrA1 itseld were precipitated with acetone. The complete digests were done with ΔN-HtrA1 and HtrA1-prot. The published primary sequences of the substrates were used to assign the molecular weights after mass spectrometry to the corresponding peptides. With both proteins a large number of different peptides were generated. However not all the peptides could have been detected by this method, where it was attempted to determine the composition of a complex mixture in a single step. Apparently, some peptides whose existence would be caused by a present neighbouring fragment were not detected. This is illustrated by the representative cleavage pattern of the citrate synthase (Fig. 4.21).

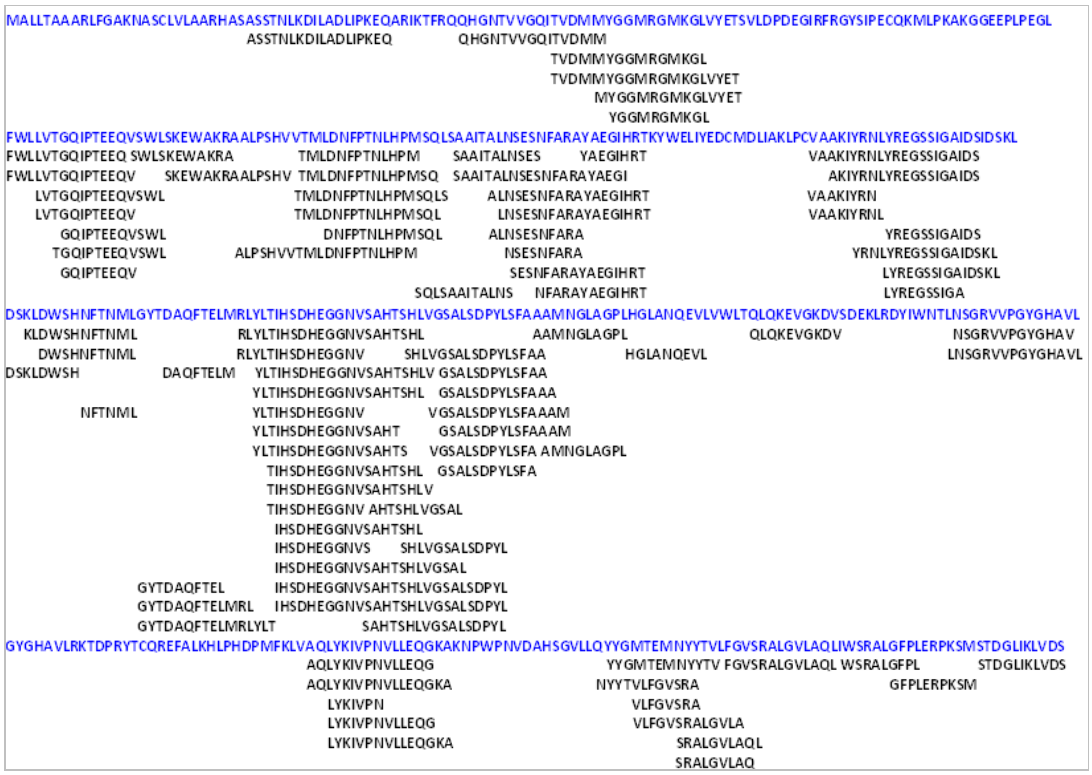

Fig. 4.21 Cleavage pattern of citrate synthase
Depicted are the peptides derived by degradation of heat denatured CS with ΔN-HtrA1.

Furthermore not all peptides were detected with the same reliability (data not shown). Especially larger peptides, containing more than 30 amino acid residues were rarely detected. However the vast majority was clearly detected, thus statistical parameters about the reliability of individual peptides were omitted in the analyses. This was also done with respect to the fact, that there is no clear cut-off value, which would allow a differentiation between a 'good' and a 'bad' peptide. In summary there were 206 peptides identified for ΔN-HtrA1, 67 for MDH and 94 for CS. For HtrA1-prot 60 peptides for MDH and 124 peptides for CS were detected. The evaluation of MDH and CS showed that the vast majority of the residues at the carboxy-terminus of the peptide fragments (P1 position) are small hydrophobic amino acids like leucine, valine, alanine and threonine (Fig. 4.22). This is in good agreement with previous studies for DegP (Krojer *et al.* 2008, Jones *et al.* 2002, Kolmar *et al.* 1996). Additionally a number of methionine, serine and isoleucine residues were identified, but other amino acids were only found occasionally.

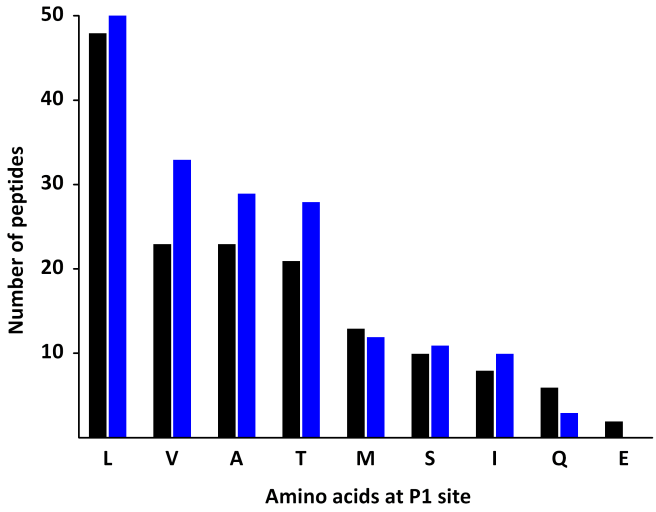

Fig. 4.22 Preferences for small hydrophobic residues at P_1 site
Sequence analysis of the identified peptides resulting from citrate synthase and malate dehydrogenase degradation revealed the specificity of HtrA1 for the P1 position of substrates. The observed P1-occurrences of the 9 most frequently identified amino acids are shown. Black bars indicate the results for ΔN-HtrA1, blue bars for HtrA1-prot.

Further analysis of the digestion pattern was conducted to characterize possible preferences for certain amino acids in the P1´ position (the position of the leaving group of the scissile bond according to the Schechter-Berger notation). The results of the analysis are shown in figure 4.23. Here the situation is not as clear as for the P_1 position. Although the majority of the amino acids belong to the class of small residues (S, A, V, L) a significant number belongs to bigger residues like lysine and tyrosine. The charge of the residues seems to be irrelevant.

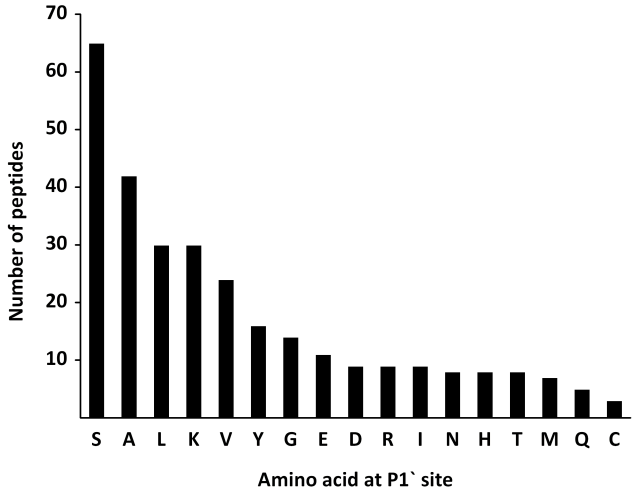

Fig. 4.23 Preferences at P_1´site
Sequence analysis of the identified peptides resulting from citrate synthase and malate dehydrogenase degradation revealed the preference of ΔN-HtrA1 for the P1´ position of substrates. The observed P1´-occurrences are shown.

4.5.2 Length distribution of degradation products

To further characterize the proteolytic activity of HtrA1, the length distribution of the degradation products for ΔN-HtrA1 and HtrA1-prot were analyzed. The majority of the generated peptides had a length between 6 and 30 residues for both proteins. Fragments longer than 25 residues were only occasionally detected and these peptides were most often of little reliability. Furthermore, no peptides shorter than six amino acid residues were found. In principle peptides shorter than six amino acids could have been produced but were not detected due to the identification technic.

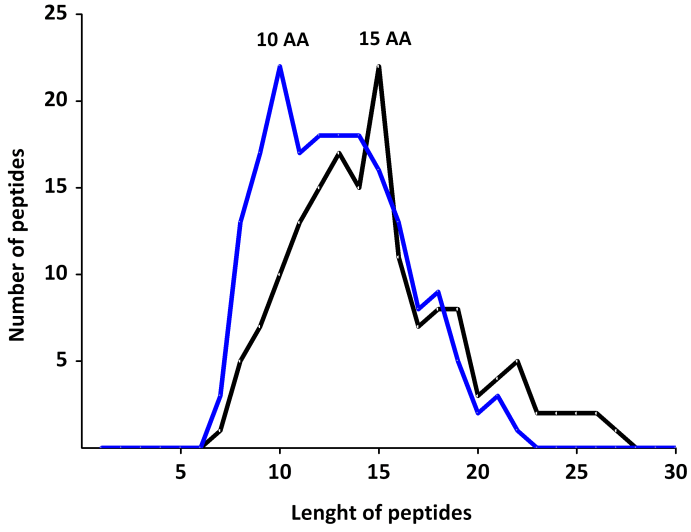

Fig. 4.24 Length distribution of peptide products generated in MDH and CS digests
Product sizes of complete digests of citrate synthase and malate dehydrogenase with wt ΔN-HtrA1 and HtrA1-prot were determined by mass spectrometry. The identified products were counted and plotted. The blue curve shows the results for HtrA1-prot, the black curve for ΔN-HtrA1.

Plotting the length of the peptide products (Fig. 4.24) revealed that the average length of the peptides was 15 residues for ΔN-HtrA1 and 10 residues for HtrA1-prot. This significant difference implicates a role for the PDZ domain in shaping cleavage products.

4.6 Liposome binding assay

ΔN-HtrA1 and HtrA1-prot were further characterized in liposome binding assays. The bacterial homolog DegP was shown to bind via its PDZ domains to liposomes. Thus liposome binding assays were conducted for ΔN-HtrA1 and HtrA1-prot to determine if the human homolog displays a similar behaviour and to study the role of the PDZ domains. Additionally the human homolog HtrA2 (lacking the first 133 N-terminal residues) was tested. Brain extracts from bovine were incubated with ΔN-HtrA1, HtrA1-prot and mature HtrA2 (Fig. 4.25).

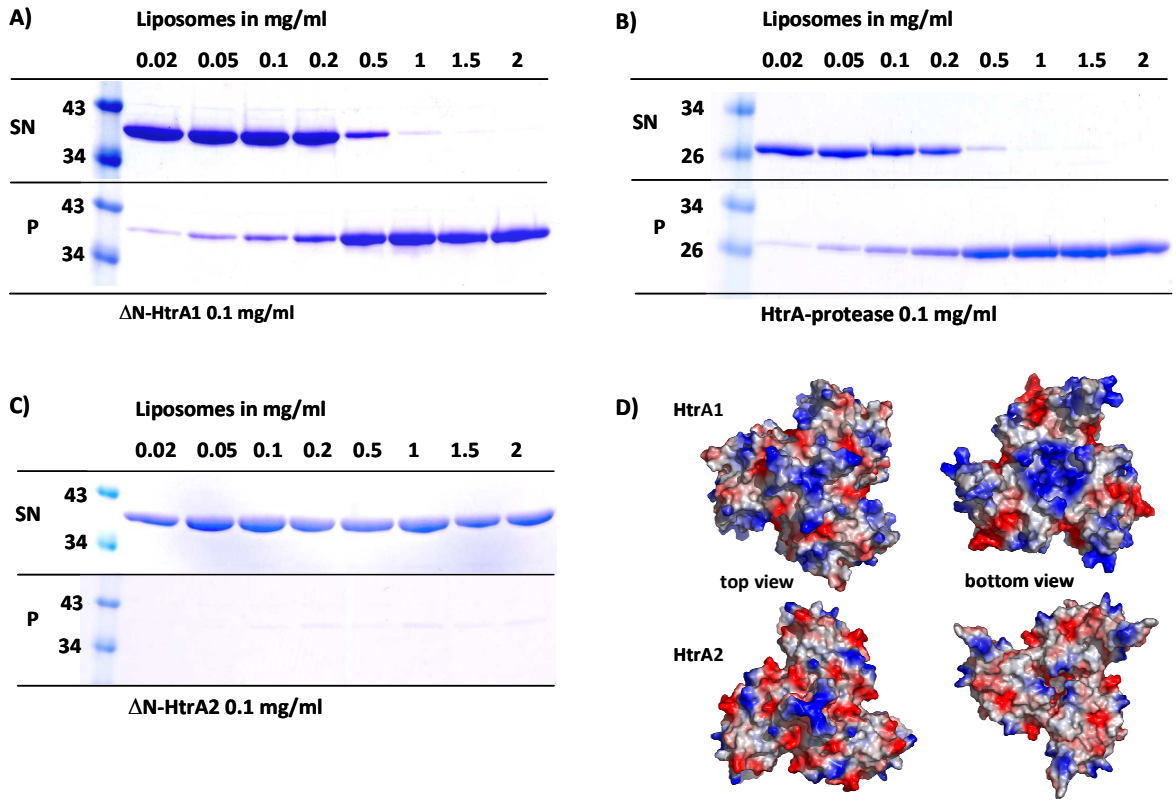

Fig. 4.25 Liposome binding assay
Co-sedimentation assays show binding of ΔN-HtrA1 and HtrA1-prot to bovine brain liposomes. Titration experiments were carried out with a fixed amount of HtrA1 and HtrA2 (0.1 mg/ml) and increasing concentrations of liposomes as indicated. HtrA1 and HtrA2 were incubated with liposomes 10 min at 37°C and ultra centrifuged for 30 min. "S" and "P" refer to proteins present in the supernatant or pellet after centrifugation. A) ΔN-HtrA1$_{S328A}$ B) HtrA1-prot$_{S328A}$ C) ΔN-HtrA2$_{SA}$ D) The electrostatic potential of the protease domains of HtrA1 and HtrA2

was calculated with PYMOL and mapped on the molecular surface of the particle. Red indicates negatively charged regions, blue positively charged regions. The protease domain is shown as a trimer in top and bottem view.

It could be shown that both HtrA1 proteins co-sediment with liposomes as the amount of protein increases in the pellet fraction with increasing amounts of liposomes. HtrA2 does not show binding to liposomes.

The obtained results indicate that the PDZ domains are dispensable for binding to liposomes as no differences between ΔN-HtrA1 and the protease domain could be observed. Analysing the surface potential of the protease domain of HtrA1 and HtrA2 identifies more positive charged residues for HtrA1 than for HtrA2 (Fig. 4.25 D) which could explain why HtrA2 does not co-sediment with liposomes.

4.7 Protein crystallization

4.7.1 Crystallization of ΔN-HtrA1$_{S328A}$

4.7.1.1 *Screening for initial crystallization conditions*

Initial crystallization trials were done in 96 well plates by using the commercially available Hampton Research Screens Index, Crystal 1 & 2, Membfac/Peg/Ion, Cryo 1 & 2, Wizard and from Jena Bioscience JBS 1 - 10. Initial screening was done first with the non methylated ΔN-HtrA1$_{S328A}$ and finally with the methylated mutant protein as non methylated protein did not produce a single hit in any screen. Crystalization trials were setup with the sitting-drop vapour diffusion method at 19°C and the drop ratio was 1:1 and 1:2, i.e. 0.1 µl of protein and 0.1 µl or 0.2 µl of reservoir solution in 96-well plates. The concentration of the protein solution was approx. 30mg/ml for all different crystallization trials. After approx. one week small cubic crystals appeared at 19°C (Fig. 4.26).

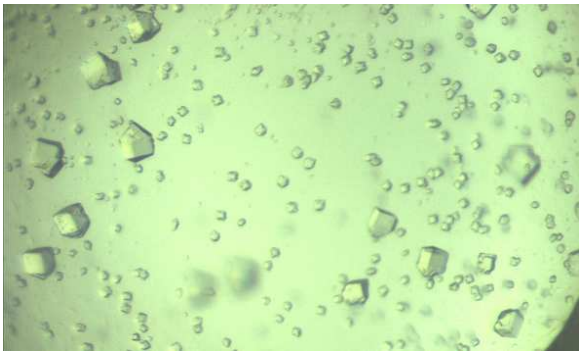

Fig. 4.26 Crystals from the initial crystallization condition in 96 well plates

Crystallization condition: 0.5 M $(NH_4)_2SO_4$, 0.1 M Na-citrate pH 5.4, 1 M $LiSO_4$

The crystals were stained with Izit (Hampton Research) to confirm that these crystals are made of protein. Interstingly, the same condition did not give any crystals for the methylated protein. Subsequently this condition was used for further fine-screening to obtain bigger crystals for testing their diffraction potential at the in-house x-ray generator.

4.7.1.2 *Optimization*

In order to grow bigger and more compact crystals, suitable for data collection, the components of the crystallization solution were varied, i.e. different buffer substances, different pH values and different drop ratios were tested. Moreover, a variety of additives, i.e. salts like $MgCl_2$ or organics like ethanol were added to the initial crystallization solution with a drop ratio of 2 µl of protein solution, 0.3 µl additive and 1 µl of reservoir solution. The final crystallization condition yielded compact cubic crystals grown in 24-well plates (Fig. 4.27).

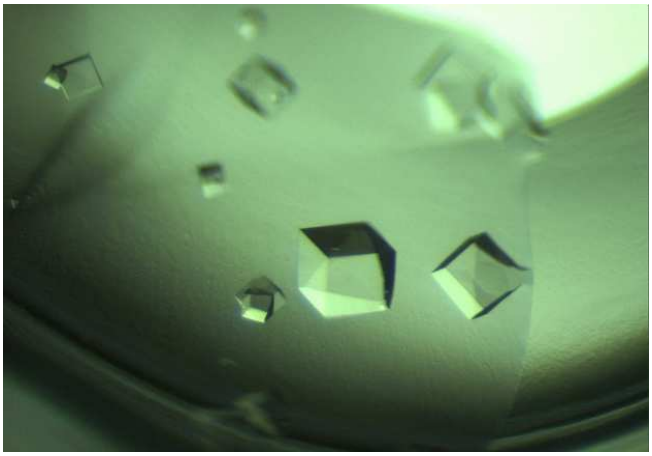

Fig. 4.27 Optimized crystals in 24-well plates
Crystallzation condition: 0.6 M $(NH_4)_2SO_4$, 0.1 M Na-citrate pH 5.4, 5.6, 5.8, 6.0 and 6.3, 1 M $LiSO_4$. Drop ratio: 2 µl $HtrA1_{S328A}$ (30 mg/ml) and 1 µl crystallization solution.

4.7.2 Crystallization of wt ΔN-HtrA1

The methylated wild type protein was crystallized in exactly the same refined conditions as described for the mutant version directly in 24-well plates and yielded crystals with comparable size and shape after 2 to 3 days.

4.7.2.1 *Co-crystallization of wt ΔN-HtrA1 with a boronic acid inhibitor*

The catalytically active methylated protein was furthermore co-crystallized with the DPMFKLboroV peptide containing a boronic acid group at the C-terminus. The aim was to lock the protease in an active conformation as boronic acids are described to bind covalently to the active site serine (Kettner and Shenvi 1984). The Ki of the boronic inhibitor was 2.6 µM as determined by using VFNTLPMMGKASPV-pNA as a substrate in an HtrA1 cleavage assay (personal communication) and inhibited ΔN-HtrA1 in a ß-casein cleavage assay as shown in 4.4.3. Inhibition was only achieved in the presence of a 10 fold molar excess of the inhibitor. This was taken into consideration when setting up crystal trials. The peptide inhibitor was co-crystallized in a 1:2 molar and 1:20 molar ratio and crystallization plates were set up with the same conditions as for the inactive mutant in 24-well plates. Successful crystallization was only achieved with 2 mM inhibitor concentrations. Quasi crystals appeared in the 1:20 molar ratio set up, showing no sharp edges and were not taken for refinement. Crystals for the 1:2 molar ration appeared after 2 to 3 days but no single crystals could be obtained as they were growing into each other (Fig. 4.28). They diffracted to 8 Å.

4.7.2.2 *Optimization of crystal quality with seeding*

Co-crystallization with the DPMFKLboroV peptide yielded crystals in the same conditions as mentioned for ΔN-HtrA1$_{S328A}$. Nervertheless these crystals had to be refined and the method of choice was seeding. Seeding allows one to grow crystals in the metastable zone. Crystallization in this zone provides control, reproducibility and an improved likelihood of a successful crystallization experiment. By placing a seed or solution of seeds in a drop which is saturated to the metastable zone, one can use the seeds to grow larger single crystals. By controlling the number of seeds introduced into the drop, one can control the number of crystals grown. Different dilutions of seeds were tested and crystal growth took 4 weeks yielding cubic single crystals with good diffraction properties.

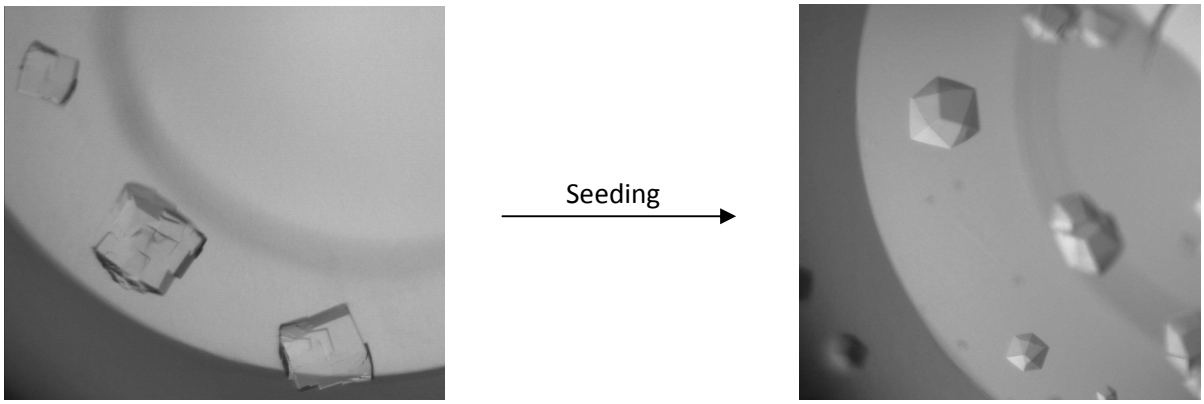

Fig. 4.28 Crystals can be improved by seeding
Drop ratio: 2 µl ΔN-HtrA1 incubated with inhibitor, 1 µl reservoir, 0.3 µl seeds 10^{-5} and 10^{-6} diluted in reservoir. Seeds were derived from co-crystals of wt HtrA1 and inhibitor.

4.7.3 Crystallization of HtrA1-prot

Crystallization of the protease domain of HtrA1 was done using the initial screens described for ΔN-HtrA1 crystallization with non methylated mutant protein. The protease domain crystallized in many different conditions and crystals were found in many different shapes like illustrated in examples in the figure below.

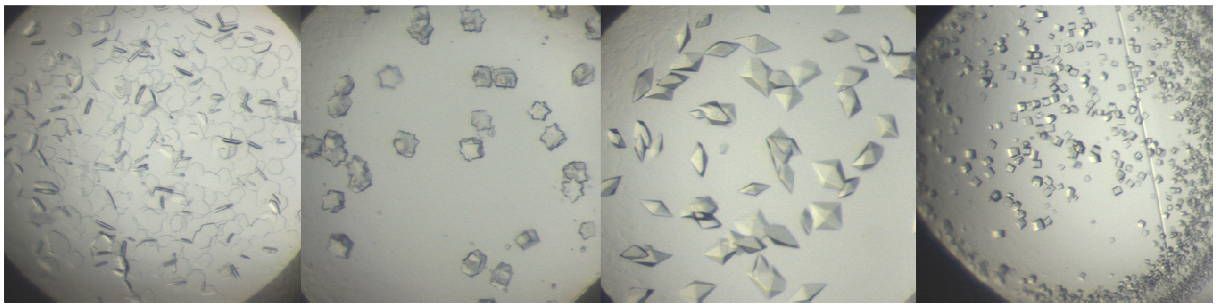

Fig. 4.29 HtrA1-prot$_{S328A}$ crystals from initial screens
Hexagonal plates, stars bipyramidal and cubic crystals were observed in many different conditions in initial screens. Fine screened crystallization condition contained 0.1 M Na-acetate pH 4.6 and 2 M $(NH_4)_2PO_4$.

Hexagonal and bipyramidal crystals were fine screened (see legend Fig. 4.29) and datasets for the bipyramidal crystals were collected and analysed.

All crystallization conditions had in common that the pH was around 5. HtrA1 was found to be not active at that low pH (data not shown) and conclusively the solved structure showed the protease domain in the inactive conformation. To promote the active conformation crystals were shifted from a low to a higher pH. There was no possibility to to collect x-ray diffraction data for these shifted crystals as they suffered too much in the new reservoir and broke.

4.7.4 Further improvement of HtrA1 crystals

4.7.4.1 *Improvement of diffraction properties*

The final electron density maps showed no clear density for the PDZ domain which had therefore to be omitted from the model. Nevertheless the maps for ΔN-HtrA1 showed a lot of additional density and the PDZ domain was tried to model in without success. Given the possibility that the PDZ domain is too flexible and stabilization could help to visiualize the domain, different optimization strategies were applied. The first possibility is to increase the resolution to be able to model the PDZ domain. Therefore strategies included crystallization at 4°C, shifting of crystals from 19 to 4°C as this might stabilize the PDZ domain and crystallization in hanging drops. The hanging drop method differs from the sitting drop method in the vertical orientation of the protein solution drop within the system. Nevertheless crystallization in hanging drops did not improve the resolution. Crystallization at 4°C was successful but gave neither a different unit cell nor better resolution. The crystals shifted from 19°C to 4°C kept growing for weeks and defracted to 2.5 Å. The structure was solved by moleculare replacement (MR) with HtrA1. Still these datasets showed no clear density for the PDZ domain.

4.7.4.2 *Co-crystallization of ΔN-HtrA1$_{S328A}$ with peptide KKKDSRIWWV*

Another strategy to stabilize the PDZ domain or to decrease the flexibility was the co-crystallization of ΔN-HtrA1$_{S328A}$ with the peptide KKKDSRIWWV which was found to bind to the PDZ domain by ITC measurements. Co-crystallization was carried out in a 1:1 molar ratio using 900 µM ΔN-HtrA1 and 900 µM peptide (i.e. > 50x Kd of the peptide) and crystals could be observed. They diffracted poorly and it was not possible to improve them. Crystals were also soaked with peptide. Some of the soaked crystals started to “melt” but one dataset could be collected. The crystal diffracted to 2.9 Å with very similar unit cell dimensions as for the crystals without peptide. The structure was solved by molecular replacement with the protease domain of HtrA1$_{S328A}$. The initial model showed no density for the PDZ domain.

4.7.4.3 *Crystallization of selenomethionine substituted wt ΔN-HtrA1*

HtrA1 contains six methionine residues one as the starting amino acid, four in the PDZ domain and one in loop L3 which is a mechanistically important loop. Methionine can be substituted by selenomethionine which anomalous scattering properties can be exploited for solving the crystallographic phase problem. The anomalous dispersion of the selenium atoms can be taken to

calculate initial phases. The crystals of the ΔN-HtrA1 wild type co-crystallized with the inhibitor peptide showed the protease domain in the active conformation. One characteristic of this conformation is that loop L3 and subsequently the methionine as well as the side chain are present in an ordered conformation. Semet-protein was successfully expressed, purified and co-crystallized with the inhibitor peptide. The dataset could be refined to 2.5 Å and the presence of selenium in the protein could be confimred by an absorption edge scan before proceeding with the MAD diffraction experiment. An X-ray absorption spectrum of the crystal was collected near the selenium K absorption edge by measuring the fluorescent signal perpendicular to the beam during an energy scan performed at the ESRF. Only very weak anomalous signal was detected and the position of the selenomethionine could not be determined.

4.8 Crystal structure of HtrA1

4.8.1 Data collection and structure determination

Data collection experiments have been performed at beamline ID 14-4 at the ESRF (Grenoble, France) to collect datasets for ΔN-HtrA1$_{S328A}$ and HtrA1-prot. The crystals were briefly soaked with cryobuffer before flash frozen in liquid nitrogen. The experiments were made with native crystals. All diffraction data were processed and scaled with the programs DENZO and SCALEPACK. All crystals of ΔN-HtrA1 belonged to the trigonal space group H3 with one ΔN-HtrA1 monomer in the asymmetric unit and unit cell constants of a = 108 Å b = 108 Å c = 113 Å and α = 90, ß = 90 and γ = 120. Data of improved ΔN-HtrA1-inhibitor crystals were collected at beamline X06SA at the SLS (Zurich, Swiss) at λ = 0.9724 Å using a Pilatus detector (Dectris). The crystals belonged to spacegroup H3 with slightly different cell constants of a = 105.965 Å, b = 105.965 Å, c = 118.336 Å.

Crystals of the protease domain belonged to the tetragonal spacegroup $P4_32_12$ with unit cell constants of a = 153.671 Å, b = 53.671 Å, c = 89.835 Å containing three molecules per asymmetric unit. A summary of the data collection statistics is given in Table 4.4.

Tab. 4.4 Summary of data collection statistics

Data Collection	ΔN-HtrA1 + inhibitor	ΔN-HtrA1$_{S328A}$	HtrA1-prot
Space Group	H3	H3	$P4_32_12$
Unit Cell Parameter Å	105x105x118 90x90x120	108x108x113 90x90x120	153x153x89 90x90x90
Resolution Å[1]	50 - 2.75	50 - 2.75	50 – 3.0
Completeness %	99.9 (99.9)	95.7 (87.5)	91 (89.1)
Rsym %[2]	7.2 (46.3)	6 (39.5)	10.2 (62.5)
I/sigma (I)	6.4 (3.9)	9.3 (3.9)	27.7 (25.3)
Redundancy	4.8 (5.1)	3.3 (3.3)	2.0 (1.7)

Tab. 4.4 Summary of data collection statistics [1]Numbers in parentheses refer to the highest resolution shell. [2]Rsym is the unweighted R-value on I between symmetry mates. Co-crystals with ΔN-HtrA1 and inhibitor showed the active conformation, the SA mutant of ΔN-HtrA1 and the protease domain showed the inactive conformation.

4.8.2 Structure solution

The structure for ΔN-HtrA1$_{S328A}$ and for HtrA1-prot were determined by molecular replacement (MR) using the program Phaser of the CCP4 package (CCP4, 2002) and the protease domain (residues 140 - 340) of human HtrA2 (Protein Data Bank ID 1LCY) as a search model. Human HtrA2 shows the highest similarity to human HtrA1. Electron density maps based on the coefficients 2Fo-Fc and 3Fo-2Fc were calculated from the phases of the initial model.

The structure of wild type ΔN-HtrA1 in complex with the inhibitor peptide was solved as well by MR with the protease domain of ΔN-HtrA1$_{S3298A}$ as a search model. Clear, additional density was observed in the active site and allowed insertion of the entire inhibitor molecule except the side chains of the P3-lysine and the P7-aspartate, which were replaced by alanine.

4.8.3 Model building and refinement

The program O was used for model building. For the ΔN-HtrA1$_{S328A}$ structures just one molecule was present in the asymmetric unit (AU). The electron density map was of good quality in the protease region but showed no clear density for the PDZ domain which had to be excluded from the model (residues 371 to 480). Additionally, the residues 158 to 160 and 301 to 314 (Loop L3) could not be fitted into the electron density. The current model has an R-factor of 25.43% (R_{Free}=28.52%).

For the ΔN-HtrA1-Inhibitor crystals also one molecule per asymmetric unit was present. During refinement of the HtrA1 inhibitor complex, clear electron density developed for one inhibitor molecule within the active site of the protein. In contrast to ligand-free HtrA1, the entire protease domain was well defined. Especially for the proteolytic site that underwent pronounced conformational changes remodeling was carefully inspected. In these maps, residues 158 - 159 and 371 - 480 had to be omitted from the model due to high flexibility. The current model has an R-factor of 22.38% (R_{Free}=27.82%)

For HtrA1-prot three molecules were present per AU which will be referred to as molecule A, B and C. Protein segments including residues 158–160, 301–314 (loop L3) and 365-373 were hardly visible or invisible and were therefore omitted from the model. The stereochemistry of all three models was validated with PROCHECK. The refinement statistics are summarized in table 4.5.

Tab. 4.5 Refinement statistics

	ΔN-HtrA1 + inhibitor active	**ΔN-HtrA1$_{S328A}$ inactive**	**HtrA1-prot**
Resolution Å	20 – 2.75	20 - 2.75	20 – 3.2
Rcryst/Rfree[1]	22.38 / 27.82	25.43 / 28.52	25.36 / 27.95
Number of reflections Rwork/Rfree	12208 / 651	11473 / 603	16725 / 900
Number of protein atoms / ligand atoms (C / N / O / S / B)	1013 / 275 / 304 / 1 35 / 7 / 8 / 1 / 1	946 / 249 / 281	914 / 239 / 266
Average B-factor protein / ligand Å^2	70.18 / 111	63.2	56.55
Root mean square deviations			
Bond *length* Å / angles Å / bonded Bs Å^2	0.0075 / 1.5 / 1.6	0.008 / 1.46 / 1.7	0.009 / 1.48 / 1.6
Ramachandran statistics %			
Most favoured / additionally allowed / generously allowed / disallowed region[2]	71 / 27.4 / 0.5 / 0.0	81.5 / 17.3 / 1.2 / 0.0	77 / 21.3 / 1.4 / 0.2

Tab. 4.5 Refinement statistics [1]$R_{cryst} = \Sigma_{hkl} \mid |F_{obs}(hkl)| - k|F_{calc}(hkl)| \mid / \Sigma_{hkl}|F_{obs}(hkl)|$ for the working set of reflections; R_{free} is the R-value for 5% of the reflections excluded from refinement. [2]The stereochemistry of the model was validated with PROCHECK.

4.8.4 Tertiary structure of the inactive HtrA1

Similar to other members of the trypsin family, the protease domain of HtrA1 is formed by two perpendicular ß-barrel lobes (β1−β6 and β7−β12) with an N-terminal and C-terminal helix. The

catalytic triad is located in the crevice between the two lobes (Fig. 4.30). The activation domain of the protease constituted by the active site loops L1, L2 and LD (nomenclature according to Perona and Craik 1995 and Krojer *et al.* 2008) is severely distorted impeding the proper adjustment of the catalytic triad, formation of the oxyanion hole and the S1 specificity pocket. For example, ß3 following the active site His220 is, causing an improper localization of His220 with respect to Asp250 and Ser328 (Fig. 5.3). Therefore, the protease domain is present in an inactive conformation. Furthermore, loop L3 that in HtrA proteases was too flexible to be traced in the electron density. A flexible loop L3 and in addition a misarranged activation domain are typical features of inactive HtrA protease states as previously observed in DegP and DegS (Krojer *et al.* 2002, Wilken *et al.* 2004).

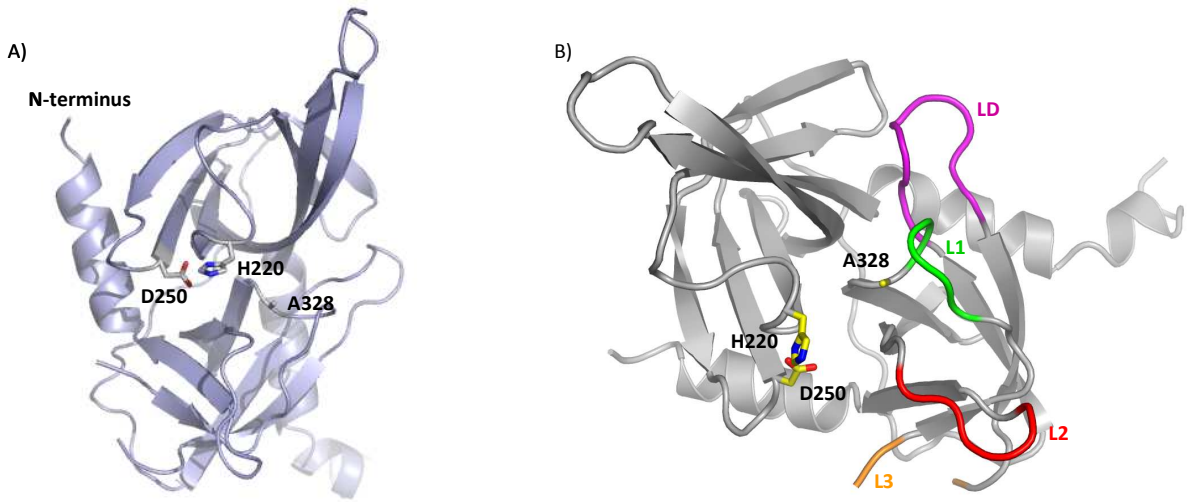

Fig. 4.30 HtrA1 in an inactive conformation
A) The active site is sandwiched between two ß-barrel lobes building up the HtrA1 protease domain. Residues of the catalytic triad are labelled and shown in ball and stick representation. Serine 328 is replaced by alanine. B) Mechanistically important loops are labelled. Note that loop L3 is not ordered and had to be omitted from the model.

4.8.4.1 *Assembly of the trimer*

Size exclusion chromatography revealed an apparent molecular mass of 120 kDa suggesting the presence of HtrA1 trimers (Mw 36.8 kDa) in solution. Consistently, in the crystals, three monomers are arranged around a crystallographic three-fold axis with the N-termini located to the opposite face as the active site. The PDZ domains were not defined by electron density.

Homotrimerization is mediated exclusively by the protease domain, in particular by N-terminal residues and ß-sheet interactions. At the top, three conserved residues, Tyr169, Phe171 and Phe278 from each monomer, stack against each other. They form a hydrophobic, aromatic cylinder at the interface of the HtrA1 monomers (Fig. 4.31). This interaction is further stabilized by H-bonds within ß-sheet 8 from each monomer and the side chain of Asp320 (Fig. 4.32). The side chain of Asp320 forms inter- and intramolecular H-bonds to the main chain amid of Ile296 and Thr294* in the

neighboring monomer. Furthermore, ß-sheet 8 from each monomer forms three hydrogen bonds to the adjacent monomer. Consistently, the HtrA1 trimer is remarkably stable in solution, even at low µM concentrations (e.g. 1.5 µM) no HtrA1 monomers could be detected by SEC.

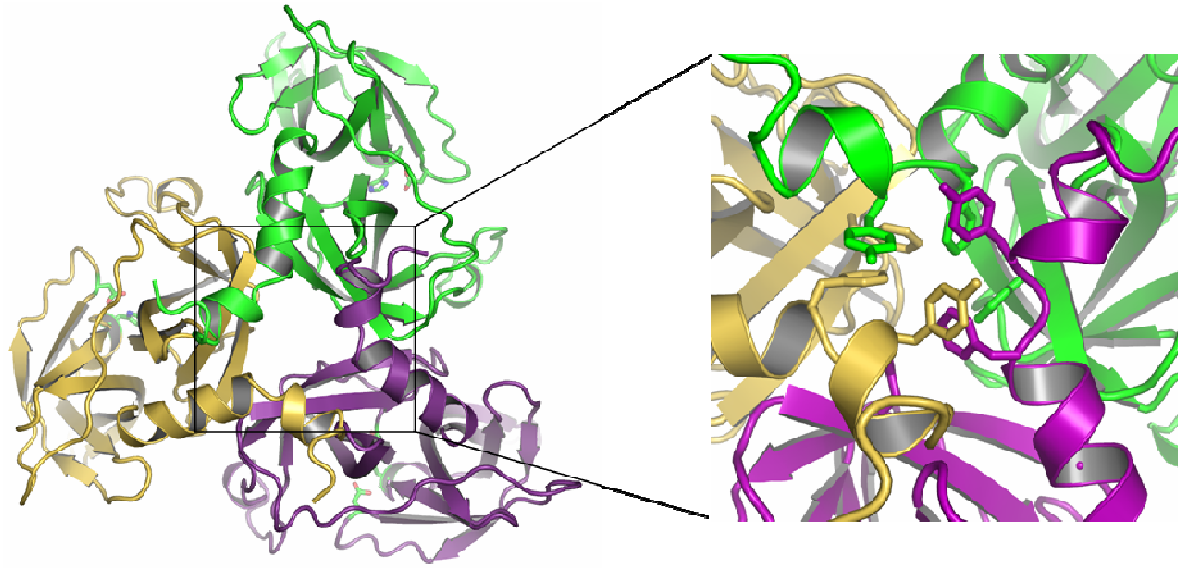

Fig. 4.31 Homotrimer formation in HtrA1 by conserved hydrophobic residues
A) Cartoon representation of the homotrimer from the top. The individual monomers are coloured differently. B) Close up view of the trimer interface. Residues Tyr169, Phe171 and Phe278 of each monomer form ring stacking interactions to build the homotrimer. These residues are presented in a ball-and-stick model.

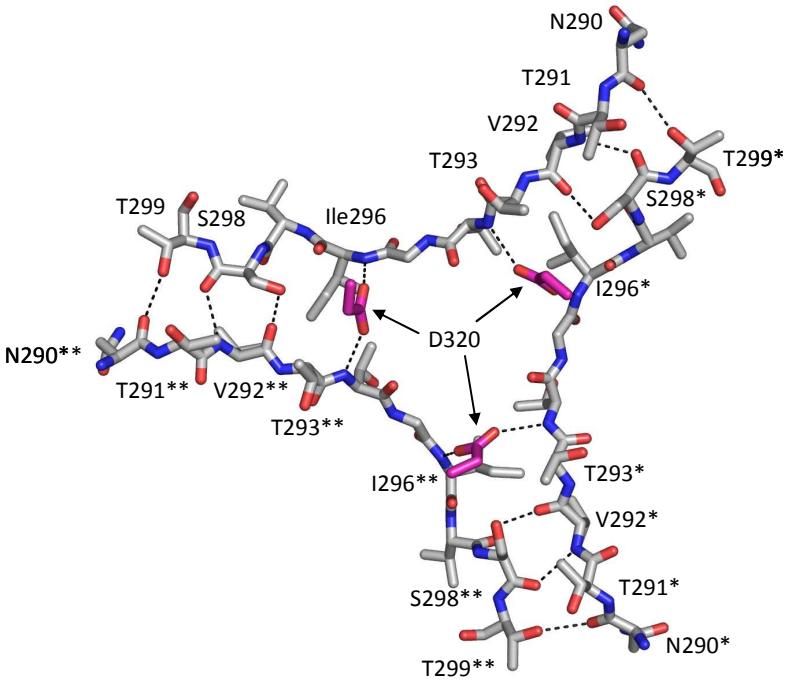

Fig. 4.32 Homotrimerization is stabilized by serveral hydrogen bonds
Residues are shown in ball and stick representation and labelled if they form hydrogen bonds to the neighbouring monomer. Residues of monomer 2 and 3 are indicated with * and **, respectively. Asp320 forms inter- and intramolecular hydrogen bonds thereby connecting two monomers.

4.8.5 Tertiary structure of the active HtrA1

The catalytically active protein was co-crystallized with the DPMFKLboroV peptide containing a boronic acid group at the C-terminus. After molecular replacement with the protease domain of HtrA1 clear, additional density was observed in the active site and allowed insertion of the entire inhibitor molecule except the side chains of the P3-lysine and the P7-aspartate, which were replaced by alanine.

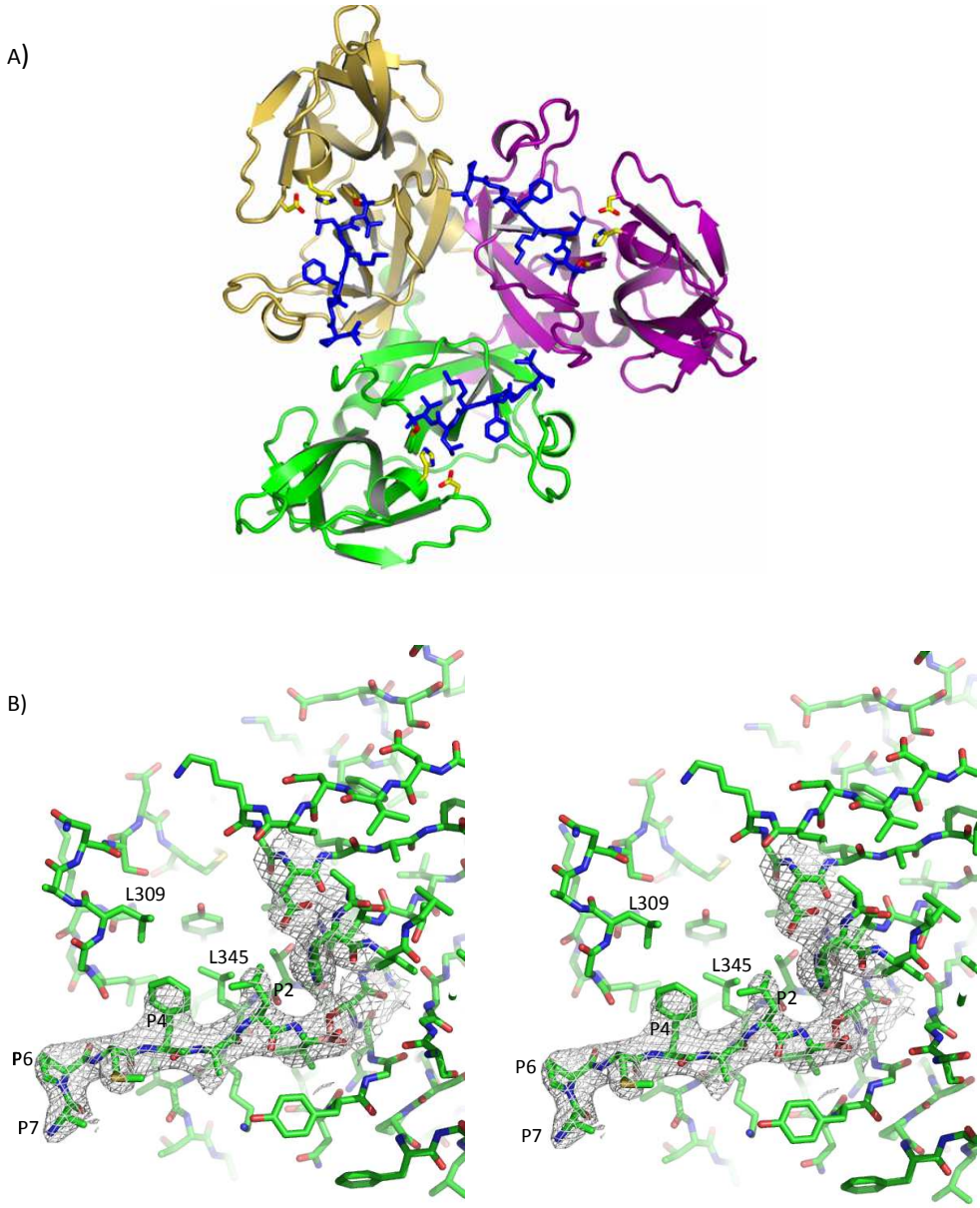

Fig. 4.33 The inhibitor peptide DPMFKLboroV is bound to the active site
A) Cartoon representation of the homotrimer shown from the bottom. Each monomer is coloured differently. The inhibitor peptide (blue) is bound to the active site. Inhibitor peptide and active site residues are shown in ball and stick representation. B) Stereo view. 2FoFc - electron density for the covalently attached inhibitor DPMFKLboroV, contoured at 1 sigma. The protease domain (green) and the inhibitor peptide are shown in ball and stick representation.

The inhibitor molecule is covalently attached to the active site Ser328 via the boronic acid group, forming a tetrahedral boronate complex (Fig. 4.33). The inhibitor undergoes numerous interactions with the protease domain. These interactions lead to a rearrangement of the active site loops (Fig. 4.34) converting the protease from the resting into the active conformation.

The active conformation was evident from the following observations: First, the active site residues His220, Asp250 and Ser328 reorient upon inhibitor binding and are now properly positioned to set up a functional catalytic triad. e.g. the interatomic distances between components of the His/Asp/Ser proton relay system are 2.65 Å between Asp250 and His220 and 2.87 Å between His220 and Ser328 in the active conformation (Fig. 4.34 A) while they are for example 9.5 Å between His220 and Ala328 in the inactive conformation. Second, loop L3 undergoes a disordered-order transition and is now present in a well-defined conformation contributing to a functional activation domain required for efficient protein cleavage. Third, a proper oxyanion hole is formed by the peptide stretch 325-327 preceding the active site serine. Formation of the oxyanion hole is achieved by a peptide flip of Gly326 (loop L1: Ile322-Ile323-Asn324-Tyr325-Gly326-Asn327) allowing accommodation of the O^- -group of the boronic inhibitor. In addition, the inhibitor is captured by participating in a composite hydrophobic cluster that is constituted by Leu307, Leu309 and Tyr316 (loop L3), Leu345, Thr344 and P2-Leu, P4-Phe of the inhibitor (Fig. 4.34 B).

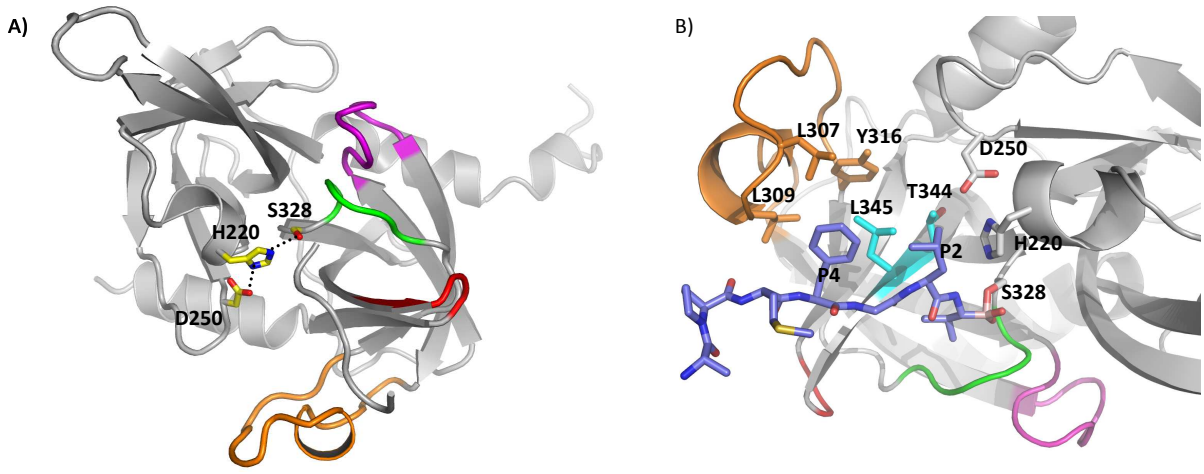

Fig. 4.34 Active conformation of HtrA1
A) The protease domain in the active conformation. Residues of the catalytic triad are shown in ball and stick representation. H-bonds are indicated. Mechanistically important loops are labelled. Loop L3 is now in an ordered conformation interacting with the inhibitor peptide. B) Close up view of the interactions between protein and inhibitor showing the hydrophobic cluster. P1-Val points into S1 specificity pocket; P4-Phe and P2-Leu undergo hydrophobic interactions with Leu305, Leu 309 and Tyr316 in loop L3 and Leu345 as well as Thr344.

Moreover, the P1-valine of the inhibitor is deeply buried within the S1 specificity pocket, which is formed by the aliphatic side chain of Lys346 and the side chain of Ile323 (Fig. 4.35). In figure 4.37 the interactions between the inhibitor peptide and HtrA1 are summarized.

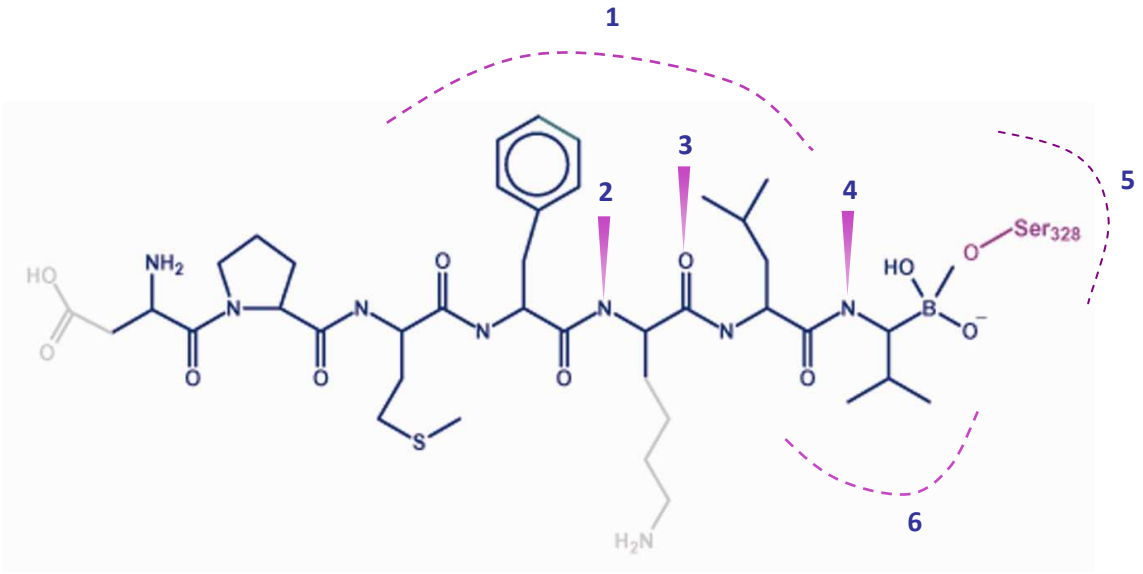

Fig. 4.35 DPMFKLboroV undergoes numerous interactions with the HtrA1 protease domain
Schematic view of interactions between protein and inhibitor was made with chemgraph. 1: P4-Phe and P2-Leu undergo hydrophobic interactions with HtrA1; 2, 3, 4: indicate hydrogen bonds to the backbone of HtrA1; 5: covalent binding of the boronic acid group to the carbonyl of the active site Ser328; 6: the P1-Val points into the S1 specificity pocket. In grey are the side chains of P3 lysine and P7 aspartate depicted which have been replaced by alanine in the structure.

5 Discussion

5.1 HtrA1 can be over expressed in and purified from *E. coli* cells

The N-terminus of HtrA1 comprises a Kazal-like inhibitory domain and an IGFBP-like domain containing 18 cysteines. So far these domains are uncharacterized as is was not possible to express and purify the full length protein in large amounts. Purification of the protein from insect cells resulted in small amounts not suited for crystallization (personal communication). It is very common for recombinant proteins expressed in *E. coli* to form insoluble, misfolded cytoplasmic complexes known as “inclusion bodies” (Mitraki and King 1989). Inclusion body formation is unpredictable but seems to increase in proportion to the size and complexity of the protein (LaVallie 2002).

One useful strategy to express proteins in *E. coli* cells is the fusion to proteins like GST, MBP or thioredoxin which may enhance solubility of the target protein. Even though there are studies on the effects of different tags the mechanism behind the solubilizing effect remains unclear (Dyson *et al.* 2004, Hammarström *et al.* 2006). In the case of thioredoxin, it has been proposed that it could exert its effect either by acting as a covalently linked chaperone (Berndt *et al.* 2008, Liu *et al.* 2007, Sun *et al.* 2007), aiding in protein folding, or as an oxidoreductase, which would catalyze the correct formation of disulfide bonds. Furthermore most proteins containing disulfide bonds require not only fusion to thioredoxin, but also expression in genetically modified *E. coli* strains having an oxidizing cytoplasm (e.g. Origami B(DE3) cells) (Peisley and Gooley 2007, Xiong *et al.* 2005, Lauber *et al.* 2001, Lehmann *et al.* 2003). This would suggest that thioredoxin could also be catalyzing proper disulfide bond formation. Nevertheless the expression in fusion with thioredoxin was described for proteins containing Kazal-type inhibitory domains (Vitzithum *et al.* 2008, Lauber *et al.* 2001). In this work His-tagged full length HtrA1 was not expressed in soluble form in BL21(DE3)pLysS cells, and only little expression was observed with expression in Origami B(DE3) cells as indicated by Western Blot analysis. However, a fusion construct comprising HtrA and a thioredoxin-tag showed dramatically improved expression in Origami B(DE3) cells. This suggests that thioredoxin promotes the solubility of HtrA1 by catalyzing proper disulfide bond formation.

To further investigate the folding status of full length HtrA1 different approaches could be considered. First of all it would be possible to map disulfide bonds and more easily to identify cysteines which are not involved in disulfide bond formation. Furthermore circular dichroism spectroscopy, a method to determine the secondary structure of proteins, could be applied to investigate the secondary structure of HtrA1. The N-terminus of HtrA1 was purified separately during this thesis and could be taken for these experiments in addition.

As the N-terminus contains a kazal-like inhibitory motif, it would be interesting to discover its inhibiting ability towards trypsin-like proteases. Possible candidates would be proteases from the ECM as HtrA1 is predicted to be secreted to the ECM. To establish an assay to show the inhibition of HtrA1 towards other proteases would be in addition a proof for HtrA1 to be folded.

Taken together, being able to express and purify full length HtrA1 from *E. coli* cells in large amounts offers for the first time the possibility to crystallize the protein in the future and to characterize it in detail. As the N-terminus shows an inhibitory motif for trypsin like proteases it would be interesting to assess the influence of this domain on HtrA1 itself as well as other trypsin like proteases especially in the ECM.

5.2 Inactive conformation of HtrA1

The basic building block for HtrA family members is a trimer as described for human HtrA2 (Li *et al.* 2002), the protease domain of HtrA from *Thermotoga maritima* (Kim *et al.* 2003) as well as for DegS and DegP from *E. coli* (Wilken *et al.* 2004, Krojer *et al.* 2002) and the HtrA protease from *M. tuberculosis* (Mohamedmohaideen *et al.* 2008). Homotrimerization was also observed for HtrA1. Interactions between monomers include hydrogen bonds and hydrophobic interactions as shown in Fig. 4.31 and 4.32 for the inactive conformation.

The inactive conformation of ΔN-HtrA1 shows a misarranged activation domain as well as a flexible loop L3 and therefore typical features of an inactive HtrA protease as described for DegP (Krojer *et al.* 2002) and DegS (Wilken *et al.* 2004). Another typical feature for inactive serine proteases is a not properly formed oxyanion hole. This characteristic is described for human HtrA2, HtrA from T. maritima and inactive DegS. Here the NH donor of residue 193 (using the trypsin nomenclature) is flipped to the opposite side of the protein backbone. Therefore an oxyanion intermediate can not be stabilized (Fig. 5.1 A).

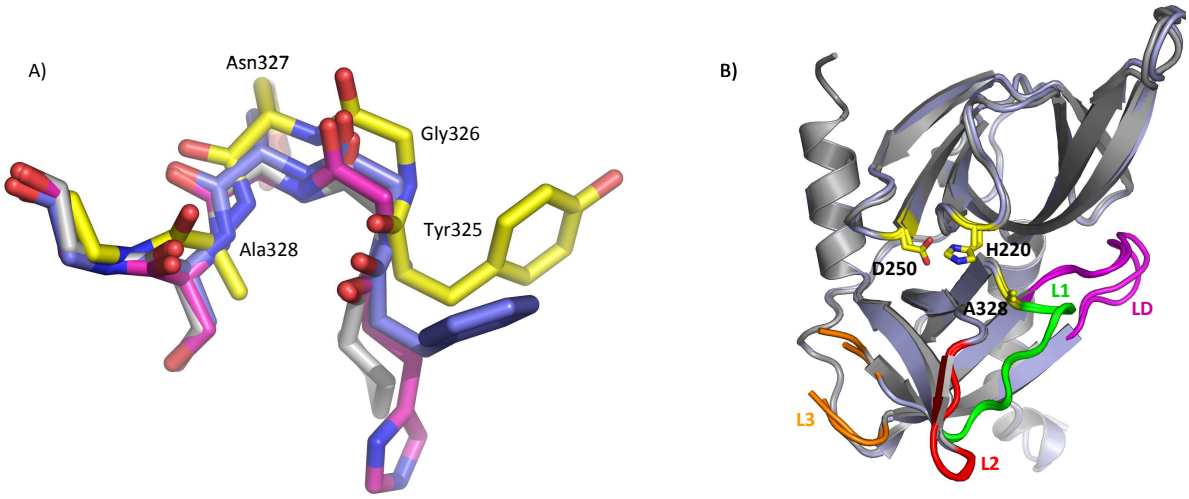

Fig. 5.1 Inactive conformation of HtrA1
A) Alignment of human HtrA2 (blue, residues 170-174, PDB entry code 1LCY), HtrA from *T. maritima* (grey, residues 203-207, PDB entry code 1L1J), inactive DegS from *E. coli* (magenta, residues 198-202, PDB entry code 1SOT) and human HtrA1 (yellow, residues 325-329) B) Alignment of inactive and active conformation of human HtrA1 (yellow and green respectively). The structures of the protease domain of HtrA1 (light blue) and for the inactive mutant of ΔN-HtrA1 (grey) are superimposed. Mechanistically important loops are indicated: loop L1 in green, loop L2 in red, loop L3 in orange and loop LD in magenta. The side chains for catalytic triad are shown in stick and ball mode. Note that loop L3 is disordered in both structures.

A superimposition of the structures of the HtrA-prot and ΔN-HtrA1 shows that both proteins are present in an inactive conformation (Fid. 5.1 B). They align with an rmsd of 0.6 Å showing no significant differences neither for the loops setting up the catalytic site nor for the remaining part of the protease domain. As the protein without the PDZ domain is active it would have been also possible to observe the active conformation. Loop L3 is not defined in both inactive conformations of ΔN-HtrA1 and HtrA1-prot therefore a possible interaction with the PDZ domain and any influence on the conformation of the protease domain can not be discussed.

5.3 Active conformation of HtrA1

To solve the crystal structure of an enzyme-inhibitor complex is a general tool to assess the mechanism of a certain enzyme. Here ΔN-HtrA1 was co-crystallized with a boronic acid based inhibitor. Peptide boronic acids are described as potent proteasome (Adams *et al.* 1998) and serine protease inhibitors (Bode and Huber, 2000). The inhibition can take place in two different modes. Boronic acids which are analogues of substrates bind in a canonical manner with the boron atom

covalently attached to the active site serine. In contrast boronic acids which are not substrates analogous can form complexes with the active site histidine (Bachovchin *et al.* 1988).

The first mode is characterized by several inter-main chain hydrogen bonds of the inhibitor with proteinase binding sites. The scissile peptide bond is partially added to the active site serine. The P1 side chain is pointing into the S1 specificity pocket. Altogether the peptide inhibitor undergoes numerous substrate-like interactions (Bode and Huber, 2000).

The peptide boronic acid DPMFKLboroV interacts with HtrA1 in a canonical mode. Three hydrogen bonds between P1, P2, P3 and the backbone of HtrA1 in beta sheet 11 stabilize the binding of the inhibitor (Fig. 5.2 A). The boron atom is covalently bound to the active site serine forming a tetrahedral state with the O^- stabilized by hydrogen bonds in the oxyanion hole and the P1 residue pointing into the S1 specificity pocket (Fig. 5.2 B).

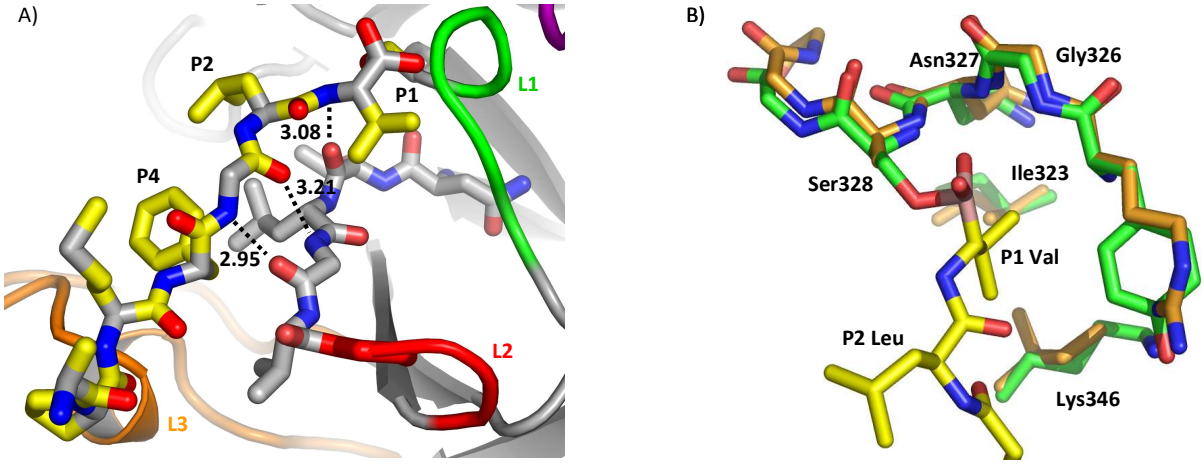

Fig. 5.2 Binding of the peptide boronic acid inhibitor in a substrate like manner
A) Residues are shown in stick and ball presentation. Loop L1 (green), L2 (red), and L3 (orange) are indicated. The peptide inhibitor is hydrogen bonded to residues in beta sheet 8 binding in a canonical fashion. B) The peptide inhibitor is covalently attached to the active site serine. B) The O^- of the boronic acid is stabilized by hydrogen bonds in the oxyanion hole. Residues are despicted in stick and ball mode, HtrA1 protease residues in green (325-329 in loop L1 and Ile323 and Lys346 building the S1 specificity pocket), inhibitor residues in yellow (LboroV). The DegP active conformation of loop L1 (residues 207-211, PDB entry 3CS0) is superimposed in orange.

Interestingly, the bacterial homologs of HtrA1 exhibit exactly the same active site geometry in their respective active states. In the activated form of DegS and DegP the backbone atoms are rearranged and loop L1 adopts a conformation similar to trypsin. This can be also observed for HtrA1 (Fig. 5.2 B).

A structure based sequence alignment with homologues of HtrA1 indicates that residues Ile323 and Lys346 are equivalents of the positions 192 and 216 in trypsin-like serine proteases and Ile205 and Ile228 in DegP. These amino acids usually extend into the S_1 pocket, where they partially or fully block access to the base of the pocket. For HtrA1 it can be proposed that the conserved isoleucine and the aliphatic side chain of lysine play a similar role in the active protease, providing the basis for

the interaction with small, hydrophobic P_1 residues of substrates. Consistent with this notion, complete digests of CS and MDH indicated a corresponding preference (Fig. 4.21). Consistently, DegP has a preference for an aliphatic β-branched residue such as valine at the P_1 position but no obvious preference for the P_1' position (thesis Tobias Krojer, 2004) which is also true for HtrA1 (Fig. 4.22).

More interestingly the peptide inhibitor was able to trigger the active conformation of HtrA1. This was also possible even though HtrA1 shows no proteolytic activity at pH 5.4 to 6.3 where co-crystallization trials were set up. Superimposements of the active conformation of HtrA1 with the active conformations of DegS and DegP shows that loops L1 and LD aligned perfectly to each other and loop L2 and L3 aligned in the stem region (Hasselblatt *et al.* 2007, data not shown) which is confirming the active conformation of HtrA1. Nevertheless the HtrA structures also display significant differences in their active site architecture. Sequence alignments of human HtrA1 and HtrA2 and *E. coli* DegP and DegS, illustrate that the human proteins exhibit specific truncations in several loop regions with respect to DegP including for example loop L3 which shows an insertion of 5 amino acids for HtrA1 in comparison to DegP. In contrast loop L2, which determines the substrate specificity, consists of only 2 residues in HtrA1 and shows an insertion of three amino acids for DegS compared to DegP. Loop LA is completely absent in human HtrA1 and HtrA2.

For DegP the release of loop LA from the active site of the opposite monomer is crucial to obtain the active conformation. During oligomerization conformational changes take place which lead to the release of loop LA. Subsequently loop L1 can fold into the turn structure needed to build up a proper oxyanion hole (Krojer *et al.* 2008).

For DegS Loop L3 is communicating with the PDZ domain sensing a bound stress peptide and interacting with the -1 position in the peptide. Thereby loop L3 undergoes conformational changes which lead in turn to the rearrangement of loops L1, L2 and LD and an active site conformation.

In the HtrA1 structure co-crystallization with the peptide inhibitor leads to a disorders orderd transition of loop L3. This is due to hydrophobic interactions with the inhibitor peptide at position P4 and P2 and leads to the rearrangement of loop L1 and a proper set-up of the oxyanion hole (Fig. 5.3 A) as well as loop L2 and LD. The catalytic triad residues are hydrogen bonded (Fig. 5.3 B).

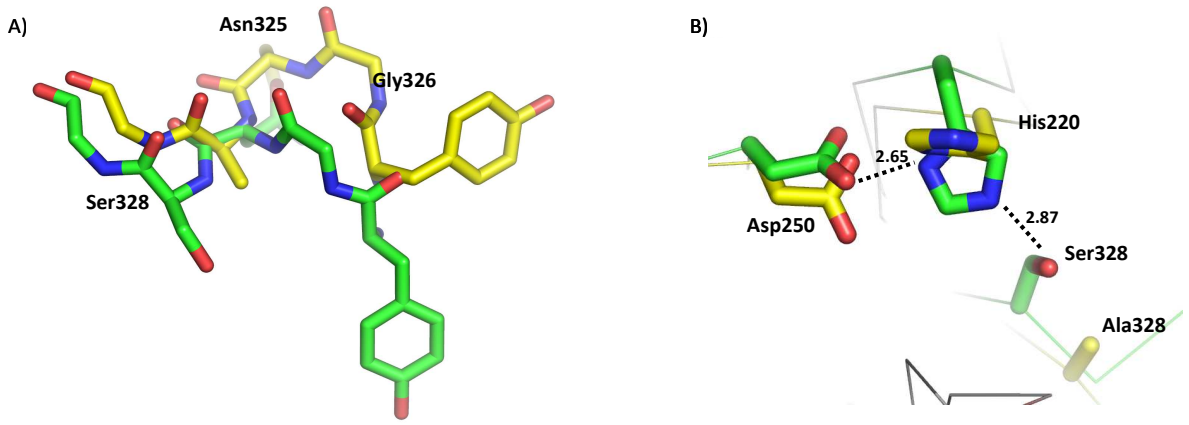

Fig. 5.3 Conversion from the inactive to the active conformation
A) Residues of the catalytic triad are shown in stick and ball presentation. Green residues confirm the active residues for the active conformation, yellow residues for the inactive conformation. In the active conformation Asp250 is in hydrogen bond distance to His220 and His220 to Ser328. In the inactive conformation Ser328 is replaced by Ala328. B) Formation of the oxyanion hole. Loop L1, residues 325-329 of inactive and active conformation.

In the active conformation loop L2 undergoes interactions with L1 in the adjacent monomer. The side chain of Thr348 in loop L2 interacts with the side chain of Asn324* (L1*) in the adjacent monomer. L1 forms also intramonomeric interactions with loop LD as Tyr325 (L1) interacts with Phe286 in loop LD. In comparison in the inactive conformation Tyr325 in loop L1 interacts with Thr348* in loop L2*. Loop L2 is 'longer' in the inactive conformation as some residues of it are part of ß sheet 11 in the active conformation.

It is quite remarkable that there was no electron density for the PDZ domains of HtrA1 in the active state. Thus conversion from the inactive into the active state is triggered without contribution of the PDZ domains. This is in contrast to all data published for structures of human or bacterial family members including tmHtrA, HtrA2, DegP and DegS (MohamedMohaideen *et al.* 2008, Krojer *et al.* 2008, Kim *et al.* 2003) where the protease-PDZ interplay is critical for enzymatic regulation. For example, in DegS, the PDZ domain regulates the proteolytic activity by offering a binding site for an allosteric peptide activator that signals protein folding stress. Moreover, in the non-stress situation, i.e. in the absence of an activator, the PDZ domain is required to keep the protease in the resting state (Wilken *et al.* 2004, Hasselblatt *et al.* 2007, Walsh *et al.* 2003). In contrast, DegP employs its PDZ domain 1 for processive substrate degradation by an interdomain protease-PDZ molecular ruler (Meltzer *et al.* 2008, Krojer *et al.* 2008). Furthermore, the PDZ domain 1 of DegP is directly involved in the conversion of the resting hexamer into the functional 12- and 24-mers by stabilizing the DegP12/24 interfaces. Finally for human HtrA2 it was proposed that the PDZ domains restrict entry to the active site thereby exerting an inhibitory effect on the catalytic activity (Li *et al.* 2002). Consequently HtrA2 shows increased activity in ß-casein digests when PDZ domain deletion

constructs are incubated with the substrate. HtrA2 exhibit full enzymatic activity only when activating peptides bind to the PDZ domain (Li *et al.* 2002).

For HtrA1 slightly increased activity could also be examined for ß-casein degradation but not for degradation of substrates like unfolded CS, MDH or Lysozyme.

Because the PDZ domains were not defined by electron density it can be concluded that they do not block the active site as observed in human HtrA2. Most likely they protrude outwards as suggested by the crystal packing.

Inhibition by the peptide inhibitor is achieved when added in more than 10 fold molar excess to HtrA1. The inhibitor binds with a Ki of 2.6 µM as determined in pNA cleavage assays (personal communication). Optimized boronic acid inhibitors containing analogous for good peptide substrates are bound in a range of 0.1 to 20 nM (Kettner *et al.* 1984). Thus the binding and inhibition of the inhibitor could be optimized. Two conclusions can be drawn from the binding mode of the peptide inhibitor for the design of improved versions of the inhibitor. First interactions between inhibitor and protease domain are mainly mediated by the side chains of threonine at P2 and phenylalanine at P4 position. A network of hydrophobic interactions formed with loop L3 and these two residues seems to be important and help to order loop L3. Second the phenylalanine at P4 position seems to be "squeezed" between the inhibitor backbone and beta sheet 8 of the protease domain as it is slightly bended (Fig. 4.34). The substitution with a smaller hydrophobic residue like valine or isoleucine could improve the binding features. Conclusively when analysing the complete digests of CS and MDH for the P4 position mainly small residues as leucine followed by serine, threonine, alanine, glycine and valine were found.

5.4 Role of the PDZ domains

Much effort was spent into the determination of the structure and position of the PDZ domains in order to clarify their role for HtrA1. As discussed above the absence of intramolecular interactions between protease and PDZ domain is in contrast to all known structures of human or bacterial family members.

Biochemical assays with ß-casein showed that for HtrA1 the PDZ domains are not required for proteolytic activity. For the bacterial homolog DegP the PDZ domains are indispensable for proteolysis (Krojer *et al.* 2008). Deletion constructs of DegS and human HtrA2 which lack their

respective PDZ domain show moderate proteolytic activity if lacking the PDZ domain (Li *et al.* 2002) and are only fully enzymatic active if activated with peptides binding to the PDZ domains. In assays with the synthetic substrate VFNTLPMMGKASPV-pNA the rate of the substrate degradation is slightly decreased by deleting the PDZ domain suggesting that the PDZ domain does not significantly contribute to the activity of HtrA1. In pNA assays with VFNTLPMMGKASPV-pNA as substrate and 5 µM of the peptide KKKDSRIWWV which was shown to bind to the PDZ domain of HtrA1, protease activity could be activated but with 30% activation was only marginal increased. Increased activity was not observed for HtrA1-prot. ITC measurements indicate that the PDZ domain is required for the binding of peptides. Taken together this would lead to the conclusion that the PDZ domain like in related structures is important for binding peptides and for modulating protease activity. Further experiments with different and optimized peptides have to be done.

In complete digests of denatured MDH or CS it became obvious that the PDZ domain has in addition an influence on the length of the peptide products. Peptides derived with HtrA1 lacking the PDZ domain appeared to be 5 AA shorter. In DegP PDZ and protease domain cooperate to cleave substrates in a processive manner (Krojer *et al.* 2008). Substrates are held by the PDZ domain and cut by the protease domain. One possible explanation for shortened peptides in HtrA1-prot cleavage assays could be that one catalytic side is holding the substrate instead of the PDZ domain. In agreement the catalytic sites in a HtrA1 trimer are separated by approx. 30 Å and could thus be bridged by a 10 amino acid peptide (Fig. 5.4).

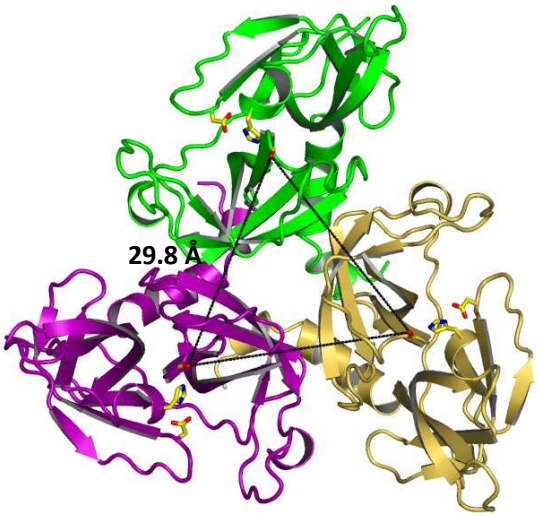

Fig. 5.4 Distance of the active sites in HtrA1 trimer
The trimer of the protease domain is shown as cartoon, coloured differently for each monomer. The catalytic sites are shown in stick and ball presentation. The triangle indicates the distance from one active site serine to the active site serine in the adjacent monomer which is calculated with 29.8 Å.

HtrA1 was found to build a homotrimer in inactive and active conformation. Interactions with the PDZ domains could not be determined due to the high flexibility of the domains. According to the model of DegP it could be speculated that the PDZ domains maintain interactions to form a 12mer of HtrA1. That would explain why they were found to be highly flexible in a trimer. In contrast HtrA1 incubated with the peptide found via ITC to bind to the PDZ domain of HtrA1 does not trigger oligomerization as concluded from SEC (data not shown). Furthermore PDZless protein forms higher oligomers. Therefore co-crystallization with an unfolded substrate like CS or lysoyzme would be an aim for the future to get insight into action of the PDZ domain. On the other hand given the results that the PDZ domain is dispensable for oligomerization and enzymatic activity one could speculate that the PDZ domains are required for tethering HtrA1 to the places within the cell where HtrA1 is required. Chien *et al.* showed recently that HtrA1 is located to microtubules and that the PDZ domain is indispensable for location (Chien et al. 2009).

In ß-casein cleavage assays ΔN-HtrA1 was decelerated in cleaving ß-casein degradation products compared to PDZless HtrA1 which higly efficiently cleaved the degradation products. As a certain cleavage product remained over minutes (Fig. 4.15) one could speculate that the PDZ domain is holding cleavage products which are not immedeatly further processed by the PDZ domain as indicated in the figure below. To date it is completely unknow if this model is true and for whatever function this feature would be necessary.

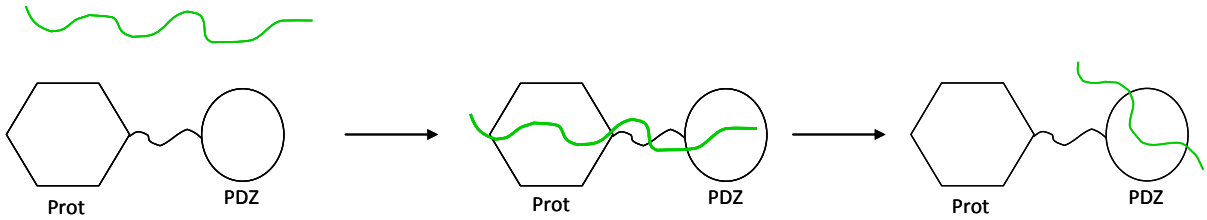

Fig. 5.5 Role of the PDZ domain
Unfolded substrates (green) are bound by protease and PDZ domain. After cleavage the peptide product remains bound to the PDZ domain.

5.5 Quaternary structure of HtrA1 in solution

Through size-exclusion chromatography and dynamic light scattering measurements, it could be verified that ΔN-HtrA1 is predominantly present as a trimer in solution. Interestingly, higher molecular species could be detected in the presence of unfolded substrates. It was shown that these

species emerge in the presence of denatured and unfolded lysozyme, CS, bacterial OmpA and ß-casein. So far no studies are available describing a high oligomeric state for HtrA1 or a human homolog in solution. For the bacterial homolog DegP it has been confirmed that it exists either as a hexamer in solution (Sassoon *et al.* 1999), but that it forms 12 and 24meric particle (Kim *et al.* 1999, Krojer *et al.* 2008). For DegP this conversion into a higher oligomeric state is accompagnied with a structural conversion of an inactive into an active proteolytic site as DegP converts from the inactive resting state (hexamer) into the active form as 12- or 24mer. Thus it is tempting to speculate that the detected oligomer for HtrA1 represents a conserved form of activation. Comparison of the elution volumes for DegP 12mer and HtrA1 show that DegP elutes slightly earlier from the column (1.08 ml DegP12mer, 1.22 HtrA1 oligomer with CS) corresponding to a difference of approx. 70 kDa. This is in agreement with the fact that DegP contains two instead of one PDZ domains (approx. 10 kDa) compared to HtrA1. Thus the species could represent a 12mer of HtrA1. Additionally this finding is supported by preliminary EM data showing particles with a diameter of 120 Å, which is comparable to the diameter of 160 Å for a DegP 12mer (Krojer *et al.* 2008). Furthermore in pNA assays activity increase in the presence of unfolded CS. To draw conclusions about the stoichiometry of HtrA1 and the substrate is rather difficult. DLS measurements reveal a particle with 670 kDa which would correspond to a 12mer of HtrA1 and 4 molecules of unfolded CS.

For DegS and HtrA2 no chaperone activity has been reported but for DegP and HtrA from *T. maritima* experiments demonstrated that this protein also possesses both functionalities (Kim *et al.* 2003, Spiess *et al.* 1999). For HtrA1 it became obvious that during incubation with lysoyzme and CS HtrA1 is able to keep both proteins in solution and to prevent aggregation a fact that points towards an activity of HtrA1 to suppress aggregation of unfolded substrates, most likely by encapsulating unfolded proteins.

DegP is capable to form 12 and 24meric particles depending on the concentration and the size of the substrate (Krojer *et al.* 2008). However both PDZ domains are involved in 24mer formation whereas the crucial contacts in the 12mer are entirely formed via the PDZ1 domain (Krojer *et al.* 2008). For HtrA1 only one oligomeric species could be observed in the presence of unfolded protein, which corresponds to the fact that it contains only one PDZ domain and thus may only be able to form 12meric complexes.

For DegP the PDZ domains are indispensable for oligomerization (Sassoon *et al.* 1999). In contrast for HtrA1 it was shown in this thesis that the PDZ domain is dispensable for oligomer conversion i.g. also without the PDZ domain higher oligomeric species could be determined. These species elute later from the column (1.18 ml) corresponding to a molecular mass difference of approx. 75 kDa. It turned

out that this complex is less stable compared to the one with the PDZ domains. When a previously isolated complex was reinjected to the column a significant amount of trimeric HtrA1-prot and CS occurred. In pNA assays the activity of HtrA1-prot was increased if incubated with unfolded CS. This suggests a new mechanism of activation due to the fact that the PDZ domains can not be part of the new interface in a higher oligomer of HtrA1-prot.

At this point further experiments will be necessary to clarify if the 12mer is one existing form for HtrA1 and for HtrA1-prot. Cryo EM studies could be one possibility. Obviously it would be absolutely interesting to solve the crystal structure of a HtrA1 12mer to get insight into the mode of action of HtrA1.

5.6 Possible activation mechanisms

Finally the question arises how HtrA1 activity is regulated. What could be the activation mechanism and how could HtrA1 be controlled? If it would be possible to control the proteolytic activity of HtrA1 it could be a good candidate for therapeutical interventions as HtrA1 was shown to be upregulated during arthrits (Grau *et al.* 2005) and ageing (Ly *et al.* 2000) and downregulated during Alzheimers`s disease (Grau *et al.* 2005). For several members of the HtrA family activation mechanisms have been described. DegP is controlled by temperature DegS by binding of substrates to the PDZ domain, HtrA2 by the binding of trimeric ligands (Li *et al.* 2002). Recently it was proposed that HtrA from *Mycobacterium tuberculosis* is regulated by auto proteolysis (Mohamedmohaideen *et al.* 2008) as in both the active site and the binding site of the PDZ domain auto proteolytic peptides were found. During purification of full length HtrA1 strong auto degradation was observed for the wt protein resulting in a fragment comprising the C-terminal protease and PDZ domain. The N-terminus of HtrA1 contains a predicted Kazal-like inhibitor domain. Kazal inhibitory domains are known to inhibit proteases of the trypsin family (Bode *et al.* 1992, Van de Locht *et al.* 1995).

At the moment it is not clear if auto proteolysis corresponds to an additional mechanism for regulating the protease activity of HtrA1. Mapping the cleavage sites by N-terminal sequencing and subsequent mutation would reveal if HtrA1 is still active under these conditions and if forming of higher oligomers upon substrate binding is still possible or if the N-terminus has to be cleaved. Additionally co-crystallization of C- and N-terminus of HtrA1 could show possible binding of the Kazal-like inhibitory domain to HtrA1 itsself.

When testing the ability of HtrA1 to form higher oligomers it was observed that oligomerization is pH dependent. HtrA1 was incubated with unfolded CS in pH 7.5, 8, 8.5 and 9. Clearly conversion into the oligomer increased with increasing pH (Fig. 5.5). Conclusively no activation was observed in pNA assays at pH 7.5.

During biochemical characterization of HtrA1 it became also obvious that only completely unfolded proteins were cleaved which could be another mechanism to prevent unwanted proteolysis. Lysoyzme was only degraded and captured when fully denatured that means denaturation with urea was not sufficient and addition of at least 20 mM DTT was required. The same result was observed for CS and MDH which had to be denatured at 42°C prior to degradation. Consistently no higher oligomers occurred when incubating HtrA1 and CS at 37°C. It can be speculated that folded substrates are too bulky to enter the active site or the S1 specificity pocket. In the trimeric structure of HtrA1 the active site is freely accessible to solvent thus one could speculate that the PDZ domains influence the access or that in a 12mer of HtrA1 only unfolded proteins can be captured.

Another activation mechanism is shown in figure 5.6. Given the fact that the peptide inhibitor is capable to trigger the active conformation, substrates or peptides binding to the active site could lead to activation in cis, i.e. within the trimer, without contribution of the PDZ domain (Fig. 5.6).

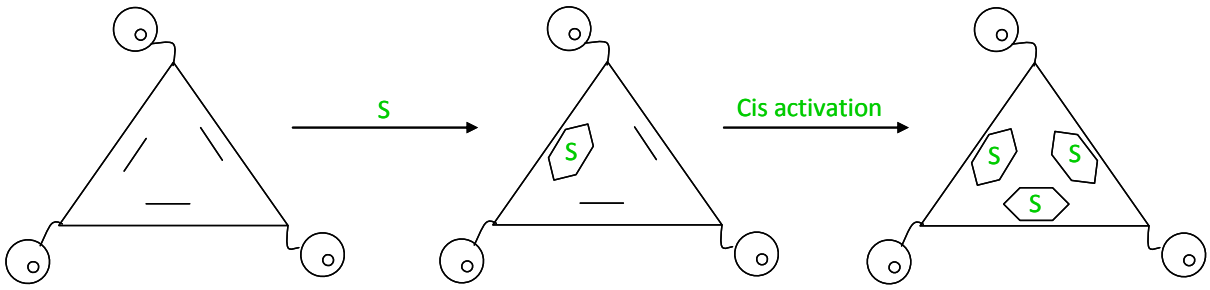

Fig. 5.6 Model for HtrA1 activation in cis
Substrates (S) bind to the one active site in a HtrA1 trimer and trigger the active conformation. This leads in turn to the activation of the other two monomers within the trimer (in cis activation).

Activation in trans, i.e. between different trimers of HtrA1 could be present if unfolded substrate is bound. As so far it can not be stated how HtrA1 binds to unfolded substrates two different modes could be considered (Fig. 5.7). Either HtrA1 is able to form defined particles like DegP or it may cluster around unfolded substrates to prevent aggregation and subsequently cleave them.

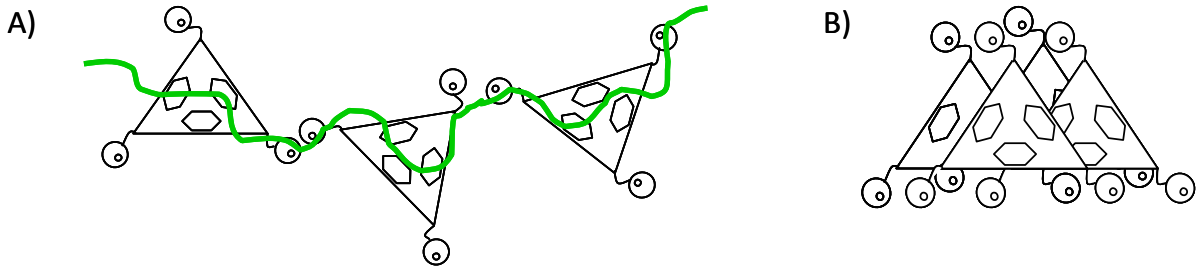

Fig. 5.7 Model for activation of HtrA1 in trans
HtrA1 binds unfolded substrates either by binding along the substrate or by forming defined particles around the substrate. Activation may occur between different trimers (in trans activation).

To decide between both models depicted in Fig. 5.7 one could identify by mass spectrometry the ration of HtrA1 to unfolded substrate which would be a clear indicator.

Taken together the results imply that HtrA1 could play a role as a rather unspecific housekeeping protease degrading unfolded proteins which may probably aggregate. HtrA1 could be thus considered playing a role in the protein quality control in the ECM like DegP in the periplam of *E. coli.*

6 Conclusions

Three crystal structures were presented for human HtrA1. They show the protease domain in the inactive and active conformation. Both states share common structural features with other members of the HtrA family. But they also show striking mechanistic differences.

Interestingly, binding of the peptide inhibitor to the active site of the protease domain alone leads to conformational changes of all active site loops setting up the active conformation. Most prominently loop L3 becomes ordered showing defined interactions with the peptide inhibitor. This observation is different to known HtrA structures where loop L3 becomes ordered by specific interactions with the PDZ domain or to a stress peptide bound to the PDZ domain in DegS.

In bacterial HtrAs the PDZ domains function as sensors of protein folding stress, binding sites for substrates, regulators of the enzymatic activity and are required for oligomerization. In human HtrA1 they are dispensable for proteolytic activity but are involved in allosteric regulation. Furthermore they influence the product size of cleaved substrates.

Most interestingly these data also suggest that human HtrA1 could be regulated by a conserved mechanism of activation by oligomerization which was first described for bacterial DegP (Krojer *et al.* 2008). It could not be shown for DegS or human HtrA2. It is therefore exciting to speculate that in analog to DegP HtrA1 establishes a packaging device that is able to sequester unfolded proteins for partitioning between refolding and degradation pathways. Thus it could be considered as a part of the protein quality control in the ECM which is not yet characterized.

Although the crystal structures of HtrA1 and biochemical analysis have enlarged our knowledge about HtrA1, there is still a great number of open questions regarding the regulation of this family member. Therefore the presented results could be the guide for future experiments that will allow a detailed view into the activation mechanism of human HtrA1.

7 Zusammenfassung

HtrA1 gehört zur Familie der HtrA (*High temperature requirement*) Serin-Proteasen, einer Gruppe hochkonservierter Proteasen, die sowohl eukaryotische als auch prokaryotische Mitglieder umfasst. Gemeinsames Merkmal dieser Serin-Proteasen ist das Vorhandensein einer hoch-konservierten Trypsin-ähnlichen Domäne und mindestens einer C-Terminalen PDZ-Domäne. HtrA1 wurde ursprünglich als weniger exprimiertes Gen in SV40-transfomierten Fibroblasten identifiziert und wird außerdem mit verschiedenen Krankheitsbildern, wie Arthritis, altersbedingter Makuladegeneration oder der Alzheimerschen Krankheit in Verbindung gebracht.

In dieser Arbeit werden drei Kristallstrukturen von HtrA1 präsentiert. Sie zeigen die Protease Domäne in der inaktiven und aktiven Konformation. Beide Konformation weisen vergleichbare strukturelle Gegebenheiten im Vergleich mit anderen HtrA Familienmitgliedern auf. Zugleich werden aber signifikante Besonderheiten für HtrA1 deutlich.

Interessanterweise ist die Bindung des Peptid-Inhibitors in das aktive Zentrum der Protease Domäne ausreichend, um konformationelle Änderungen hervorzurufen, die durch Reorientierung der Schleifen, die das aktive Zentrum gestalten, von einer inaktiven zu einer aktiven Konformation führen. Schleife L3, die in der inaktiven Konformation ungeordnet ist, zeigt jetzt eine geordnete Konformation und definierte Interaktionen mit dem Inhibitor molekül. Diese Erkenntnis ist unterschiedlich zu vergleichbaren bekannten HtrA Strukturen in denen L3 eine geordnete Konformation durch spezifische Interaktionen mit der PDZ Domäne einnimmt.

Die PDZ Domänen der bakteriellen HtrAs sind wichtig für die Erfassung von Protein Faltungsstress, sie sind Bindungsstellen für Substrate und regulieren die enzymatische Aktivität. Für das humane HtrA1 konnte gezeigt werden, dass die PDZ Domäne entbehrlich für die katalytische Aktivität ist, aber eine Rolle für die allosterische Regulation von HtrA1 spielt. Außerdem beeinflusst die PDZ Domäne die Produktlänge von geschnittenen Substraten.

Vor allem interessant ist, daß die Daten auch auf die Möglichkeit hindeuten, daß die Protease durch einen konservierten Mechanismus der Oligomerisierung reguliert wird. Dieser Mechanismus der Regulation durch Oligomerisierung wurde zuerst für das bakterielle Familienmitglied DegP beschrieben (Krojer *et al.* 2008), konnte aber nicht für bakterielles DegS oder humanes HtrA2 gezeigt werden. Es ist daher spannend zu spekulieren, dass HtrA1 analog zu DegP ein Molekül darstellt, das

in der Lage ist ungefaltete oder fehlgefaltete Proteine zu sequestrieren, um es der Rückfaltung oder dem Abbau zuzuführen. Damit könnte es ein Teil der Stressantwort auf ungefaltete Proteine in der ECM sein, ein Qualitäts-Kontrollsystem das noch nicht sehr characterisiert ist.

Obwohl die hier präsentierten Kristallstrukturen von HtrA1 und die biochemischen Analysen unser Wissen über HtrA1 erweitern, ist die Zahl der offenen Fragen immer noch immens. Die dargestellten Ergebnisse können somit die Grundlage für wichtige Experimente in der Zukunft bilden, die einen weiterführenden Einblick in den Mechanismus der Aktivierung der humanen Serin-Protease HtrA1 ermöglichen.

8 References

Ades, S. E., L. E. Connolly, *et al.* (1999). "The Escherichia coli sigma(E)-dependent extracytoplasmic stress response is controlled by the regulated proteolysis of an anti-sigma factor." Genes Dev **13**(18): 2449-61.

Alba, B. M., J. A. Leeds, *et al.* (2002). "DegS and YaeL participate sequentially in the cleavage of RseA to activate the sigma(E)-dependent extracytoplasmic stress response." Genes Dev **16**(16): 2156-68.

An, E., S. Sen, *et al.* "Identification of novel substrates for the serine protease HTRA1 in the human RPE secretome." Invest Ophthalmol Vis Sci.

Anfinsen, C. B. (1973). "Principles that govern the folding of protein chains." Science **181**(96): 223-30.

Bakay, M., P. Zhao, *et al.* (2002). "A web-accessible complete transcriptome of normal human and DMD muscle." Neuromuscul Disord **12 Suppl 1**: S125-41.

Bailey, S. (1994). "The CCP4 Suite - Programs For Protein Crystallography." Acta Crystallographica Section D-Biological Crystallography **50**: 760-763.

Baldi, A., A. De Luca, *et al.* (2002). "The HtrA1 serine protease is down-regulated during human melanoma progression and represses growth of metastatic melanoma cells." Oncogene **21**(43): 6684.

Baldi, A., M. Mottolese, *et al.* (2008). "The serine protease HtrA1 is a novel prognostic factor for human mesothelioma." Pharmacogenomics **9**(8): 1069-77.

Barrett, A. J. (1994). "Classification of peptidases." Methods Enzymol **244**: 1-15.

Beebe, K. D., J. Shin, *et al.* (2000). "Substrate recognition through a PDZ domain in tail-specific protease." Biochemistry **39**(11): 3149-55.

Beleford, D., R. Rattan, *et al.* "High temperature requirement A3 (HtrA3) promotes etoposide- and cisplatin-induced cytotoxicity in lung cancer cell lines." J Biol Chem **285**(16): 12011-27.

Berndt, C., C. H. Lillig, *et al.* (2008). "Thioredoxins and glutaredoxins as facilitators of protein folding." Biochim Biophys Acta **1783**(4): 641-50.

Blow, D. (2000). "So do we understand how enzymes work?" Structure **8**(4): R77-81.

Blow, D. M. (1997). "The tortuous story of Asp ... His ... Ser: structural analysis of alpha-chymotrypsin." Trends Biochem Sci **22**(10): 405-8.

Bode, W. and R. Huber (2000). "Structural basis of the endoproteinase-protein inhibitor interaction." Biochim Biophys Acta **1477**(1-2): 241-52.

Bowden, M., A. E. Drummond, *et al.* (2009). "Evolutionary conservation of mammalian HTRA3 and its developmental regulation in the rat ovary." J Exp Zool B Mol Dev Evol **312**(7): 701-13.

Bowden, M. A., L. A. Di Nezza-Cossens, *et al.* (2006). "Serine proteases HTRA1 and HTRA3 are down-regulated with increasing grades of human endometrial cancer." Gynecol Oncol **103**(1): 253-60.

Brunger, A. T., P. D. Adams, *et al.* (1998). "Crystallography & NMR system: A new software suite for macromolecular structure determination." Acta Crystallogr D Biol Crystallogr **54**(Pt 5): 905-21.

Chamberland, A., E. Wang, *et al.* (2009). "Identification of a Novel HtrA1-susceptible cleavage site in human aggrecan: evidence for the involvement of HtrA1 in aggrecan proteolysis in vivo." J Biol Chem **284**(40): 27352-9.

Chien, J., G. Aletti, *et al.* (2006). "Serine protease HtrA1 modulates chemotherapy-induced cytotoxicity." J Clin Invest **116**(7): 1994-2004.

Chien, J., J. Staub, *et al.* (2004). "A candidate tumor suppressor HtrA1 is downregulated in ovarian cancer." Oncogene **23**(8): 1636-44.

Clausen, T., C. Southan, *et al.* (2002). "The HtrA family of proteases: implications for protein composition and cell fate." Mol Cell **10**(3): 443-55.

Cortes, G., B. de Astorza, *et al.* (2002). "Role of the htrA gene in Klebsiella pneumoniae virulence." Infect Immun **70**(9): 4772-6.

Czapinska, H. and J. Otlewski (1999). "Structural and energetic determinants of the S1-site specificity in serine proteases." Eur J Biochem **260**(3): 571-95.

Dagda, R. K. and C. T. Chu (2009). "Mitochondrial quality control: insights on how Parkinson's disease related genes PINK1, parkin, and Omi/HtrA2 interact to maintain mitochondrial homeostasis." J Bioenerg Biomembr **41**(6): 473-9.

Danese, P. N., W. B. Snyder, *et al.* (1995). "The Cpx two-component signal transduction pathway of Escherichia coli regulates transcription of the gene specifying the stress-inducible periplasmic protease, DegP." Genes Dev **9**(4): 387-98.

De Luca, A., M. De Falco, *et al.* (2004). "The serine protease HtrA1 is upregulated in the human placenta during pregnancy." J Histochem Cytochem **52**(7): 885-92.

Degterev, A., M. Boyce, *et al.* (2003). "A decade of caspases." Oncogene **22**(53): 8543-67.

DeLano, W. L. (2004). Pymol. San Carlos, California, U.S.A, DeLano Scientific LLC.

Demuro, A., E. Mina, *et al.* (2005). "Calcium dysregulation and membrane disruption as a ubiquitous neurotoxic mechanism of soluble amyloid oligomers." J Biol Chem **280**(17): 17294-300.

Dewan, A., M. Liu, *et al.* (2006). "HTRA1 promoter polymorphism in wet age-related macular degeneration." Science **314**(5801): 989-92.

Dobson, C. M. (2004). "Principles of protein folding, misfolding and aggregation." Semin Cell Dev Biol **15**(1): 3-16.

Doyle, D. A., A. Lee, *et al.* (1996). "Crystal structures of a complexed and peptide-free membrane protein-binding domain: molecular basis of peptide recognition by PDZ." Cell **85**(7): 1067-76.

Dyson, M. R, S. Shadbolt, *et al.* (2004). "Production of soluble mammalian proteins in Escherichia coli: identification of protein features that correlate with successful expression." BMC Biotechnol **4**: 32.

Ehrmann, M. and T. Clausen (2004). "Proteolysis as a regulatory mechanism." Annu Rev Genet **38**: 709-24.

Engh, R. A. and R. Huber (1991). "Accurate Bond and Angle Parameters For X-Ray Protein-Structure Refinement." Acta Crystallographica Section a **47**: 392-400.

Erickson, J. W. and C. A. Gross (1989). "Identification of the sigma E subunit of Escherichia coli RNA polymerase: a second alternate sigma factor involved in high-temperature gene expression." Genes Dev **3**(9): 1462-71.

Ferré-d'Amaré, A. R. and S. K. Burley (1994). "Use of Dynamic Light-Scattering to Assess Crystallizability of Macromolecules and Macromolecular Assemblies." Structure **2**(5): 357-359.

Friedrich, R., P. Panizzi, *et al.* (2003). "Staphylocoagulase is a prototype for the mechanism of cofactor-induced zymogen activation." Nature **425**(6957): 535-9.

Gottesman, S. (2003). "Proteolysis in bacterial regulatory circuits." Annu Rev Cell Dev Biol **19**: 565-87.

Grau, S., A. Baldi, *et al.* (2005). "Implications of the serine protease HtrA1 in amyloid precursor protein processing." Proc Natl Acad Sci U S A **102**(17): 6021-6.

Gouet, P., E. Courcelle, *et al.* (1999). "ESPript: analysis of multiple sequence alignments in PostScript." Bioinformatics **15**(4): 305-8.

Grau, S., P. J. Richards, *et al.* (2006). "The role of human HtrA1 in arthritic disease." J Biol Chem **281**(10): 6124-9.

Gray, C. W., R. V. Ward, *et al.* (2000). "Characterization of human HtrA2, a novel serine protease involved in the mammalian cellular stress response." Eur J Biochem **267**(18): 5699-710.

Guillin, M. C., A. Bezeaud, *et al.* (1995). "Thrombin specificity." Thromb Haemost **74**(1): 129-33.

Gupta, S., R. Singh, *et al.* (2004). "The C-terminal tail of presenilin regulates Omi/HtrA2 protease activity." J Biol Chem **279**(44): 45844-54.

Hammarstrom, M., E. A. Woestenenk, *et al.* (2006). "Effect of N-terminal solubility enhancing fusion proteins on yield of purified target protein." J Struct Funct Genomics **7**(1): 1-14.

Hanahan, D. (1983). "Studies on transformation of Escherichia coli with plasmids." J Mol Biol **166**(4): 557-80.

Hara, K., A. Shiga, *et al.* (2009). "Association of HTRA1 mutations and familial ischemic cerebral small-vessel disease." N Engl J Med **360**(17): 1729-39.

Harris, B. Z., B. J. Hillier, *et al.* (2001). "Energetic determinants of internal motif recognition by PDZ domains." Biochemistry **40**(20): 5921-30.

Harris, B. Z. and W. A. Lim (2001). "Mechanism and role of PDZ domains in signaling complex assembly." J Cell Sci **114**(Pt 18): 3219-31.

Hasselblatt, H., R. Kurzbauer, *et al.* (2007). "Regulation of the sigmaE stress response by DegS: how the PDZ domain keeps the protease inactive in the resting state and allows integration of different OMP-derived stress signals upon folding stress." Genes Dev **21**(20): 2659-70.

Hedstrom, L. (2002). "Serine protease mechanism and specificity." Chem Rev **102**(12): 4501-24.

Hegde, R., S. M. Srinivasula, *et al.* (2002). "Identification of Omi/HtrA2 as a mitochondrial apoptotic serine protease that disrupts inhibitor of apoptosis protein-caspase interaction." J Biol Chem **277**(1): 432-8.

Hillier, B. J., K. S. Christopherson, *et al.* (1999). "Unexpected modes of PDZ domain scaffolding revealed by structure of nNOS-syntrophin complex." Science **284**(5415): 812-815.

Hu, S. I., M. Carozza, *et al.* (1998). "Human HtrA, an evolutionarily conserved serine protease identified as a differentially expressed gene product in osteoarthritic cartilage." J Biol Chem **273**(51): 34406-12.

Huang, X., C. T. Knoell, *et al.* (2001). "Modulation of recombinant human prostate-specific antigen: activation by Hofmeister salts and inhibition by azapeptides. Appendix: thermodynamic interpretation of the activation by concentrated salts." Biochemistry **40**(39): 11734-41.

Huber, R., D. Kukla, *et al.* (1974). "Structure of the complex formed by bovine trypsin and bovine pancreatic trypsin inhibitor. II. Crystallographic refinement at 1.9 A resolution." J Mol Biol **89**(1): 73-101.

Huesgen, P. F., H. Schuhmann, *et al.* (2006). "Photodamaged D1 protein is degraded in Arabidopsis mutants lacking the Deg2 protease." FEBS Lett **580**(30): 6929-32.

Iwanczyk, J., D. Damjanovic, *et al.* (2007). "Role of the PDZ domains in Escherichia coli DegP protein." J Bacteriol **189**(8): 3176-86.

Jones, C. H., T. C. Bolken, *et al.* (2001). "Conserved DegP protease in gram-positive bacteria is essential for thermal and oxidative tolerance and full virulence in Streptococcus pyogenes." Infect Immun **69**(9): 5538-45.

Kettner, C. A., R. Bone, *et al.* (1988). "Kinetic properties of the binding of alpha-lytic protease to peptide boronic acids." Biochemistry **27**(20): 7682-8.

Kettner, C. A. and A. B. Shenvi (1984). "Inhibition of the serine proteases leukocyte elastase, pancreatic elastase, cathepsin G, and chymotrypsin by peptide boronic acids." J Biol Chem **259**(24): 15106-14.

Khan, A. R. and M. N. James (1998). "Molecular mechanisms for the conversion of zymogens to active proteolytic enzymes." Protein Sci **7**(4): 815-36.

Kim, D. Y., D. R. Kim, *et al.* (2003). "Crystal structure of the protease domain of a heat-shock protein HtrA from Thermotoga maritima." J Biol Chem **278**(8): 6543-51.

Kim, D. Y. and K. K. Kim (2002). "Crystallization and preliminary X-ray studies of the protease domain of the heat-shock protein HtrA from Thermotoga maritima." Acta Crystallogr D Biol Crystallogr **58**(Pt 1): 170-2.

Kim, D. Y. and K. K. Kim (2005). "Structure and function of HtrA family proteins, the key players in protein quality control." J Biochem Mol Biol **38**(3): 266-74.

Kim, K. I., S. C. Park, *et al.* (1999). "Selective degradation of unfolded proteins by the self-compartmentalizing HtrA protease, a periplasmic heat shock protein in Escherichia coli." J Mol Biol **294**(5): 1363-74.

Kolmar, H., P. R. Waller, *et al.* (1996). "The DegP and DegQ periplasmic endoproteases of Escherichia coli: specificity for cleavage sites and substrate conformation." J Bacteriol **178**(20): 5925-9.

Kolmar, H., P. R. Waller, *et al.* (1996). "The DegP and DegQ periplasmic endoproteases of Escherichia coli: specificity for cleavage sites and substrate conformation." J Bacteriol **178**(20): 5925-9.

Krem, M. M. and E. Di Cera (2003). "Conserved Ser residues, the shutter region, and speciation in serpin evolution." J Biol Chem **278**(39): 37810-4.

Krishnaswamy, S. (2005). "Exosite-driven substrate specificity and function in coagulation." J Thromb Haemost **3**(1): 54-67.

Krojer, T., M. Garrido-Franco, *et al.* (2002). "Crystal structure of DegP (HtrA) reveals a new protease-chaperone machine." Nature **416**(6879): 455-9.

Krojer, T., K. Pangerl, *et al.* (2008). "Interplay of PDZ and protease domain of DegP ensures efficient elimination of misfolded proteins." Proc Natl Acad Sci U S A **105**(22): 7702-7.

Krojer, T., J. Sawa, *et al.* (2008). "Structural basis for the regulated protease and chaperone function of DegP." Nature **453**(7197): 885-90.

Kuninaka, S., S. I. Iida, *et al.* (2007). "Serine protease Omi/HtrA2 targets WARTS kinase to control cell proliferation." Oncogene **26**(17): 2395-406.

Larsen, C. N. and D. Finley (1997). "Protein translocation channels in the proteasome and other proteases." Cell **91**(4): 431-4.

Laskowski, R. A., M. W. Macarthur, *et al.* (1993). "Procheck - a Program to Check the Stereochemical Quality of Protein Structures." Journal of Applied Crystallography **26**: 283-291.

Lauber, T., U. C. Marx, *et al.* (2001). "Accurate disulfide formation in Escherichia coli: overexpression and characterization of the first domain (HF6478) of the multiple Kazal-type inhibitor LEKTI." Protein Expr Purif **22**(1): 108-12.

LaVallie, E. R., E. A. DiBlasio-Smith, *et al.* (2003). "Thioredoxin and related proteins as multifunctional fusion tags for soluble expression in E. coli." Methods Mol Biol **205**: 119-40.

Lazure, C. (2002). "The peptidase zymogen proregions: nature's way of preventing undesired activation and proteolysis." Curr Pharm Des **8**(7): 511-31.

Lehmann, K., S. Hoffmann, *et al.* (2003). "High-yield expression in Escherichia coli, purification, and characterization of properly folded major peanut allergen Ara h 2." Protein Expr Purif **31**(2): 250-9.

Leslie, A. G. W. (1992). "Recent changes to the MOSFLM package for processing film and image plate data." Joint CCP4 + ESF-EAMCB Newsletter on Protein Crystallography **26**.

Li, W., S. M. Srinivasula, *et al.* (2002). "Structural insights into the pro-apoptotic function of mitochondrial serine protease HtrA2/Omi." Nat Struct Biol **9**(6): 436-41.

Liu, Q., J. Lin, *et al.* (2007). "Large scale preparation of recombinant human parathyroid hormone 1-84 from Escherichia coli." Protein Expr Purif **54**(2): 212-9.

Ly, D. H., D. J. Lockhart, *et al.* (2000). "Mitotic misregulation and human aging." Science **287**(5462): 2486-92.

Macario, A. J. and E. Conway de Macario (2005). "Sick chaperones, cellular stress, and disease." N Engl J Med **353**(14): 1489-501.

Martins, L. M., A. Morrison, *et al.* (2004). "Neuroprotective role of the Reaper-related serine protease HtrA2/Omi revealed by targeted deletion in mice." Mol Cell Biol **24**(22): 9848-62.

Maurizi, M. R. (2002). "Love it or cleave it: tough choices in protein quality control." Nat Struct Biol **9**(6): 410-2.

Meltzer, M., S. Hasenbein, *et al.* (2008). "Allosteric activation of HtrA protease DegP by stress signals during bacterial protein quality control." Angew Chem Int Ed Engl **47**(7): 1332-4.

Milev, S., S. Bjelic, *et al.* (2007). "Energetics of peptide recognition by the second PDZ domain of human protein tyrosine phosphatase 1E." Biochemistry **46**(4): 1064-78.

Mo, E., S. E. Peters, *et al.* (2006). "Single, double and triple mutants of Salmonella enterica serovar Typhimurium degP (htrA), degQ (hhoA) and degS (hhoB) have diverse phenotypes on exposure to elevated temperature and their growth in vivo is attenuated to different extents." Microb Pathog **41**(4-5): 174-82.

Mohamedmohaideen, N. N., S. K. Palaninathan, *et al.* (2008). "Structure and function of the virulence-associated high-temperature requirement A of Mycobacterium tuberculosis." Biochemistry **47**(23): 6092-102.

Moradian-Oldak, J., W. Leung, *et al.* (1998). "Temperature and pH-dependent supramolecular self-assembly of amelogenin molecules: A dynamic light-scattering analysis." Journal of Structural Biology **122**(3): 320-327.

Mullis, K., F. Faloona, *et al.* (1992). "Specific enzymatic amplification of DNA in vitro: the polymerase chain reaction. 1986." Biotechnology **24**: 17-27.

Murwantoko, M. Yano, *et al.* (2004). "Binding of proteins to the PDZ domain regulates proteolytic activity of HtrA1 serine protease." Biochem J **381**(Pt 3): 895-904.

Nie, G., K. Hale, *et al.* (2006). "Distinct expression and localization of serine protease HtrA1 in human endometrium and first-trimester placenta." Dev Dyn **235**(12): 3448-55.

Nie, G., Y. Li, *et al.* (2005). "Serine protease HtrA1 is developmentally regulated in trophoblast and uterine decidual cells during placental formation in the mouse." Dev Dyn **233**(3): 1102-9.

Nie, G. Y., Y. Li, *et al.* (2003). "A novel serine protease of the mammalian HtrA family is up-regulated in mouse uterus coinciding with placentation." Mol Hum Reprod **9**(5): 279-90.

Oka, C., R. Tsujimoto, *et al.* (2004). "HtrA1 serine protease inhibits signaling mediated by Tgfbeta family proteins." Development **131**(5): 1041-53.

Otwinowski, Z. and W. Minor (1997). Processing of X-ray diffraction data collected in oscillation mode. Macromolecular Crystallography, Pt a. **276:** 307-326.

Pace, C. N., F. Vajdos, *et al.* (1995). "How to measure and predict the molar absorption coefficient of a protein." Protein Sci **4**(11): 2411-23.

Pallen, M. J. and B. W. Wren (1997). "The HtrA family of serine proteases." Mol Microbiol **26**(2): 209-21.

Park, H. J., S. S. Kim, *et al.* (2006). "Beta-amyloid precursor protein is a direct cleavage target of HtrA2 serine protease. Implications for the physiological function of HtrA2 in the mitochondria." J Biol Chem **281**(45): 34277-87.

Patil, C. and P. Walter (2001). "Intracellular signaling from the endoplasmic reticulum to the nucleus: the unfolded protein response in yeast and mammals." Curr Opin Cell Biol **13**(3): 349-55.

Peisley, A. A. and P. R. Gooley (2007). "High-level expression of a soluble and functional fibronectin type II domain from MMP-2 in the Escherichia coli cytoplasm for solution NMR studies." Protein Expr Purif **53**(1): 124-31.

Perona, J. J. and C. S. Craik (1995). "Structural basis of substrate specificity in the serine proteases." Protein Sci **4**(3): 337-60.

Plun-Favreau, H., K. Klupsch, *et al.* (2007). "The mitochondrial protease HtrA2 is regulated by Parkinson's disease-associated kinase PINK1." Nat Cell Biol **9**(11): 1243-52.

Polgar, L. (2005). "The catalytic triad of serine peptidases." Cell Mol Life Sci **62**(19-20): 2161-72.

Rajan, R. S., M. E. Illing, *et al.* (2001). "Specificity in intracellular protein aggregation and inclusion body formation." Proc Natl Acad Sci U S A **98**(23): 13060-5.

Rawlings, N. D. and A. J. Barrett (1994). "Families of cysteine peptidases." Methods Enzymol **244**: 461-86.

Rawlings, N. D. and A. J. Barrett (1994). "Families of serine peptidases." Methods Enzymol **244**: 19-61.

Rawlings, N. D. and A. J. Barrett (1995). "Evolutionary families of metallopeptidases." Methods Enzymol **248**: 183-228.

Rawlings, N. D. and A. J. Barrett (1995). "Families of aspartic peptidases, and those of unknown catalytic mechanism." Methods Enzymol **248**: 105-20.

Runyon, S. T., Y. Zhang, *et al.* (2007). "Structural and functional analysis of the PDZ domains of human HtrA1 and HtrA3." Protein Sci **16**(11): 2454-71.

Sassoon, N., J. P. Arie, *et al.* (1999). "PDZ domains determine the native oligomeric structure of the DegP (HtrA) protease." Mol Microbiol **33**(3): 583-9.

Shi, Y. (2002). "Mechanisms of caspase activation and inhibition during apoptosis." Mol Cell **9**(3): 459-70.

Shridhar, V., A. Sen, *et al.* (2002). "Identification of underexpressed genes in early- and late-stage primary ovarian tumors by suppression subtraction hybridization." Cancer Res **62**(1): 262-70.

Songyang, Z., A. S. Fanning, *et al.* (1997). "Recognition of unique carboxyl-terminal motifs by distinct PDZ domains." Science **275**(5296): 73-7.

Spiess, C., A. Beil, *et al.* (1999). "A temperature-dependent switch from chaperone to protease in a widely conserved heat shock protein." Cell **97**(3): 339-47.

Stoscheck, C. M. (1990). "Quantitation of protein." Methods Enzymol **182**: 50-68.

Strauss, K. M., L. M. Martins, *et al.* (2005). "Loss of function mutations in the gene encoding Omi/HtrA2 in Parkinson's disease." Hum Mol Genet **14**(15): 2099-111.

Sun, Z., W. Lu, *et al.* (2007). "Expression, purification and characterization of human urodilatin in E. coli." Protein Expr Purif **55**(2): 312-8.

Suzuki, H., D. N. Watkins, *et al.* (2004). "Epigenetic inactivation of SFRP genes allows constitutive WNT signaling in colorectal cancer." Nat Genet **36**(4): 417-22.

Swamy, K. H., C. H. Chung, *et al.* (1983). "Isolation and characterization of protease do from Escherichia coli, a large serine protease containing multiple subunits." Arch Biochem Biophys **224**(2): 543-54.

Tocharus, J., A. Tsuchiya, *et al.* (2004). "Developmentally regulated expression of mouse HtrA3 and its role as an inhibitor of TGF-beta signaling." Dev Growth Differ **46**(3): 257-74.

Urano, T., K. Narusawa, *et al.* "Association of HTRA1 promoter polymorphism with spinal disc degeneration in Japanese women." J Bone Miner Metab **28**(2): 220-6.

van de Locht, A., D. Lamba, *et al.* (1995). "Two heads are better than one: crystal structure of the insect derived double domain Kazal inhibitor rhodniin in complex with thrombin." Embo J **14**(21): 5149-57.

van Loo, G., M. van Gurp, *et al.* (2002). "The serine protease Omi/HtrA2 is released from mitochondria during apoptosis. Omi interacts with caspase-inhibitor XIAP and induces enhanced caspase activity." Cell Death Differ **9**(1): 20-6.

Vande Walle, L., M. Lamkanfi, *et al.* (2008). "The mitochondrial serine protease HtrA2/Omi: an overview." Cell Death Differ **15**(3): 453-60.

Verhagen, A. M., J. Silke, *et al.* (2002). "HtrA2 promotes cell death through its serine protease activity and its ability to antagonize inhibitor of apoptosis proteins." J Biol Chem **277**(1): 445-54.

Vitzithum, K., T. Lauber, *et al.* (2008). "LEKTI domain 15 is a functional Kazal-type proteinase inhibitor." Protein Expr Purif **57**(1): 45-56.

Waller, P. R. and R. T. Sauer (1996). "Characterization of degQ and degS, Escherichia coli genes encoding homologs of the DegP protease." J Bacteriol **178**(4): 1146-53.

Walsh, N. P., B. M. Alba, *et al.* (2003). "OMP peptide signals initiate the envelope-stress response by activating DegS protease via relief of inhibition mediated by its PDZ domain." Cell **113**(1): 61-71.

Walter, T. S., C. Meier, *et al.* (2006). "Lysine methylation as a routine rescue strategy for protein crystallization." Structure **14**(11): 1617-22.

Wickner, S., M. R. Maurizi, *et al.* (1999). "Posttranslational quality control: folding, refolding, and degrading proteins." Science **286**(5446): 1888-93.

Wiederanders, B., G. Kaulmann, *et al.* (2003). "Functions of propeptide parts in cysteine proteases." Curr Protein Pept Sci **4**(5): 309-26.

Wilken, C., K. Kitzing, *et al.* (2004). "Crystal structure of the DegS stress sensor: How a PDZ domain recognizes misfolded protein and activates a protease." Cell **117**(4): 483-94.

Xiong, S., Y. F. Wang, *et al.* (2005). "Solubility of disulfide-bonded proteins in the cytoplasm of Escherichia coli and its "oxidizing" mutant." World J Gastroenterol **11**(7): 1077-82.

Yang, Z., N. J. Camp, *et al.* (2006). "A variant of the HTRA1 gene increases susceptibility to age-related macular degeneration." Science **314**(5801): 992-3.

Ye, S. and E. J. Goldsmith (2001). "Serpins and other covalent protease inhibitors." Curr Opin Struct Biol **11**(6): 740-5.

Zumbrunn, J. and B. Trueb (1996). "Primary structure of a putative serine protease specific for IGF-binding proteins." FEBS Lett **398**(2-3): 187-92.

Zurawa-Janicka, D., J. Narkiewicz, *et al.* (2007). "[Characterization of the HtrA family of proteins]." Postepy Biochem **53**(1): 27-36.

Curriculum Vitae

For data protection reasons the curriculum vitae is not included in the online version of this thesis.

The experiments presented in this work have been carried out at the Institute for Microbiology II at the University Duisburg-Essen in Germany and at the Research Institute for Molecular Pathology in the group of Dr. Tim Clausen in Vienna, Austria.

First referee:
Second referee:
Third referee:

President of the audit commitee:
Day of the oral examination:

Die der vorliegenden Arbeit zugrunde liegenden Experimente wurden am Institut für Mikrobiologie II der Universität Duisburg-Essen und am Institut für molekulare Pathologie (IMP) in Wien durchgeführt.

1. Gutachter:
2. Gutachter:
3. Gutachter:

Vorsitzender des Prüfungsausschusses:
Tag der mündlichen Prüfung:

Author´s Declarations

Unless otherwise indicated in the text or references, or acknowledged above, I declare according to § 6 para. 2 no. 6 for doctoral regulations of the Faculty of Mathematics and Science, that this thesis is entirely the product of my own work. Any inaccuracies of fact or faults in reasoning are my own and accordingly I take full responsibility.

Essen, _____

Signature _____

I declare according to § 6 para. 2, no. 7 for doctoral regulations of the Faculty of Mathematics and Science that the work entitled "*Structural and Biochemical Characteriszation of the Human Serine Protease HtrA1"* belongs to my field of expertise, that I teach and lead research in this field, and that I support the application of Linda Trübestein.

Essen, _____

Signature _____

I declare according to § 6 para. 2, no. 8 for doctoral regulations of the Faculty of Mathematics and Science that this thesis has not been submitted, either in whole or part, for a degree at this or any other university or institution, and that I have not tried to receive a doctor's degree in the past.

Essen, _____

Signature _____

Erklärung:

Hiermit erkläre ich, gem. zur Erlangung des Dr. rer. nat., dass ich die vorliegende Dissertation selbständig verfasst und mich keiner anderen als der angegebenen Hilfsmittel bedient habe.

Essen, den _____ _____

Unterschrift des Doktoranden

Erklärung:

Hiermit erkläre ich, gem. § 6 Abs. 2, Nr. 7 der Promotionsordnung der Math.-Nat.-Fachbereiche zur Erlangung des Dr. rer. nat., dass ich das Arbeitgebiet, dem das Thema *„Structural and Biochemical Characterization of the Human Serine Protease HtrA1“* zuzuordnen ist, in Forschung und Lehre vertrete und den Antrag von Linda Trübestein befürworte.

Essen, den _____ _____

Unterschrift eines Mitglieds der Universität Duisburg-Essen

Erklärung:

Hiermit erkläre ich, gem. § 6 Abs. 2, Nr. 8 der Promotionsordnung der Math.-Nat.-Fachbereiche zur Erlangung des Dr. rer. nat., dass ich keine anderen Promotionen bzw. Promotionsversuche in der Vergangenheit durchgeführt habe und dass diese Arbeit von keiner andern Fakultät abgelehnt worden ist.

Essen, den _____ _____

Unterschrift des Doktoranden